

POLITECNICO DI TORINO

Corso di Laurea Magistrale in Ingegneria Civile



Tesi di Laurea Magistrale

Scissor crossover: numerical analysis of the viability of an underground interchange alternative and comparison with a real case

Relatore:

Prof. Ing. Daniele Peila

Candidato:

Tomas Santolalla

Correlatori:

Ing. Daniele Martinelli

Ing. Moreno Pescara

Ing. Patricio Garcia De Haro

Anno Accademico 2019/2020

Acknowledgments

To the Universidad Nacional de Córdoba, for keeping its public character that allowed me and many other students to pursue an engineering vocation and for giving me the opportunity to expand my knowledge in a different country, promoting my personal and professional growth.

To the Politecnico di Torino, for opening its doors and providing everything I needed for this experience, making me feel like home from the first moment. Especially I would like to express my gratitude to Professors Daniele Peila and Daniele Martinelli, director and co-director of this work for their support during the development of the thesis and for the opportunity of continuing my studies in this passionate field.

To Tunnelconsult Engineering SL, for trusting me with the realization of this study and giving me my first professional experience surrounded by an experienced staff that provided me uninterested guidance since the moment I arrived to the company. In this respect, I would like to mention particularly to Nicola Della Valle, director of the company, Moreno Pescara and Patricio García de Haro, co-directors of this work, and José Ruiz and Pablo Fernández Coto.

To CSPFEA Engineering Solutions for providing me with a full license of Midas GTS NX, without which the realization of this work would not have been possible, and the assistance given whenever needed.

Last and most importantly, I would like to thank my family for all their support throughout all these years. To my parents Raquel and Carlos for their countless sacrifices made to give me the opportunity of achieving my goals and my sister Alfonsina, who has been the most important person in this process, believing in me even when I doubted myself.

Abstract:

The constant growth of the populations and the increase in the needs of transportation obligate engineers to propose efficient infrastructures that minimize costs of construction with better results. In metropolitan railway systems, underground constructions are widely used not only to materialize the needed space where trains perform their route, but can also hold stations and interchanges. Crossovers are necessary in metro lines, and generally are performed inside a cavern of big dimensions where rails develop a change of directions. Structures of this magnitude imply high levels of coordination, important time increments and serious deformations in the surface that, if are not correctly controlled, can produce severe consequences, especially in urban areas. The work developed in this thesis intends to analyze the possibility of using a different crossover method, the so-called “scissor” methodology.

Using geotechnical investigations performed for a real case, two models of the scissor crossover are designed: one considering favorable ground conditions and another where the characteristics of the formation are adverse. Additionally, two other models of the typical solution are done in order to compare results in the same ground conditions.

The whole excavation process is analyzed, from the undisturbed ground to the finalization of the necessary works. So, two different excavation methodologies are studied: a mechanized procedure for the running tunnels and a conventional tunnelling approach for the caverns that materialize the crossover.

Through a geotechnical analysis software based on the Finite Element Method (FEM), it is possible to simulate the construction sequence and understand how the ground behaves during and after the excavation. Results show that the scissor crossover is perfectly viable in the ground with good characteristics and possible in the more unfavorable case, applying corresponding interventions. Nevertheless, the most typical solution presents more advantages in this particular case, probably due to the geometric characteristics of the railway design.

Table of Contents

Chapter 1: Introduction.....	1
1.1. Introduction.....	1
1.2. Research motivation and objectives.....	2
1.3. Work methodology	2
Chapter 2: Caverns as underground constructions	4
2.1 Historical use of caverns	4
2.2 Importance of caverns for transportation infrastructure	6
2.3 Caverns construction methods. Examples	7
Chapter 3: Description of the case under study	13
3.1 The existing cavern.....	13
3.2 Definition of the proposed solution	15
3.3 Pros and Cons of the proposals.....	20
Chapter 4: Excavation methods.....	23
4.1 Conventional Tunnelling	23
4.2 Mechanized tunneling: slurry machine.....	26
4.2.1 General aspects.....	26
4.2.2 Machine used in the project.....	28
Chapter 5: Geotechnical analysis of the site.....	30
5.1 Mumbai Geology	30

5.2	Crossover Geology	31
5.3	Groundwater and permeability	34
Chapter 6: 3D Models		37
6.1	Introduction to Numerical Analysis.....	37
6.1.1	FEM models for geotechnics.....	37
6.1.2	3D Models	39
6.2	Software	40
6.2.1	Midas GTS NX.....	40
6.2.2	Software validation.....	41
6.3	Geometry	45
6.3.1	Representation of the project.....	45
6.3.2	Load and boundaries definition	47
6.4	Ground Characteristics	48
6.4.1	Failure Criteria.....	49
6.4.2	Overburden	50
6.4.3	Class III and IV Breccia	51
6.5	Support Characteristics	60
6.5.1	First Phase Lining.....	60
6.5.2	Final Lining and Segmental Lining.....	66
6.6	Groundwater	69

6.7	Construction stages	69
6.8	FEM models results	72
6.8.1	Displacements.....	72
6.8.2	Principal Stresses.....	73
6.8.3	Plastic Status.....	74
6.8.4	Original Cavern Model:.....	75
Chapter 7: Discussion.....		80
7.1	Viability of the crossover in the two rock masses	80
7.2	Comparison with original project	85
7.3	Distance between tubes.....	86
Chapter 8: Conclusions.....		88
Chapter 9: References.....		90
Chapter 10: Appendices.....		93
10.1	Appendix 1: Scissor Crossover cross sections	93
10.2	Appendix 2: Crossover geological information	99
10.3	Appendix 3: Scissor crossover results.....	103
10.3.1	Breccia Class III	104
10.3.2	Breccia Class IV	108
10.4	Appendix 4: Values of Superficial Displacements	112

Figures Index

Figure 2.1 -Aldeadávila dam and cavern scheme.....	5
Figure 2.2-Natural gas reservoir scheme.....	6
Figure 2.3-Cut and Cover. Bottom-up.....	8
Figure 2.4-Cut and cover. Top down.....	9
Figure 2.5-Cavern section. Eurotunnel, French side (left) and UK side (right).....	11
Figure 2.6-Istanbul metro crossover. Plan view and excavation sequence	12
Figure 3.1- Map of the metropolitan transportation system of Mumbai ¹	13
Figure 3.2-Original Design. Plan view.....	14
Figure 3.3-Original Design Cross Section.....	15
Figure 3.4-Scissor cross over plan view and excavation sections.....	16
Figure 3.5-Scissor crossover construction process. Plan view.....	18
Figure 3.6-Excavation sequence of each cavern	19
Figure 3.7-Alternatives confrontation	22
Figure 3.8-Potential weak points	22
Figure 4.1-Conventional tunneling. Excavation with rockheader.....	25
Figure 4.2-Examples of excavation sequences.....	25
Figure 4.3-Pressure balance must be ensured in the face	26
Figure 4.4-Parts of a slurry machine	27
Figure 4.5-17” discs hard rock Cutterhead.....	29

Figure 5.1-Boreholes location in the original project.....	31
Figure 6.1-Scissor Crossover with Midas GTS NX.....	37
Figure 6.2-Midas GTS NX.....	41
Figure 6.3-Settlement curve. (MORETTO et al., 1969).....	42
Figure 6.4- Software verification. Cavern D.....	44
Figure 6.5-Cavern D model results.....	45
Figure 6.6-Model's domain.....	46
Figure 6.7- Part of the model represented.	46
Figure 6.8-Transition Section problem and solution.....	47
Figure 6.9-Model's loads and constraints.....	48
Figure 6.10- Mohr-Coulomb's Criterion.(Hudson & Harrison, 1997).....	49
Figure 6.11-Relationship between $\sin \phi$ and plasticity index for normally consolidated soils. (Mitchel & Soga, 2005).....	51
Figure 6.12Mohr-Coulomb's fit with Hoek-Brown's criterion.....	52
Figure 6.13-Bieniawski Classification.(Bieniawski, 1989).....	55
Figure 6.14-RocData Output. Breccia Class III.....	58
Figure 6.15-RocData Output. Breccia Class IV.....	58
Figure 6.16-Aproximation of support, Grimstad and Barton (1993).....	62
Figure 6.17-Universal Ring.....	68
Figure 6.18-Excavation of TBM tunnels and installation of segment lining.....	70

Figure 6.19-Cavern I construction sequence.	71
Figure 6.20- Analyzed section.....	72
Figure 6.21-Plastic status. Plan view around cavern F. Breccia class III(left) and IV (right).	74
Figure 6.22-Original cavern model	75
Figure 6.23-Original Cavern Sequence.	78
Figure 6.24-Original Cavern superficial Settlements. Breccia Class III	78
Figure 6.25-Original Cavern superficial Settlements. Breccia Class IV	79
Figure 7.1-Alternative solutions for Breccia Class IV	81
Figure 7.2-Superficial Structures damage. Boscardin & Cordin (1989).	83
Figure 7.3-Superficial Structures damage. Boscardin & Cordin (1989).	84
Figure 10.1-Cavern A.....	94
Figure 10.2-Cavern B	94
Figure 10.3- Cavern C	95
Figure 10.4- Cavern D.....	95
Figure 10.5- Cavern E	96
Figure 10.6 - Cavern F.....	96
Figure 10.7 - Cavern G.....	97
Figure 10.8 - Cavern H.....	97
Figure 10.9 - Cavern I	98

Figure 10.10-Borehole information in the section	100
Figure 10.11- Geological profile. Cross section.....	101
Figure 10.12- Geological Profile. Longitudinal Section.....	102
Figure 10.13- Superficial Settlements. Breccia Class III.....	104
Figure 10.14- Superficial Settlements before the construction of the caverns. Breccia Class III.....	104
Figure 10.15-Cavern G face displacements in Y direction. Breccia Class III.....	105
Figure 10.16- σ_1 in the analyzed section.....	106
Figure 10.17- σ_3 in the analyzed section.....	106
Figure 10.18- Plasticity analysis. Plan view.....	107
Figure 10.19-Plasticity analysis. Cavern F cross section and plan view detail	107
Figure 10.20-Superficial settlements.....	108
Figure 10.21-Superficial Settlements before the construction of the caverns	108
Figure 10.22-Cavern G face displacements in Y direction	109
Figure 10.23- σ_1 in the analyzed section.....	110
Figure 10.24- σ_3 in the analyzed section.....	110
Figure 10.25-Plasticity analysis. Plan view.....	111
Figure 10.26-Plasticity analysis. Cavern F cross section and plan view detail	111
Figure 10.27- Building Edge, at 25 meters from Crossover center. Scissor Crossover.	114
Figure 10.28- Building Edge, at 25 meters from Crossover center. Original Crossover. ..	116

Figure 10.29- Building Edge, at 50 meters from Crossover center. Scissor Crossover. 118

Figure 10.30- Building Edge, at 50 meters from Crossover center. Original Crossover. .. 120

Tables Index

Table 3.1-Pros and Cons of the proposals	22
Table 5.1-Boreholes information.....	33
Table 5.2-Lugeon Criterion (Quiñones-Rozo, 2010).	35
Table 5.3-Water Level.....	36
Table 6.1-RMR Class III	56
Table 6.2-RMR Class IV	56
Table 6.3-Rock Mass Parameters	57
Table 6.4-Parameters used in the model.....	60
Table 6.5-Excavation Support Ratio. Burton (1947).....	61
Table 6.6- Initial support for caverns. Class III breccia	63
Table 6.7-Initial support. Class IV breccia.....	63
Table 6.8-Shotcrete Characteristics	64
Table 6.9-Lattice girders characteristics.....	65
Table 6.10-Elasticity Modulus of support.	66
Table 6.11-Rock bolts characteristics.....	66
Table 6.12-Final Lining characteristics	67
Table 6.13- Segmental rings information.	69
Table 6.14- Steel Pipes characteristics	76
Table 7.1- Boscardin & Cordin classification (1989).....	81

Table 7.2 - Bjerrum Classification (1963).....	82
Table 7.3- Horizontal strains and angular distortions of the models.....	82
Table 7.4-- Horizontal strains and angular distortions of the models.(50 meters from the center).....	83
Table 7.4-Original Model Volumes	86
Table 7.5 - Scissor Crossover volumes. *The length of each cavern is multiplied by 2.....	86
Table 10.1- Superficial Displacements Scissor Crossover. Breccia Class III. 25m from crossover center	113
Table 10.2-Superficial Displacements Scissor Crossover. Breccia Class IV. 25m from crossover center	114
Table 10.3- Superficial Displacements Original Crossover. Breccia Class III. 25m from crossover center	115
Table 10.4-Superficial Displacements Original Crossover. Breccia Class IV. 25m from crossover center	116
Table 10.5- Superficial Displacements Scissor Crossover. Breccia Class III. 50m from crossover center	117
Table 10.6-Superficial Displacements Scissor Crossover. Breccia Class IV. 50m from crossover center	118
Table 10.7- Superficial Displacements Original Crossover. Breccia Class III. 50m from crossover center	119
Table 10.8-Superficial Displacements Original Crossover. Breccia Class IV. 50m from crossover center	120

Chapter 1: Introduction

1.1. Introduction

The constant growth of the urban centers in all parts of the world in the last centuries and the consequently increase in the need of transportation of their participants have led to the permanent optimization of the communication routes. Underground structures have allowed the accommodation of the needed transportation infrastructure without permanent interferences in the surface activity, so it seems logical that they evolve in consonance with the increase of the populations and the advancement of transportation technologies.

For the construction of a metropolitan railway system, parallel twin tunnels are widely used to materialize the underground space needed to place the lines that run in two opposite directions. When the necessity to perform an interchange appears, allowing the trains to pass from one track to the other, different excavation methodologies can be proposed to solve the problem.

It is common practice to construct a cavern of big dimensions covering the complete area where the rails need to cross and providing enough space to place the railway infrastructure. This decision causes in many cases high impacts on the surface, especially in terms of vertical displacements and distortions, because of the large quantities of volume that is being extracted from the ground and for the proximity to the surface that this kind of civil work usually have.

Different from the usual approach, there are crossover methods that propose a tunnel that follows the curve of the railway track instead of excavating the whole space of the intervention, trying to be more efficient in terms of removed ground. The alternative presented in this thesis, the so-called “scissor” crossover, consists in the construction of a system of caverns capable of accommodate this diverging tunnel in their inside.

1.2. Research motivation and objectives

Crossovers represent a critical point in the alignment because their dimensions mean a disruption in the normal construction process of the running tunnels . This causes important increases in terms of time and budget, requiring a change in the construction methodology in most of cases. Although economy is a crucial variable in every project, engineers must provide cost-effective solutions with the aim to time minimize the impact generated on surroundings and environment by civil works.

The above mentioned is the reason why this thesis intends to analyze the feasibility of a solution to a social need trying to reduce as much as possible the operative costs but having safety as priority. The aims fixed to accomplish this task are to evaluate the possibility of carry out this type of solution for different ground conditions, check which variables have more influence in the design and achieve a better understanding of the method's limitations.

Also, a comparison with the most typical approach is done to evaluate if this alternative fit better with the presented railway design and with the geological characteristics established. This could define certain guidelines for future scenarios where the crossover methodology is being decided with similar geometric and ground characteristics.

1.3. Work methodology

The alternative is planned to be placed exactly where an actual crossover exists, materialized with a big-cavern approach designed by TMD(TÜNEL MÜHENDİSLİĞİ VE DANIŞMANLIK) from Istanbul. With the real project layouts, the geometry of the alternative is designed by adapting the railway curves to fit the guidelines of the scissor method. With these modifications, it is possible to create 17 caverns that progressively increase their section.

The proposed construction process involves the use of two different excavation methodologies: the running tunnels are planned to be constructed using a Tunnel Boring

Machine (TBM), while for the caverns a Conventional Method is chosen. This proposal is in accordance with the one established by the original project.

Using the geological reports of the site, it is possible to establish the essential ground parameters needed to recreate the situation with a computational simulation. Using the software Midas GST NX two models of the scissor alternative are developed, one characterized by a stable and resistant ground condition and another composed by a poor and more damaged formation. Again, the characteristics of the structural materials used in the models respect the guidelines established in the original crossover.

To simulate the constructive procedure, the models are organized in stages that include from the undisturbed ground situation to the installation of the final structural support, passing through all the necessary steps in the sequence that each method comprehends.

Additionally, two models of the big cavern approach were included with its corresponding modifications to accomplish a faithful comparison of the methodologies in the same ground characteristics. With the outputs of all four models and a simplified economic analysis, it is possible to analyze the viability of the scissor methodology and its advantages and drawbacks compared to the traditional approach.

Chapter 2: Caverns as underground constructions

2.1 Historical use of caverns

Caverns are underground structures that have their three dimensions in the same order of magnitude, differently from tunnels where the longitudinal dimension prevails over the other two(A. Fernández et al., personal communication, 2009).

They have been used since the beginnings of mankind as refuge but as a modern construction have not been developed as much as tunnels. Their shape, dimensions and construction procedures are directly linked to their purpose, that can be classified mainly into caverns for hydroelectric plants, for railway and transportation infrastructure and for the storage of hydrocarbons. Of course, there are cases of caverns that have been destined for a different use such as military bases, scientific laboratories, underground parking, even to keep in their inside entertainment activities such as museums or sport events.

Their development on a big scale can be tracked down to the Scandinavian countries, where an important tradition in underground construction exists. In 1911 in Sweden the first fully covered cavern that contained four turbines for hydroelectrical purposes was finished. For this particular purpose many caverns were constructed in Europe in the XX century, especially in valleys where the plant did not have enough space or when they wanted to obtain a higher water jump.

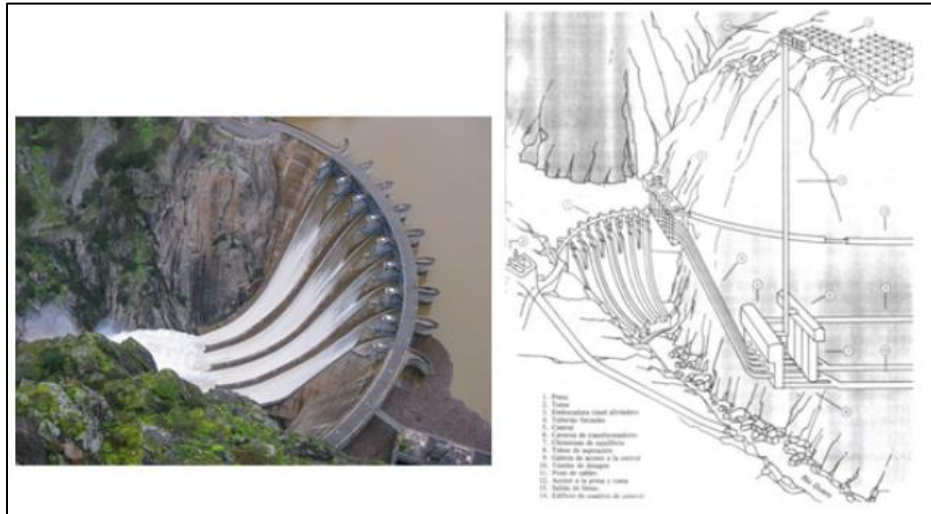


Figure 2.1 -Aldeadávila dam and cavern scheme

Besides this purpose, these underground structures have also been improved for the storage of oil derivatives and natural gas. Again, the northern countries of Europe have been pioneers in this subject, considering their preference in underground constructions due to the low temperatures and the good quality of their rock masses. In the case of liquid deposits caverns have a pretty standard dimension, similar to the ones excavated for hydroelectric plants. When the storage of natural gas is intended (in its gaseous state), vertical caverns of great depth are excavated through dissolution techniques, used especially in saline deposits that present impermeable covers.

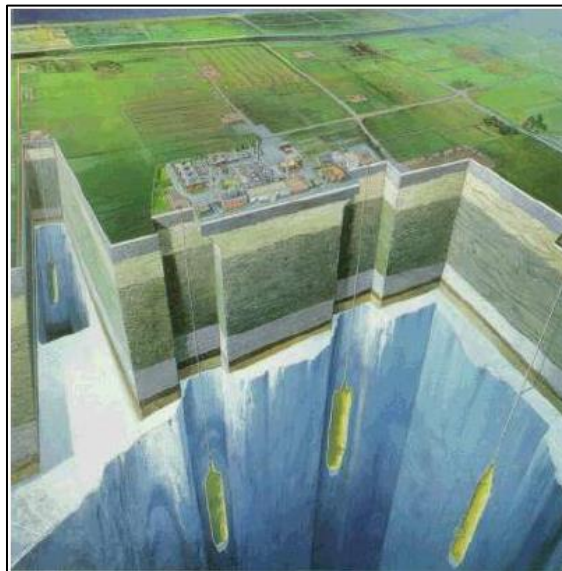


Figure 2.2-Natural gas reservoir scheme

2.2 Importance of caverns for transportation infrastructure

The tunnels where the trains perform their route comprehend the most of the part length of a project, and in most cases they are excavated using boring machines because of their high performance and low disturbance on the surrounding constructions. Although their low percentage in the excavation length, the execution of the needed caverns requires particular attention. In most cases, caverns are constructed to be destined as stations, which are mandatory in all metro lines with an interval depending on the project and the corresponding regulation.

Stations are not easy to plan, they require big spaces to contain not only the trains themselves, but also all the access facilities to the platforms and the eventual evacuation systems. This is why they represent an important variation in the transversal dimension of the project, but at the same time they are limited in order to generate the minimum disturbance to the ground and the superficial activities. It is recommended to avoid zones where complicated geological units are found with uneven sets of discontinuities and try to accomplish an adequate orientation to the present failures, if inevitable.

To construct the caverns a change in the constructive procedure is required respect to the used for the TBM tubes, needing to define excavation sequences that reduce the size of the sections to avoid compromising the stability of the process. This of course increases the working time, but it is crucial to ensure the safety of the work. Many cases can be quoted where excavations of these characteristics have failed causing important material loses and, more importantly, human lives. Carmel (El País, 2007), Heathrow (Harper, 2000) and Nicoll Highway (Hansford, 2012) are examples of how the lack of information of the ground or a wrong choice of methodology can derivate in irrecuperable loses during the execution of these complex constructions.

2.3 Caverns construction methods. Examples

Because of the advantages that present for shallow structures, it is general practice to use the *cut and cover* methodology for metro stations when working in soil conditions. This technique can follow two general procedures: *bottom-up* and *top-down* (Medaña Saavedra, 2003). Both methods consist in the excavation from the surface between retaining walls that act as lateral support, with the difference that the first one does not consider the walls as a structural part of the tunnel, while in the second case the retaining walls are part of the final structure. The construction procedures of each method are the followings:

- Bottom-up cut and cover:
 - a) It begins with the construction of the retaining walls before the excavation commences. Depending on the soil conditions and the depth of the excavation the walls can be materialized as reinforced concrete diaphragm walls, reinforced concrete bored pile walls or steel sheet pile walls.
 - b) The following operation consists in the excavation between the walls until the bottom depth is reached, installing additional temporary support when needed. The invert of the tunnel is executed.
 - c) Using conventional formworks, the whole section of the tunnel is poured including the corresponding side walls.

- d) Once the section is finished and the corresponding waterproof system is installed, the terrain is backfilled to its original level and ground activities can be resumed.

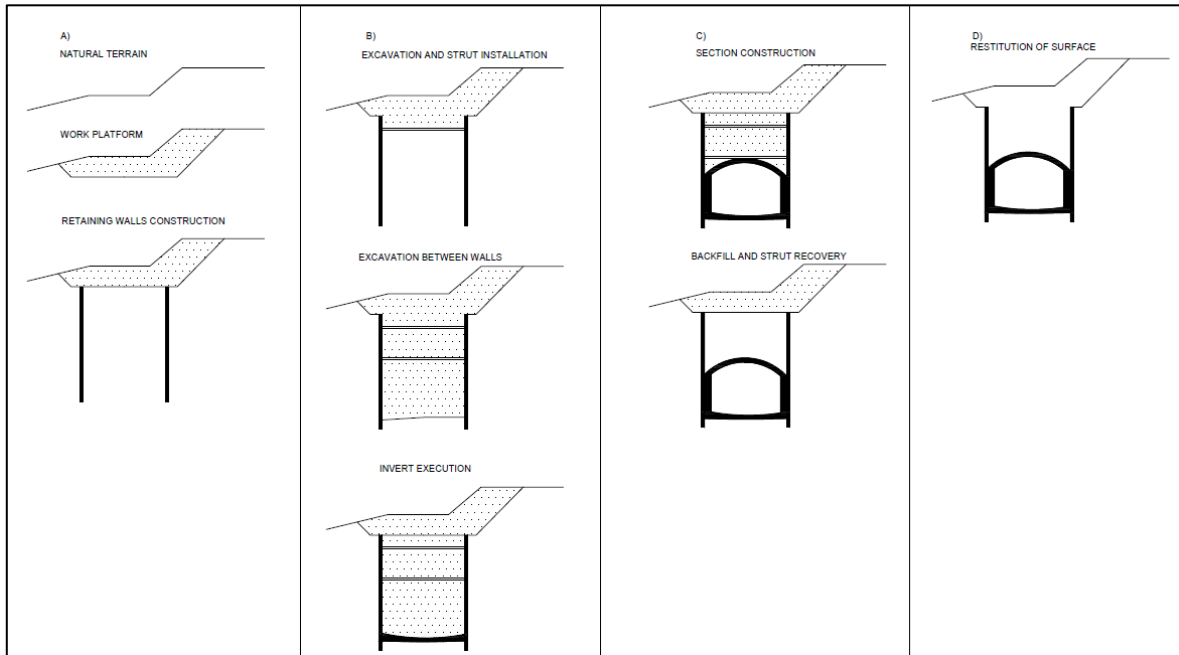


Figure 2.3-Cut and Cover. Bottom-up.

- Top-down cut and cover:
 - a) Follows the same guidelines of the previous case.
 - b) Follows the same guidelines of the previous case, but reaching only the roof level.
 - c) The crown or upper slab is constructed linked to the retaining walls. Can be poured in situ over a thin layer of mortar that separates it from the ground or using a conventional formwork. Once it is finished and the structure is impermeabilized, the terrain over the crown is filled back to its original level. If necessary, a deck on the surface can be installed.
 - d) The excavation of the tunnel section continues under the crown, finalizing with the execution of the invert that must be correctly connected to the retaining walls.

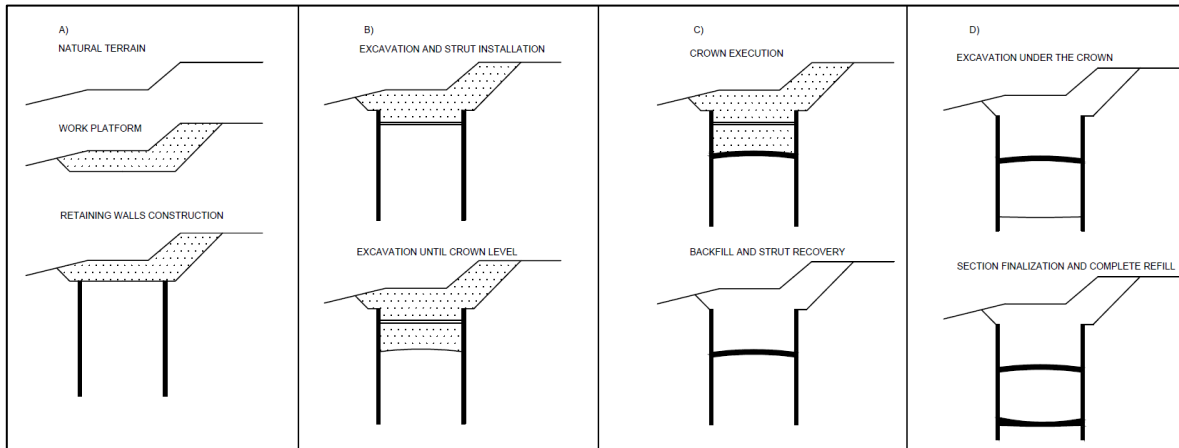


Figure 2.4-Cut and cover. Top down.

It is not easy to generalize when a method is more convenient than the other, but some differences between them can be established. The bottom-up procedure allows an easy access of the machinery to the trench and gives the possibility to waterproof the outside of the tunnel, but the surface activities must be suspended or relocated and eventually can require the dewatering of the zone to reach the invert level.

Instead, the top-down method allows an early resume of the surface activities with minor construction costs due to the use of the retaining walls as part of the structure, avoiding the execution of the side walls and translating this into minor construction times. But at the same time the lateral walls of the structure cannot be impermeabilized and the connection between the walls and the rest of the structure are potential weak points if they are not executed correctly.

Cut and cover methods present important benefits in terms of safety, reducing the uncertainties of the excavated ground and the exposure of the workers that the underground excavation comprehends, especially when working with soil. In rock condition, the procedure is reduced to the construction of a trench without the use of the walls, as long as the quality of the formation allows it.

Is possible that due to the ground condition, the activity developed on the surface or the meaningful deepness of the project this approach becomes inapplicable, so an underground execution is needed as the one presented in this work.

Caverns for crossovers or stations can present free spans of 20 meters or more, so in order to materialize these important volumes a careful procedure must be followed. This is the reason why the Sequential Excavation Method (SEM) is widely used in the field, consisting in the general concept of the division of the tunnel face in a way that allows the progressive removal of the ground in an order that the stability of the excavation is not compromised (Rafie, 2019).

The previously stated concept is followed by other methodologies, where the excavation of each part of the tunnel is followed by the immediate application of the support in a length of advancement determined depending on the ground characteristics. Because it will be temporarily unsupported, this advancement step must be able to support itself to avoid any harms to the workers exposed in this stage.

Referring to cases similar to the one under study, in one of the most important underground infrastructures of the continent such as the Eurotunnel caverns have been a frequent tool along the alignment to solve different situations when the railway system needed modifications.

For example, for the construction of a scape cavern two different procedures were followed. On the French side a series of micro tunnels were used around the area where the excavation of the face would be done afterwards to function as support in a sort of grouting system. While in the British side a more traditional work was done following a sequential excavation of the face. The French solution results more suitable for granular soil conditions, while the British approach is more typical for rock masses.

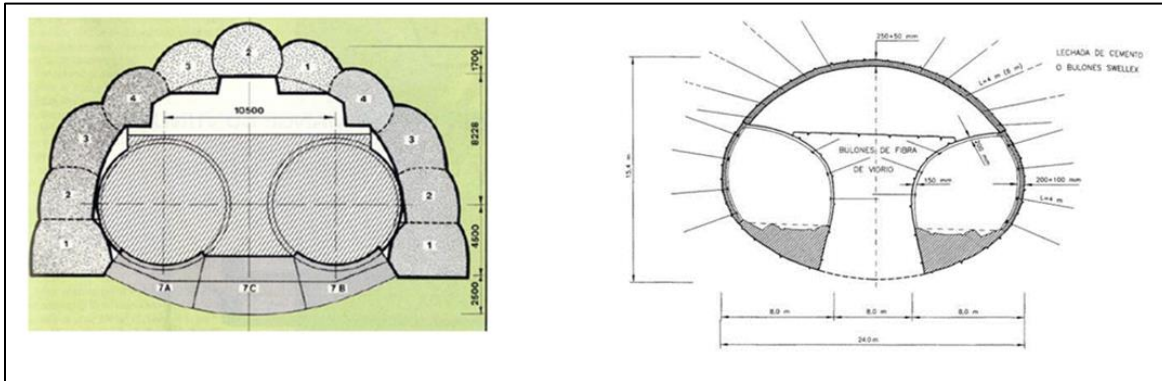


Figure 2.5-Cavern section. Eurotunnel, French side (left) and UK side (right)

As it was done in the original project of the Mumbai Metro Line, the most common procedure to solve an underground interchange of railway lines is to excavate a cavern of big dimensions, covering the complete area where the cross is performed. The geometry chosen varies depending on the project's alignment, ground conditions, machinery available and the activities carried out on the surface.

An alternative solution was used in the Uskudar – Umraniye – Cekmekoy Metro Project of the Istanbul metro system. For this case, a system of five caverns was designed to accommodate the alignments. Four of them (T3 section) allow the change of direction of the running tunnels and also have space for the passing-through rails, while in the center of the crossover, a cavern (T2 section) is constructed containing the actual cross of the rails.

This approach was possible due to the wide separation between the running tunnels. The length from the beginning of the first pair of T3 to the point where the rails finish the cross is equal to 707 meters, with a distance between tubes of 32,3 m. T2 and T3 have sections of 119 m^2 and 129 m^2 correspondingly, so the excavation of the faces was done sequentially, starting from the hole done by the TBM and growing until the final shape was obtained.

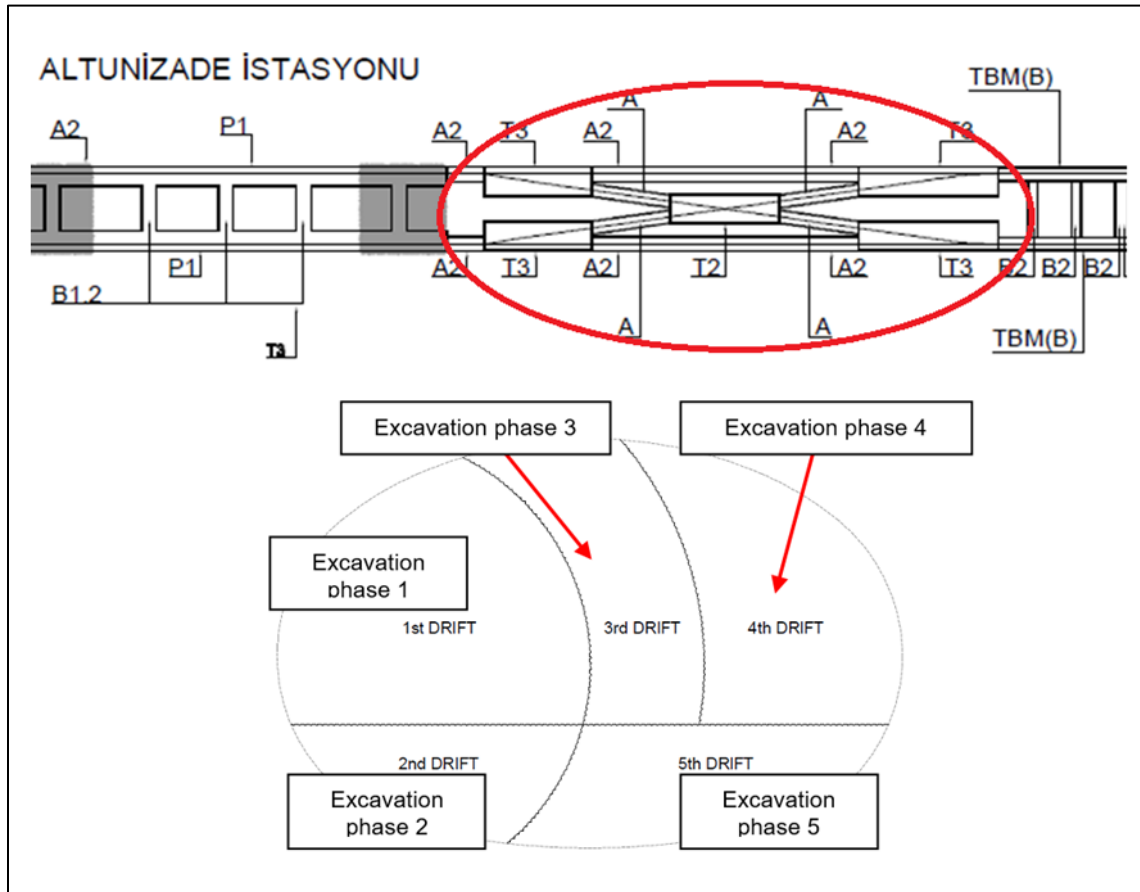


Figure 2.6-Istanbul metro crossover. Plan view and excavation sequence

Chapter 3: Description of the case under study

3.1 The existing cavern

TMD (TÜNEL MÜHENDİSLİĞİ VE DANIŞMANLIK) from Istanbul, developed one of the crossovers of the Mumbai Metro Line 3, located between the stations of Acharya Atrey Chowk and Science Museum. This original project consists in the construction of a big cavern that covers the complete zone where the metro rails need to perform the crossover. The construction of the cavern for the crossover is planned to be done after the excavation of the running tunnels. The cavern is at approximately 15 meters from ground level in an urban area, so superficial displacements are the critical parameter to be controlled in this case. The cross section of the crossover cavern is 175 m² approximately while its length of run is of 103 m.



Figure 3.1- Map of the metropolitan transportation system of Mumbai¹

¹<https://www.mapsofindia.com/mumbai/mumbai-metro-map.html>

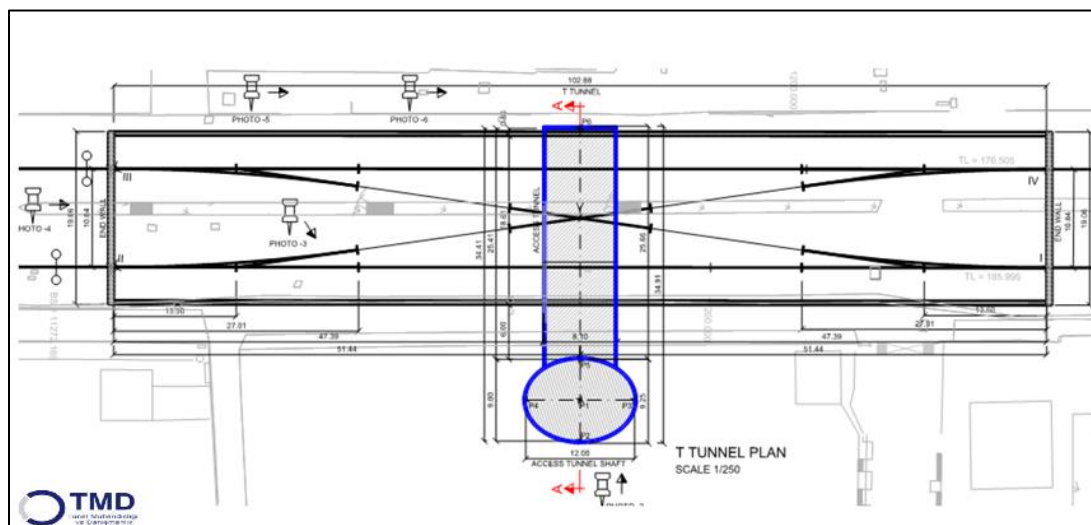


Figure 3.2-Original Design. Plan view

Although in most of Indian railways usually a broad gauge of 1676mm is used, for some metro lines in that country the Standard gauge is chosen(1435 mm), including Mumbai's metropolitan system. This particular measure is important because for a planned commercial speed of 80 km/h, minimum radius of curve shall be 190 m (STANDARDIZATION AND INDIGENISATION OF METRO RAILWAYS, SYSTEMS AND SUB-SYSTEMS, 2013), which is the value used in the original design in order to have the smallest possible cavern.

Because of the magnitude of the structure, it was required the installation of a pipe umbrella support to ensure the stability of the advancement. So, the first step in the construction process consists in the excavation of a vertical shaft, needed to get to the center of the crossover through another access tunnel and apply the corresponding reinforcement, as shown in Figure 3.2.

Once the crown reinforcement is placed, the construction follows a sequence that starts with the removal of the segments of the running tunnels and the excavation of the face divided by stages (Figure 3.3), applying intermediate reinforcement to ensure the correct advancement of every step. For the first phase lining a layer of shotcrete is applied with a

series of lattice girders, even on the temporary faces that will be removed in a following excavation stage. Also, a system of rock bolts is placed around the TBM tunnels in the length of the crossover ensuring the stability of the process.

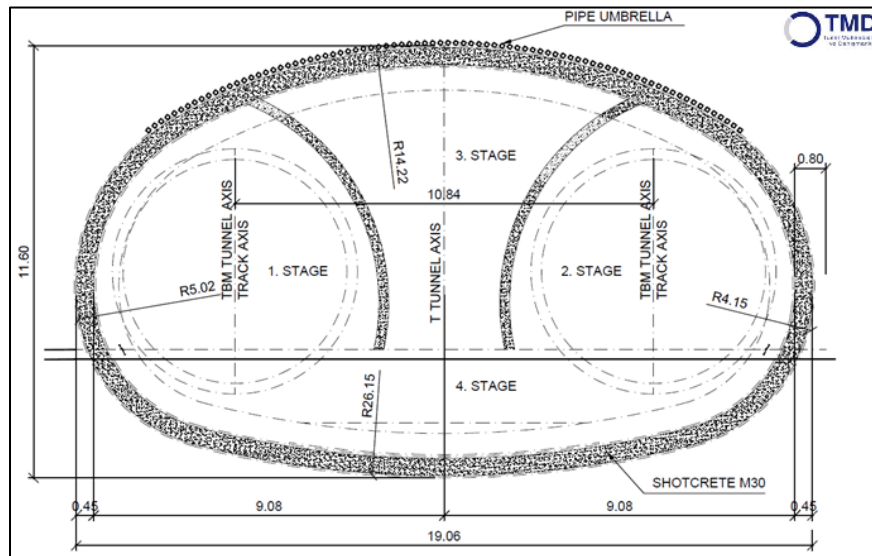


Figure 3.3-Original Design Cross Section

3.2 Definition of the proposed solution

The alternative geometry object of study consists in an arrangement of 17 cross sections of caverns. The caverns are organized in such a way that the cross section increase in order to follow the divergence of the tunnel that needs to cross to the parallel line. In this way, the encounter of the two rails will not be placed exactly between the TBM tubes but will be laid down over one of them as it is shown in Figure 3.4. The detail of the cross sections of the caverns is found in Appendix 1.

Compared to the actual cavern constructed for the crossover, the presented proposal poses an increase of the length of the work in order to correctly accommodate the diverging tunnel inside the caverns and at the same time respect the minimum curve radius of the railway curves.

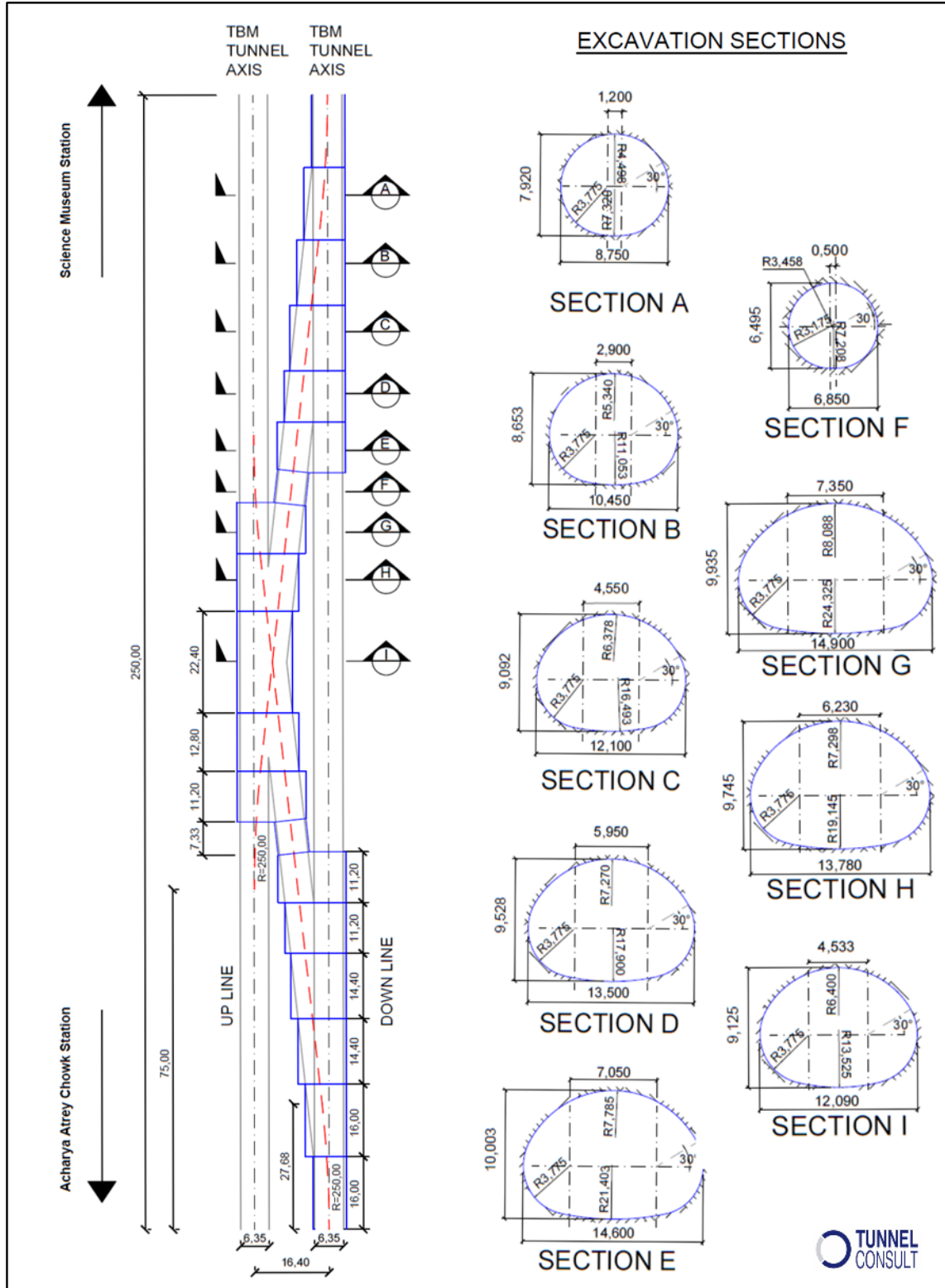


Figure 3.4-Scissor cross over plan view and excavation sections.

In this case, the rails start to curve in previous chainage in the down line respect to the up line, allowing a progressive increase in the excavation's cross section and making possible to fit the caverns between the running tunnels. This granted the possibility of using a bigger radius of 250m that increases the performance with a smaller loss of speed when entering the curve.

Figure 3.5 explains the construction procedure. A local chainage system was established in order to achieve a clear description of the operation. The process is considered from the excavation of the twin metro tunnels materialized with a Slurry TBM, with the constant placement of the correspondent segmental lining. Once they are finished, the excavation of the caverns starts following two simultaneous advancement procedures: one starting from caverns A in stations 0+016.00 and 0+234.00 towards the center of the crossover (Direction 1), and another beginning from the mid-point of cavern I (station 0+125.00) to the outside of the crossover (Direction 2).

The construction of each cavern begins with the removal of the sacrificial concrete rings, which have a length of 1,6 meters, followed by the expansion in surface from the cavity left by the TBM tunnel up to the perimeter of the planned cavern, in a longitudinal distance equal to the length of the segments. This is why the longitudes of the caverns are designed to match with the length of the rings. Caverns A and B are planned to be excavated in full-face, while because of their dimensions, from C to I the faces are divided in order to accomplish surfaces that do not compromise the stability of the work when removed.

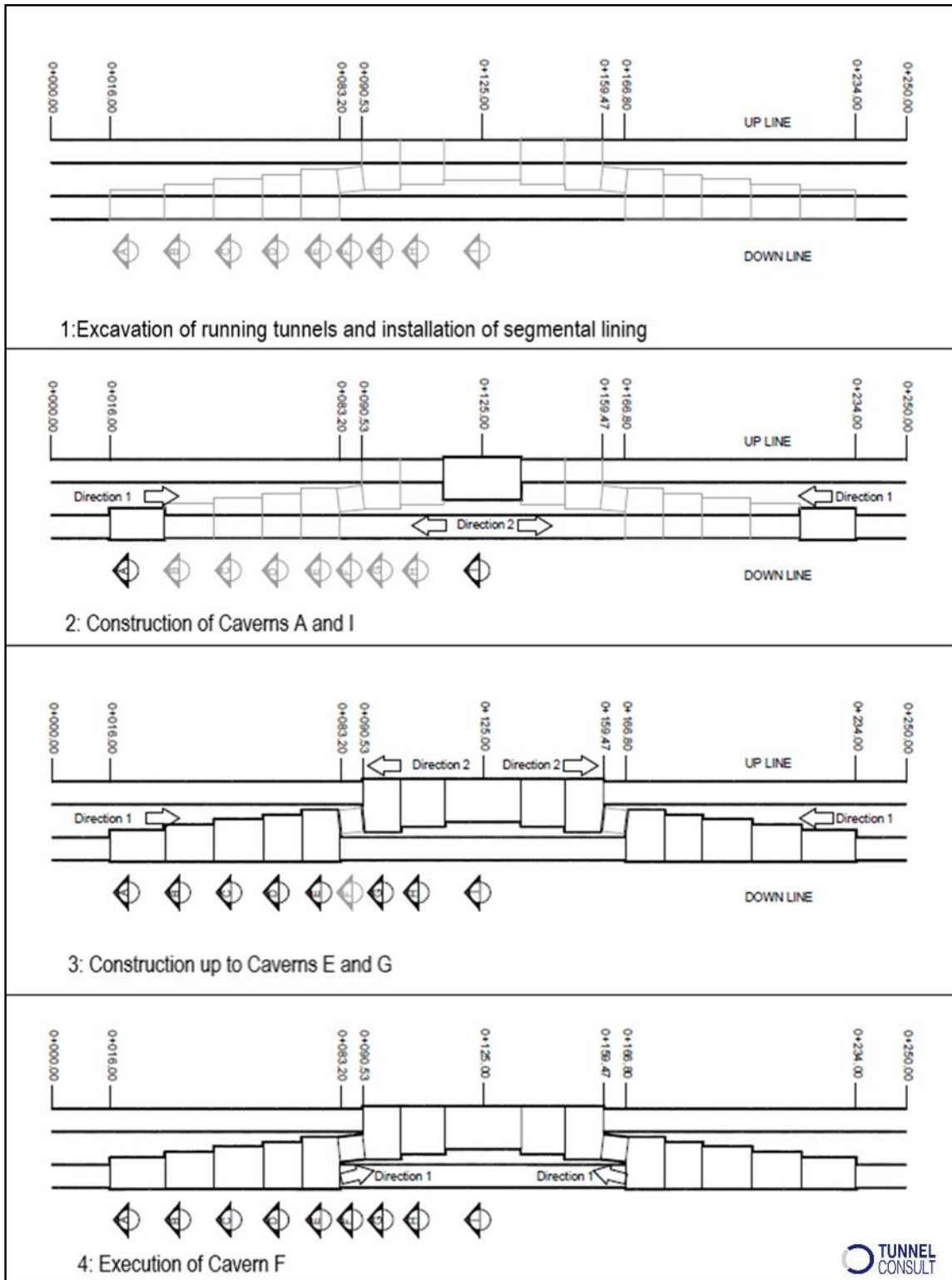


Figure 3.5-Scissor crossover construction process. Plan view.

Consequently, for caverns A and B each construction step consist in the initial removal of the ring, followed by the excavation of the remaining surface in a length equal to 1,6 meters, with the subsequent application of the initial support that consists in shotcrete, the installation of lattice girders and the a system of rock bolts in the crown. The support is determined specifically for each cavern considering the variation in the free span from one to the other.

For the rest of the caverns, the excavation begins in the section of the face that surrounds the TBM cavity with the application of the support in this part before removing the following one. Sequence shown in Figure 3.6.

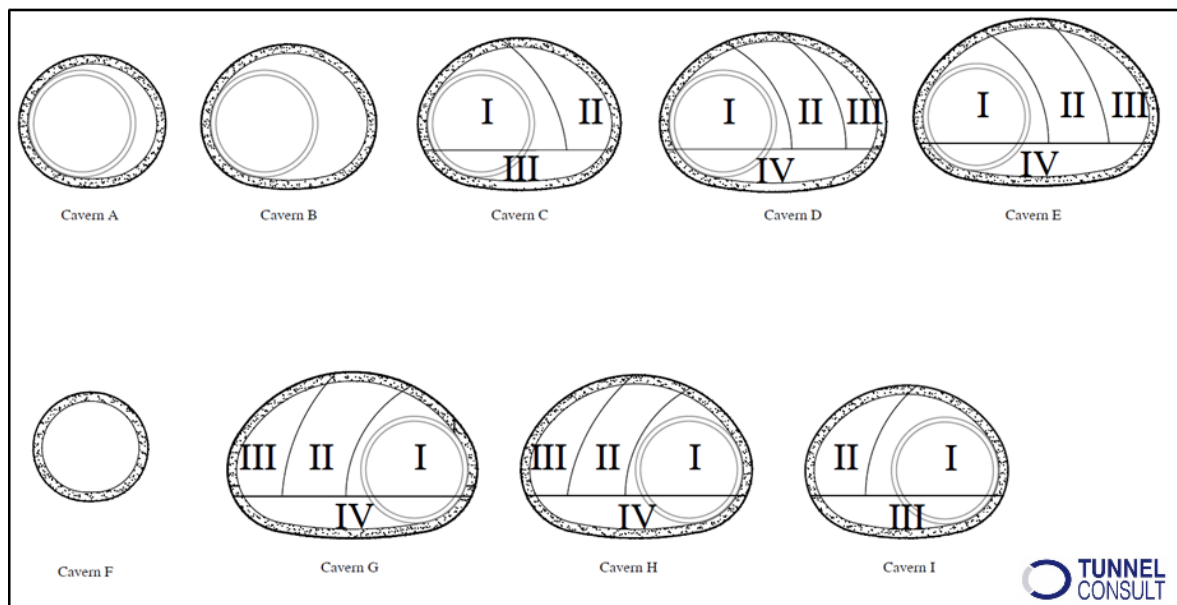


Figure 3.6-Excavation sequence of each cavern

This work continues up to cavern E in Direction 1 and Cavern G in Direction 2. At this point, from cavern E the excavation of cavern F begins with the full-face methodology with an advancement step of 1,6 meters, and the immediate application of primary support until cavern G is reached.

After this, a geotextile membrane is installed in the walls of the excavation to provide waterproofing to the structure. To end, the pouring of cast-in-place final lining is planned to be done in the same order as the cavern's excavation. This means, starting from caverns A in Direction 1 and from I in Direction 2 until caverns E and G are finished, followed by the finalization of cavern F. Considering the length of the caverns, ranging from 11 to 16 meters, it is proposed to use formworks with lengths equal to the ones of each cavern, avoiding unnecessary joints in the concrete mass. This means that the final lining of each cavern will be poured in a single stage.

3.3 Pros and Cons of the proposals

In Table 3.1 are expressed the differences between the methodologies looking to achieve a better understanding of the benefits and drawbacks that each approach comprehends. Figure 3.7 represents an overlap of the alternatives to illustrate the difference in terms of dimensions:

Big cavern crossover	Scissor crossover
Constructive procedure of the cavern(s)	
It requires the construction of an access vertical shaft and another tunnel to reach the face and allow the installation of the pipe umbrella. After this, the process becomes repetitive and capable to be industrialized in the whole crossover length.	It does not need the construction of additional structures. Nevertheless, it requires high levels of coordination between the participants of the work during the advancement because of the constant changes in the geometry and the small spaces between the running tunnels.

Cross section dimensions	
<p>The cavern has an excavation surface of 173,42 m² divided in four stages ranging from 39,98 m² to 44,89 m². Its width is equal to 19,06 m and it is 11,60 m tall. It is important to add that because of the presence of the vertical shaft, the width of the intervention has 9 additional meters.</p>	<p>The following values correspond to the range between the smallest and the biggest caverns, being these cavern A and G respectively:</p> <p>Area: 55,34 m² to 120,20 m².</p> <p>Width: 8,75 m to 14,90 m.</p> <p>Height: 7,92 m to 9,93 m</p>
Length of the intervention	
<p>The cavern is completed in a length equal to 102,88 m.</p>	<p>Considering from the point where the rails start to curve (Figure3.4), it has a total length of 250 meters. The longest cavern is 16 meters long (cavern A) while the shortest are 11,20 meters long.</p>
Modifications to the original alignment	
<p>In order to reduce as much as possible the dimensions of the excavation, approximately 100 meters before they reach the cavern the rails approximate to each other, changing the separation between them from 16,40 m to 10,84 m. This generates more interferences between the excavated tubes with increasing surface disturbances. Additionally, more curves are added to the alignment with the consequently loss of performance in terms of speed.</p>	<p>To make possible the accommodation of the scissor geometry between the running tunnels, the radius of rail curves need to be enlarged from the original solution that used the minimum value of 190 m to 250 m.</p>

Potential risks	
<p>Due to the large dimensions of the excavation, important surface disturbances are expected in terms of vertical displacements, key parameter to control in urban areas.</p>	<p>Because of the geometry of the method, the space available to accommodate the caverns between the TBM tunnels is reduced and slender columns of ground are created around cavern F (Figure 3.8), that in advance seem to be weak points of the project.</p>

Table 3.1-Pros and Cons of the proposals

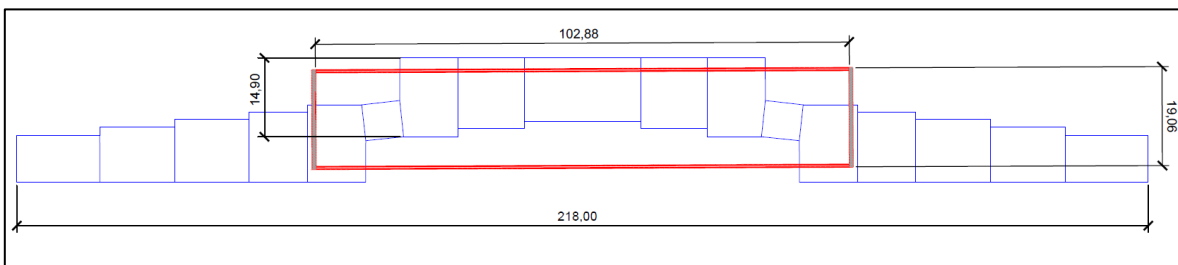


Figure 3.7-Alternatives confrontation

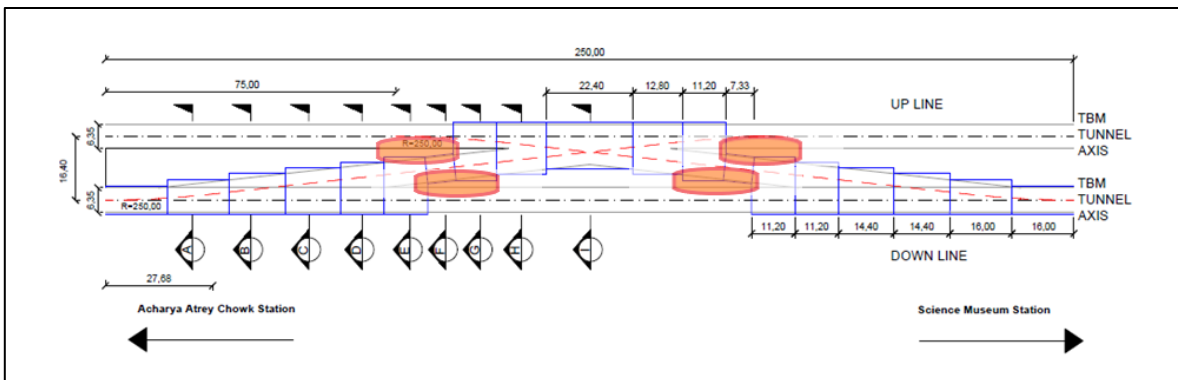


Figure 3.8-Potential weak points

Chapter 4: Excavation methods

In the present chapter the excavation methodologies proposed for the materialization of the underground structures required in the project are explained: the caverns are planned to be excavated with the Conventional Tunneling Method, meanwhile for the twin running tunnels a slurry TBM is used. These methodologies described for the scissor crossover are the same used in the actual project for Mumbai Metro Line 3.

4.1 Conventional Tunnelling

It is defined as the construction of underground openings of any shape with a cyclic construction process (ITA Working Group, 2009) composed by:

- the excavation, done with drill and blast methods or basic mechanical excavators;
- the collection of the muck, or simply mucking;
- the installation of the primary support.

This is one of the most popular methods for tunnel construction, principally due to its flexibility during the construction and its capacity to be adapted to different ground conditions. Conventional tunnelling allows the creation of complicated shapes when spaces are reduced or when the cross section presents variations, like in the case under study.

Part of the reliability of the method is based on the fact that it requires rigorous geotechnical investigations of the site to accomplish a faithful description of the ground. Geological, hydrogeological and geotechnical tests provide crucial information for the determination of the geometry, the length of the advancement that will be momentarily unsupported, the election of the excavation tools, the characteristics of the structural materials and the definition of eventual ground reinforcements.

The definition of the first phase support for this project is based on the concepts established by the New Austrian Tunnelling Method(N.A.T.M.), whose philosophy relies on using the

inherent strength of the surrounding ground to contribute to the stability of the tunnel(von Rabcewicz, 1962). This allows the use of a flexible and light initial support that is directed to enable the rock to support itself. Controlled deformation of the primary support is allowed in order to mobilize the ground strength and achieve a coordinate behavior between the surrounding material and the lining.

The first phase support is generally constituted by a layer of shotcrete that can be reinforced with a wire mesh or fibers of different materials, a system of steel arches that are especially designed for the geometry of the section placed with an interval between 0,5 and 2m, and it can be complemented with the installation of rock bolts that transmit loads to the ground when the edge of the excavation presents lousy characteristics.

This gives an economic advantage in terms of materials respect to other alternatives but also has its own harms. It is a slow methodology with rates of 3 to 5 meters per day and requires high levels of coordination, cooperation and communication between the different parts in the construction sequence. Because safety is the main priority, the surfaces excavated in every stage rarely go over 50m² and immediately after the excavation the support is placed, making the process safe but slow.

The tools chosen to perform the excavation depend on the material characteristics and the location of the work. For hard rock, drill and blast procedures are always a viable option, but the high vibrations that are produced that can affect the surface population must be considered. Alternatives when the rock's Uniaxial Compressive Strength is lower than 120 MPa are punctual tools such as road headers or high impact hammers. These methods reduce vibrations significantly and avoid the generation of fumes, with a performance similar to the one obtained using explosives. For soft ground, conventional excavation shovels are enough to create the geometry of the section, with enough flexibility to conceive complicated shapes.

The excavation procedure is conceptually the same regardless of the tool used. For the case of study, where it is proposed to use a punctual excavator, the steps to follow are basically:

excavation of one part of the section, muck charge and remove from the tunnel and placing of the correspondent support. In case of using drill and blast techniques, steps regarding the placement and ignition of the explosives and fumes ventilation must be considered.

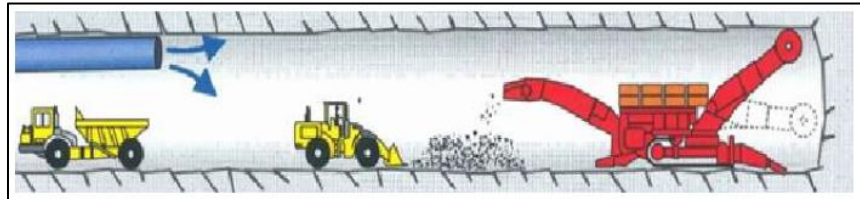


Figure 4.1-Conventional tunneling. Excavation with rockheader.

There are different ways to divide the section for the sequential excavation depending on the project characteristics, but a tunnel face is generally composed by a top head or crown, a bench and an occasional invert. The concept is to create shapes with a surface small enough to excavate them and ensure its stability while the corresponding support is being placed.

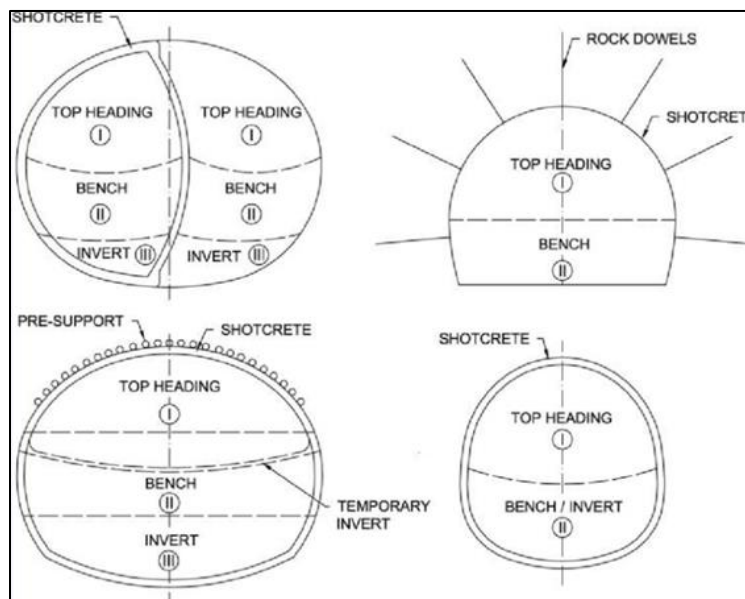


Figure 4.2-Examples of excavation sequences

4.2 Mechanized tunneling: slurry machine

4.2.1 General aspects

For the case of Line 3 of the Mumbai Metro a hard rock slurry shield was chosen to bore the running tunnels. This kind of boring machine uses a pressurized fluid to support the face. The pressure in the face must be able to counterbalance the influence of the ground above the excavation and the effect of the groundwater that can be encountered.

The suspension fluid is generally a mix of water and bentonite called slurry, that has good plasticity and a swelling capacity allowing the generation of an impermeable film-filter cake sealing the face from the entrance of water (D. Peila, personal communication, 2019). The mechanical properties and viscosity of the mix are adapted to the ground requirements and must be continuously controlled. It is crucial to permanently monitor the pressure of the face, because if the effect of the ground overpasses the resistance of the face, important volume loss can be produced translating this into considerable superficial displacements.

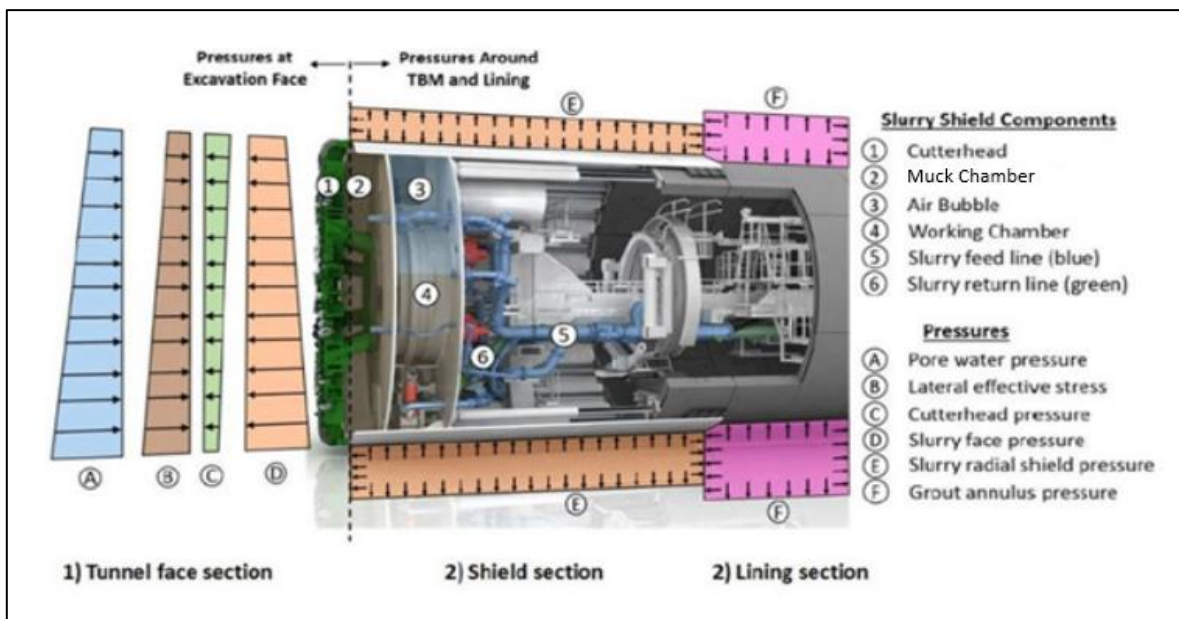


Figure 4.3-Pressure balance must be ensured in the face

The cutterhead design varies depending on the project, as the tools used to excavate the ground. Behind it, there is an excavation chamber with a bulkhead that separates the chamber itself (area under pressure) from the rest of the TBM and the already built tunnel.

The excavation chamber is divided in two: a muck chamber, filled with the slurry and the debris of the ground just before the cutting wheel; and the working chamber where the air bubble for pressure control is placed (Figure 4.3)(Maidl, 2011).

In the excavation chamber a mass balance takes place composed by three terms: the muck coming from the excavated ground and entering through the openings of the cutting head, the slurry composed by water and fresh bentonite pumped from outside and the slurry with debris suspension that is pumped out to the separation plant.

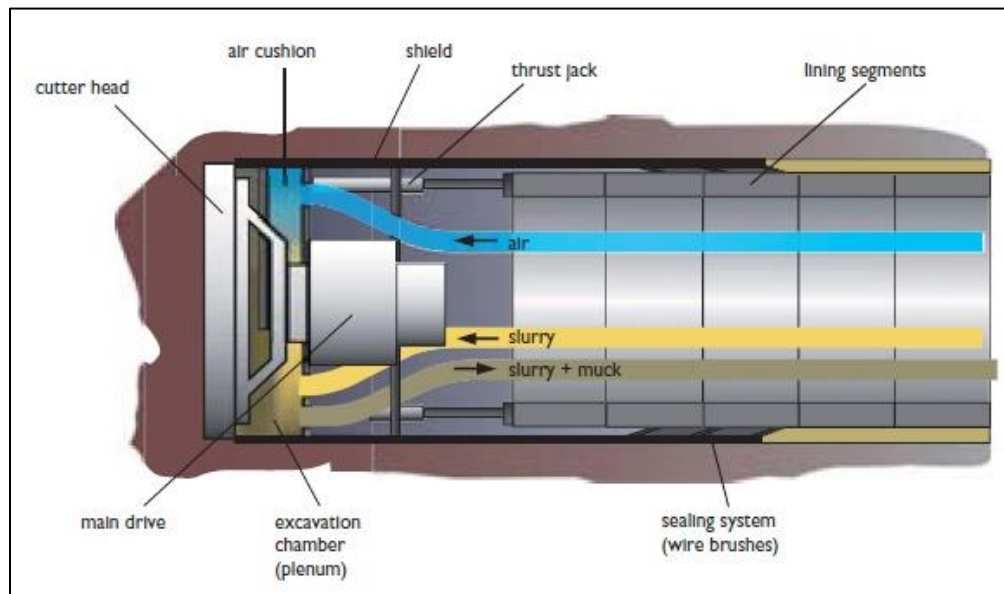


Figure 4.4-Parts of a slurry machine

The machine is also equipped with a stone crusher in the bottom of the muck chamber to use when rock blocks are encountered. The slurry with the excavated soil in suspension is pumped out towards the Slurry Treatment Plant (STP) by means of a pipe that connects directly the TBM and the STP, where the debris are separated from the slurry with the aim

of reusing the bentonite contained in the suspension. This procedure consists in the initial separation of grains bigger than 5mm through sieves, passing to smaller sieves or by cycling separation for particles bigger than 75 μ m to end with chemical separation with flocculant additives.

The lining is installed using an erector placed inside the TBM, materialized with precast concrete segments that form a ring in the perimeter of the excavation acting as support and waterproofing the tunnel, ensured by the gaskets placed in the four contact faces around each segment. The advancement of the machine is done through hydraulic jacks that apply thrust force to the precedent closed ring. This force is the most important one to be considered in the calculation of the concrete segments.

4.2.2 Machine used in the project

Speaking particularly of the construction of the Mumbai metro Line 3, the machine has a 6,35m excavation diameter and was used to excavate 4.600m of tunnel. The machine was constructed by the Robbins Company.

The depth used for the calculations is equal to 25m, adopting a pressure at the face up to 4 bar, and achieving an instantaneous speed of advancement of 50mm/min. The cut of the rock is performed by a total of 42-disc cutters of 17" (267kN) with a spacing of 86mm in the face. The spaces in the face allow a maximum size of rock boulder of 275mm.

To control the possible inflow of water into the tunnel, in the tail shield a grease injection system is available that provides water-tightness to the steel bristle brushes lines sealing the gap between the outer side of the segmental lining and the inner side of the tail shield.

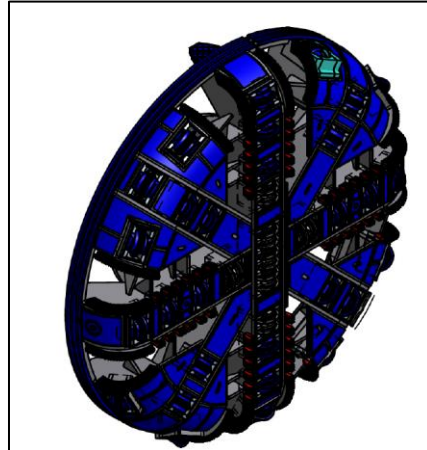


Figure 4.5-17” discs hard rock Cutterhead

Because of the rock’s abrasiveness and the long distance that the machine has to cover, the cutting-wheel tools have to be frequently replaced. There are two ways to do this: one is to change the tools when the machine is crossing a station or is inside a treated space that allows to work with no pressure. Alternatively, the replacement must be done under hyperbaric conditions by specialized operators (divers) and the transition between pressurized and non-pressurized areas requires compartmented and hermetic devices called manlocks. In this case, the TBM has available two manlocks optimizing the time required to change the tools.

The injection of the suspension fluid is done by the pumps with a maximum rate of $1000\text{m}^3/\text{h}$ in excavation mode and a maximum muck extraction of $1150\text{ m}^3/\text{h}$ in the same mode. The air bubble in the excavation chamber can be regulated with a precision of $\pm 0,05$ bar. The slurry shield is also equipped with a stone crusher that can manage boulders with a diameter of 400mm.

The shield is articulated and formed by three bodies, prepared to follow correctly the curves in the alignment and to correct eventual driving imprecisions. The lining is materialized by universal rings with a length of 1,6m and are composed of 5 segments and a closing key segment with 16 possible positions and a thickness of 275mm.

Chapter 5: Geotechnical analysis of the site

5.1 Mumbai Geology

The entire area is placed in the Deccan Basaltic formation, which is one of the largest volcanic features on the planet and started its formation 66 million years ago, at the end of the Cretaceous period. Basalts with different characteristics and weathering conditions are encountered along the formation, most of them are either compact (with no gas cavities), or amygdaloidal with gas cavities filled with secondary minerals. Zeolites are the commonest secondary minerals filling these cavities, but in some cases also silica and calcite are encountered. To a lesser degree, vesicular basalts were found; this means that they have vessels generated by gas or water but are not filled.

The volcanic flows found are mostly horizontal, showing in very particular places westerly dips ranging between 5° and 12°. Faults are rare to find in the whole area, but vertical fractures are widespread in the West area of the Deccan trap, where on the surface it is common to find Basaltic flow underlain beds formed by ash and laminated shale. In the East part there are also ash beds in the base overlain by Basalt, and in this area there are hills that show breccia formations in the top with basaltic fragments embedded in the rock.

In the west coast of Mumbai sandy and rocky beaches formed as a result of the intense wave action of the Arabic Sea. On the Eastern coast the wave activity is calmer, allowing the formation of unconsolidated clay layers underlain the sand. Because it was formed as a consequence of silting over the geological years, these clay layers are unconsolidated and very soft in nature.

5.2 Crossover Geology

To characterize the zone of interest, a total of six boreholes are available and from them a geological profile was designed. Furthermore, with these samples the different materials encountered have been identified and are used to obtain the required information to estimate the ground parameters. In this section the documents prepared to define the geological profile for the original project are analyzed and in the next chapter the particular considerations taken for the numerical model will be explained (section 6.4.).

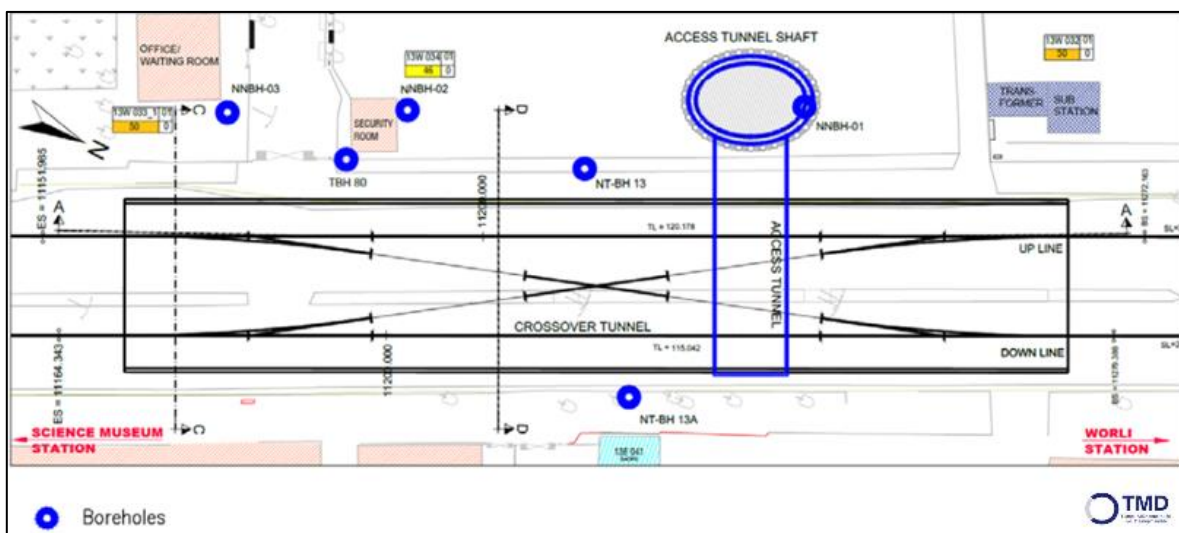


Figure 5.1-Boreholes location in the original project

The geological profile designed for the original project is presented in Appendix 2. The ground is divided in an upper residual soil layer, over a fill and clayey layer underline a Breccia bedrock that changes its conditions along the crossover length.

The fill, consisting of brownish soil with boulders and pebbles was encountered from ground surface in the boreholes. Beneath it, a clayey layer is encountered, consisting of brownish silty clay with gravels, founded at a depth between 6.0m and 9.0m below ground surface.

The upper level of the bedrock is affected by weathering, showing a clear discoloration. The depth of discoloration varies between 10.5 to 15.0m. In this layer, the following geotechnical units are defined, according strength and degree of fracturing:

- Weathered Grade Five (WG-5): breccia rock with RQD values below 10 and complete discoloration due to weathering.
- Weathered Grade Four (WG-4): breccia rock with RQD values from 10 to 40 and complete discoloration due to weathering.
- Weathered Grade Three (WG-3): breccia rock with RQD values from 40 to 75 and complete discoloration due to weathering

Beneath that level, non-discolored breccia rock is encountered. The Geotechnical units defined at that depth are as follows:

- Grade Five (G-5): breccia rock with RQD values below 10 and no-discoloration.
- Grade Four (G-4): breccia rock with RQD values from 10 to 40 and no-discoloration.
- Grade Three (G-3): breccia rock with RQD values from 40 to 75 and no-discoloration.
- Grade Two (G-2): breccia rock with RQD values from 75 to 90 and no-discoloration.

The information of the boreholes is presented in the following table:

Borehole N°	Northing	Easting	Borehole termination depth (m)
NNBH-03	2101608.13	270450.031	30
TBH-80	2101622.12	270448.91	20
NNBH-02	2101625.65	270441.143	25
NTBH-13	2101647.18	270432.06	35
NTBH-13A	2101661.02	270465.83	38.2
NNBH-01	2101664.37	270421.749	30

Table 5.1-Boreholes information

To obtain the required information, different tests were performed on these samples, in particular:

- Standard Penetration Test (SPT);
- Pressure meter Test (PMT);
- Permeability test

Additionally, some laboratory investigations were carried out to the soil samples founded in the boreholes to establish Atterberg limits, dry density, porosity and water abortion.

From samples TBH-80 and NTBH-13A important data was obtained after performing the following tests:

- Direct Shear Test (UU)²;
- Triaxial Test (UU);
- Consolidation Test;
- Unconfined Compression Test;
- Point Load Test
- Brazilian Test.

With the data obtained, the different layers are characterized as follows:

- Fill: consisting of brownish soil with murrum, pebbles and boulders was encountered from ground surface in all the 6 boreholes. The thickness of this layer is between 0.5m and 3.0m.
- Clayey Layer: consisting of brownish silty clay with gravels, encountered up to a depth between 5.5m and 9.0m below ground surface. Based on Standard Penetration Tests (SPT), consistency of cohesive soil (clay) was typically stiff. Composition and description of this layer differs from borehole to borehole. SPT carried out in this material range from very low values ($N_{spt} = 2$ in borehole NNBH-03) to medium values ($N_{spt} = 22$ in borehole NTBH-13).
- Breccia Rock: at a depth of 5.5m to 9.37m below existing ground surface in the boreholes. In this layer, the rock core recoveries varied typically between 54% and 97%, while the Rock Quality Designation (R.Q.D) ranged between Nil and 55%. The upper level of the bedrock is affected by weathering, showing a clear discoloration. The depth of weathering discoloration varies up to between 12.5 to 14.0m.

As it was said before, the weathered part of the rock mass was divided in three classes, while the non-discolored part was divided in four classes. The information regarding class 3 and 4 of this last group is going to be used to define the geotechnical parameters that consequently will work as input in the FEM models.

5.3 Groundwater and permeability

Groundwater levels have been measured in each borehole and have been recorded during drilling operations. Furthermore, stand-pipe piezometers have been installed in two of the drilled boreholes, monitoring the ground water level oscillations.

Whereas in soils hydraulic conductivity is mostly controlled by the size, shape and arrangement of its voids, in rock masses the conductivity depends on the aperture, spacing and infilling characteristics of its discontinuities.

The Lugeon test (also called Packer test) is widely used to estimate average hydraulic conductivity of rock masses. The test is a constant head type test that is performed along an isolated portion of the investigated borehole. Water at constant pressure is injected into the rock mass through a slotted pipe bounded by pneumatic packers. The test is conducted in five stages, with a particular water pressure magnitude associated with each stage. A single stage consists of keeping a constant water pressure at the test interval for 10 minutes by pumping as much water as required. The hydraulic conductivity is expressed in terms of the Lugeon value, which is empirically defined as the hydraulic conductivity required to achieve a flow rate of 1 liter/minute per meter of test interval under a reference water pressure equal to 1Mpa. If the material is homogeneous and isotropic, one Lugeon is equal to $1,3 \times 10^{-5}$ cm/s. In the following table different conditions for the rock mass discontinuities are associated with Lugeon values:

Lugeon range	Classification	Hydraulic conductivity (m/s)	Condition of rock mass discontinuities
<1	Very low	$<1 \times 10^{-7}$	Very tight
1-5	Low	$1 \times 10^{-7} - 6 \times 10^{-7}$	Tight
5-15	Moderate	$6 \times 10^{-7} - 2 \times 10^{-6}$	Few partly open
15-50	Medium	$2 \times 10^{-6} - 6 \times 10^{-6}$	Some open
50-100	High	$6 \times 10^{-6} - 1 \times 10^{-5}$	Many open
>100	Very high	$>1 \times 10^{-5}$	Open closely spaced or voids

Table 5.2-Lugeon Criterion (Quiñones-Rozo, 2010).

After performing permeability tests to the samples at different depths, it can be stated that the breccia formation represents a fractured aquifer with a mean permeability of 1.5×10^{-6} m/s; all tests resulted within a permeability range between medium and low permeability. A single test was carried out in clayey soil and the obtained permeability in this geotechnical unit was 1.59×10^{-8} m/s.

The groundwater level has been measured in the samples taken, obtaining the following results:

Borehole N°	Water table below Ground Level	Date of measurement
NNBH-03	8.25	16/10/2018
TBH-80	15	6/12/2012
NNBH-02	8.63	17/10/2018
NTBH-13	6.1	26/7/2017
NTBH-13 ^a	8	3/3/2017
NNBH-01	8.74	17/10/2018

Table 5.3-Water Level

Chapter 6: 3D Models

6.1 Introduction to Numerical Analysis

6.1.1 FEM models for geotechnics

Even though numerical analysis for structure calculation has been widely studied, it was not until the last 40 years that its application in geotechnics began, probably because of the particularities that every geotechnical project comprehends, and the uncertainties that exist whenever an underground construction is planned.

The aim of these models is to achieve a faithful representation of the real problem with the computational resources available in order to estimate as much as possible the effects that the construction of the structure will produce to the surrounding ground and how the constructive materials will react. In geotechnical analysis, displacements are usually the primary variable to study because of their influence on the surface structures.

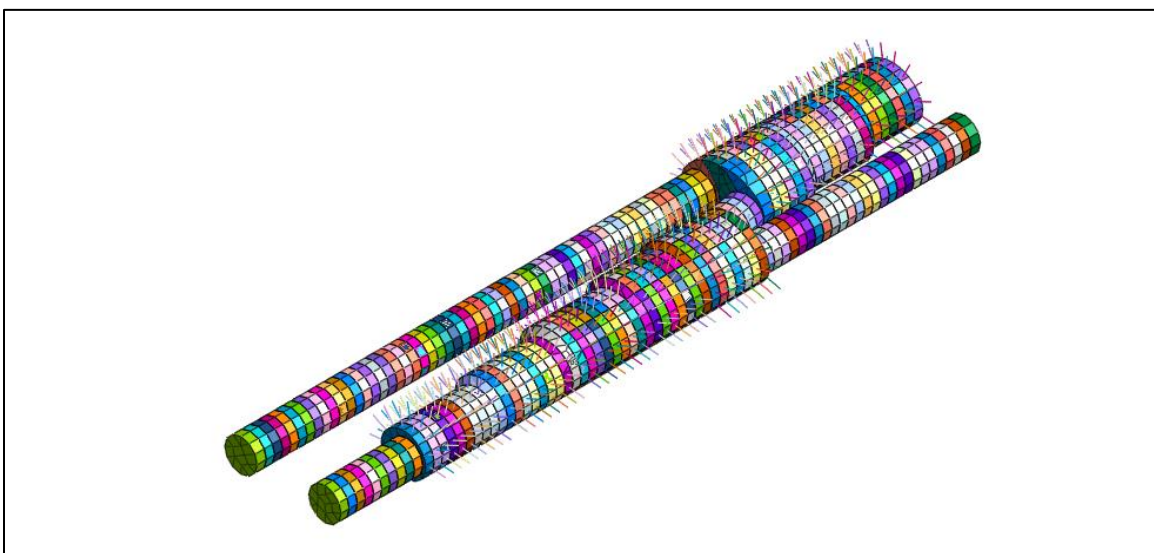


Figure 6.1-Scissor Crossover with Midas GTS NX

In Finite Element Methods, the problem is subdivided into discrete elements which provide a physical approximation to the continuity of displacements and stresses within the continuum (Potts & Zdravkovic, 2001). The governing equations are written and solved

exactly for points called nodes, through which the adjacent element is connected. Hence, the Finite Element Method gives an exact solution to a differential approximation of the problem.

Generally speaking, a theoretical solution must satisfy Equilibrium, Compatibility, material Constitutive behavior and Boundary conditions.

The evaluation of the force equilibrium, either internal or external, is done through the analysis of the stresses calculated in the model. The magnitude and direction and the way that varies inside the continuum indicates how the forces are transferred.

When talking about compatibility, it can be separated into two groups: physical and mathematical compatibility. The first one is referred to avoiding overlapping and holes in the continuum. This means that the elements that form the geometry must remain connected after a deformation and the accumulation of more than one element in the same space must be avoided. This can be expressed mathematically through the concept of strains. These, defined as variations in the dominion of the functions that represent the model's deformations, must exist in the three directions and be continuous to at least the second order to allow the displacement field to be compatible.

The constitutive behavior describes the stress-strain response of the soil. It usually takes the form of a relationship between stresses and strains, providing a link between equilibrium and compatibility. Young's modulus and Poisson's ratio are values that generally appear in these kinds of expressions. The constitutive behavior can be expressed either in terms of total or effective stresses, so the pore fluid pressure takes relevance.

To define boundary conditions means to establish rules in the borders of the domain that must be fulfilled when solving the problem's equations. So, a solution to a boundary problem will be represented by the solution of the differential equations of the model that respects the boundary conditions at the same time.

The finite elements method involves different steps:

- Discretize the elements, where the geometry represented in the model is replaced by an equivalent finite element mesh, which is composed by small regions called finite elements. For 2D analysis, these shapes are generally triangular or quadrilateral and for 3D models their three-dimensional equivalents are used (tetrahedron and cubes). In the case of Midas GTS NX also exists the hybrid mesh, that is a combination of tetrahedral and hexahedral elements united by a pyramidal shape allowing a better fit for difficult geometries.
- Approximate the primary variable, not only establishing displacements as the critical unknown to obtain, but also defining how are going to vary throughout the domain under study satisfying compatibility conditions. Stresses and strains are considered as secondary variables.
- Define the element equations that govern the deformational behavior of the elements of the mesh combining compatibility, equilibrium and constitutive conditions obtaining a global set of equations. This procedure provides a unique global stiffness matrix to solve the problem as a whole.
- Transform distributed forces or established displacements in equivalent nodal forces at the boundaries.
- Solve the global equations by defining the unknowns of the system, given by the number of nodes times the unknowns of each node.

6.1.2 3D Models

Until the beginning of this century, most of the numerical models were done in two dimensions. With plain strain, plain stress or axisymmetric conditions, important simplifications were taken in order to simplify the unknowns of the model and allow an acceptable representation of the reality. However, most geotechnical problems are three-dimensional and although in many cases the 2D representation could give important information, in some cases it is necessary to treat the problem with three directions. Mathematically, this implies that three components of displacements must be calculated for

each node in the mesh. In computational terms, this implies an important increase in the stiffness matrix size that needs to be inverted to solve the equations.

This is translated into excessive calculation times, when it was possible to create the model. But in the last years and thanks to the computational advancements, it is possible to work with three dimensional models with a good geometric accuracy obtaining more reliable results. Most of these software use iterative numerical methods to solve the stiffness matrix, rather than direct methods. These techniques are based on avoiding the use of the empty terms of the matrix, making the calculations of the displacements much lighter. Jacobi Iteration or Gradients Methods are examples of this technique.

6.2 Software

6.2.1 Midas GTS NX

GTS NX (MIDAS Information Technology, 2019) is a simulation program developed for the evaluation of soil-structure interaction based on the finite element method. This software allows the modeling of all kinds of scenarios like tunnel construction, retaining walls, landslide stability, underground water flow, deep structural foundations and more.

Settings for all types of field conditions can be simulated using non-linear analysis methods (such as linear/non-linear static analysis, linear/non-linear dynamic analysis, seepage and consolidation analysis, slope safety analysis) and various coupled analysis.

It is versatile when it comes to the creation of the geometry, providing intuitive tools based in other CAD programs or allowing to import files from a different software. It is also provided with a wide library of constitutive models to represent the behavior either of the ground or the different structural elements in the model.

Giving different options when generating the mesh, provides the designer more freedom to ensure a good behavior of the finite elements and a faithful representation of the geometry. With the Stage Wizard added in more recent versions the organization of a model based on

a construction stage analysis becomes easier to coordinate and the identification of circumstantial problems results faster.

GTS NX provides a variety of options to represent the stresses, strains, displacements and forces obtained in the numerical model. 3D vectors, stresses diagrams, result tables and graphs are possible outcomes representations that can also be exported in different formats.

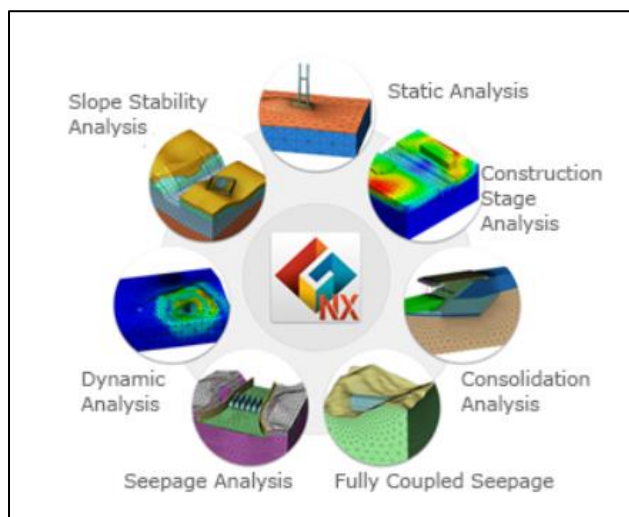


Figure 6.2-Midas GTS NX

6.2.2 Software validation

In order to ensure the reliability of the results of the numerical model done for the scissor crossover, a small simulation is presented and their results will be compared with an analytical formulation. To this aim, only the excavation of a cavern is considered, excluding the construction of the TBM tunnel.

The idea is to calculate the superficial settlements produced by the excavation of one of the caverns of the model (cavern D) with Midas GTS NX and confront the maximum value with the theoretical analysis proposed by Moretto and Peck in 1969 and studied in Spain (Chamorro Ramos, 2005). This theory relates the deformation produced in the surface with an inverted Gaussian distribution, defined by the equation:

$$Sv = S_{max} * e^{\frac{-x^2}{2i^2}} \quad (6.1)$$

Where Sv is the vertical settlement, S_{max} is the maximum settlement produced in the tunnel axis, x is the horizontal distance from the tunnel axis and I is the horizontal distance from the tunnel axis to the inflection point of the curve.

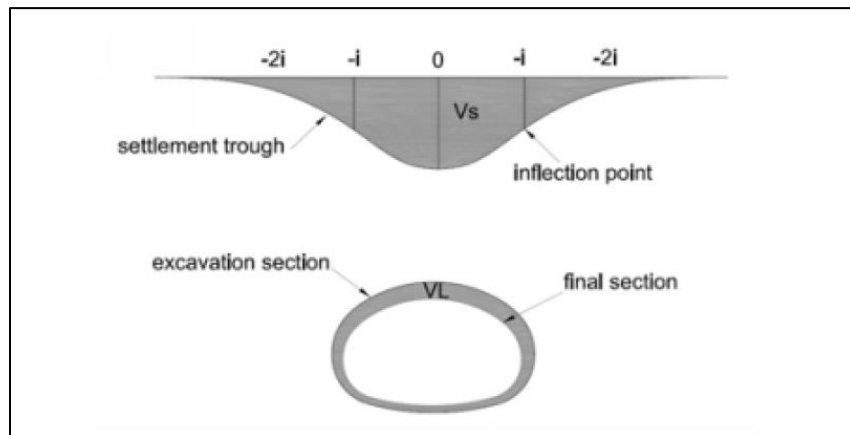


Figure 6.3-Settlement curve. (MORETTO et al., 1969)

Integrating the area under the curve the following expression is obtained:

$$S_{max} = \frac{V_s}{i * \sqrt{2\pi}} \quad (6.2)$$

The distance to the inflection point is related to the depth of the excavation and the ground characteristics. Many studies were done to achieve a good estimation of this value, but for this case of analysis the expression chosen is the one proposed by New and O'Riley in 1982. They proved that I can be expressed as a linear function:

$$i = K * z_0 \quad (6.3)$$

The value of K depends exclusively on the ground properties. These authors have proposed values from 0,1 to 0,3 for rocks and granular soil, and 0,5 for clays and soft soils. Because of the good characteristics of the rock and the influence of the clayey layer the value of 0,3 is used.

The volume loss depends on the ground conditions and the excavation method used. In the bibliography there is not much information about volume loss in rock excavated with sequential methods. For the case of hard clays and sands a value of 0,1% was measured in the field with the same excavation procedure, so considering the good properties of the material (class III breccia) a value of 0,07% is taken.

It is commonly accepted that this volume loss is equal to the superficial depression:

$$V_L \sim V_S$$

So, to obtain the maximum settlement over the tunnel axis the value of volume loss must be obtained. The surface of the face of the actual tunnel is equal to 103,82 m², measured with the software.

Then, the maximum settlement is obtained:

$$S_{max} = \frac{103,82m^2 * \frac{0,07}{100}}{0,3 * 20m * \sqrt{2\pi}} = 0,00483m = 4,83mm$$

For the software simulation, the excavation is done following a sequential procedure as follows, for a length equal to 11,2 meters:

- Initial Stage: The ground is at its natural state, displacements are cleared.

- Stage 1: Excavation of section I with an advancement of 1,6m.
- Stage 2: Colocation of shotcrete support and bolting in the excavated section.
- Stage 3: Excavation of section II with an advancement of 1,6m.
- Stage 4: Colocation of shotcrete support and bolting in the excavated section.
- Stage 5: Excavation of section III with an advancement of 1,6m.
- Stage 6: Colocation of shotcrete support and bolting in the excavated section.
- Stage 7: Excavation of section IV with an advancement of 1,6m.
- Stage 8: Colocation of shotcrete support in the excavated section.

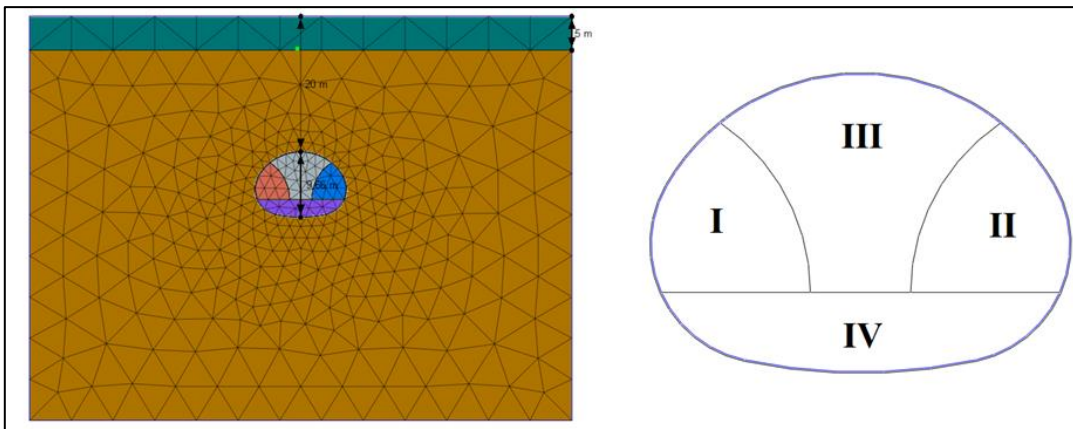


Figure 6.4- Software verification. Cavern D

As it can be appreciated in the results, the maximum superficial displacement is of 4,22mm, presenting higher values in the surroundings of the excavation. Comparing this value with the calculated using Peck's formulation, it can be said that both methods of calculation of the maximum superficial settlement on the tunnel axis present almost the same result, with a variation of ± 1 mm.

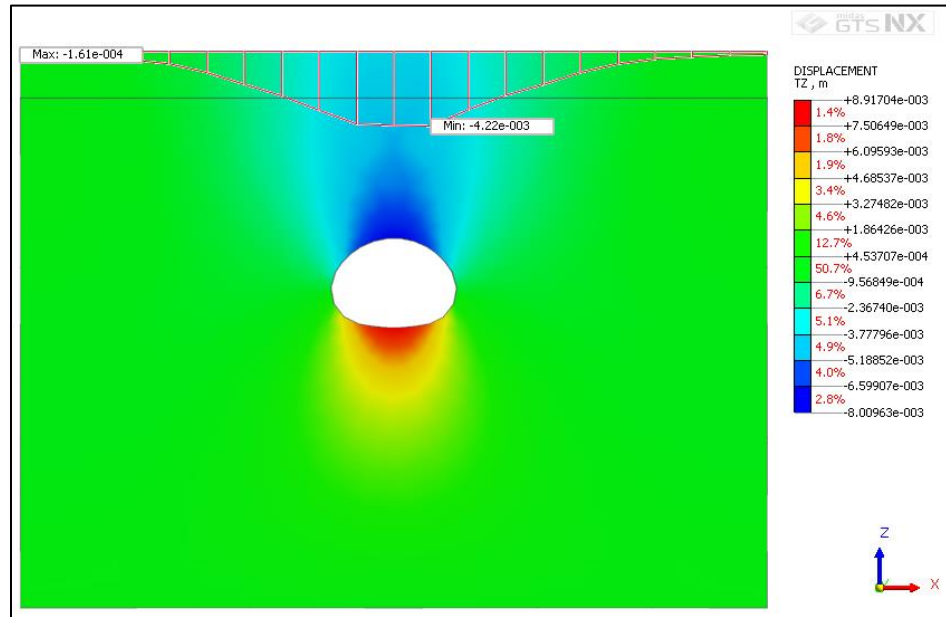


Figure 6.5-Cavern D model results

6.3 Geometry

6.3.1 Representation of the project

As presented in section 1.2, the project comprises the construction of 17 caverns with widths ranging from 8 to almost 15 meters and variable height that follow the path of the diverging tunnel with the aim of minimizing as much as possible the excavated volume. The running tunnels excavation diameter is equal to 6,35 meters supported by segmental rings with a length of 1,6. Due to the fact that to start the excavation of the caverns the segment must be removed, their length has been chosen as distance of advancement, so the lengths of the caverns were thought to respect this distance.

The total length of the crossover is equal to 250m, being symmetric in the direction perpendicular to the movement of the trains at the center of Cavern I. This is why in the model only half of the geometry is represented, saving computational resources avoiding the calculation of results that would not add any additional information.

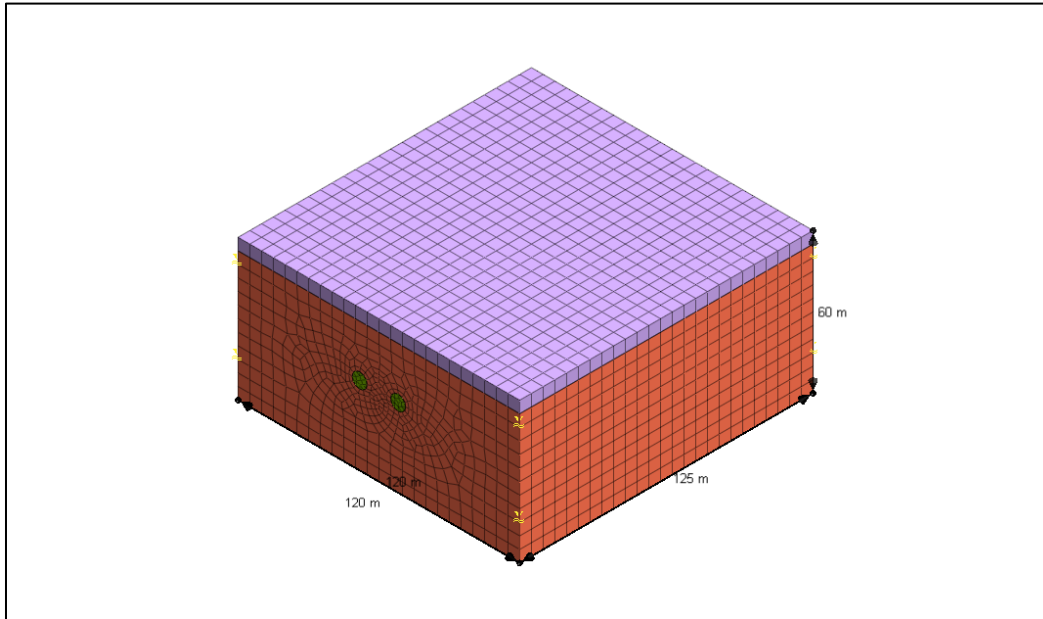


Figure 6.6-Model's domain

The size of the domain was thought to avoid interference of the boundaries in the result and give the ground enough space to develop stresses and displacements correctly. From the bottom of the excavation additional 30 meters are added (3 times the height of the caverns approximately) and the total width of the model is 120m, remembering that between the tubes the distance is equal to 16,40m.

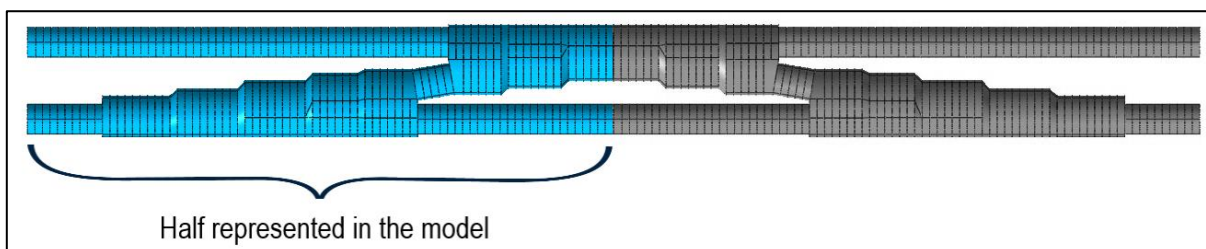


Figure 6.7- Part of the model represented.

To discretize the geometry designed in the model, the hybrid mesher was chosen because of its capacity of adapting to complicated shapes and versatility. For all the excavated parts of the ground (TBM tubes and caverns) and their corresponding 2D supports, the size of the elements is equal to 1,6m as the length of advancement of the excavation, creating a mesh

correlated to the excavation sequence. For the surrounding ground, the element size is of 5m in order to reduce the number of nodes in the parts of the model where results are less important and to match with the thickness of the overburden layer.

Also, because of the tangency in the transition from one cavern to the next one, imperfect faces were created that give problems to the software to create appropriate meshes. To solve this, in the sections where the caverns changed sizes a transition section was created to ensure the continuity of the solid.

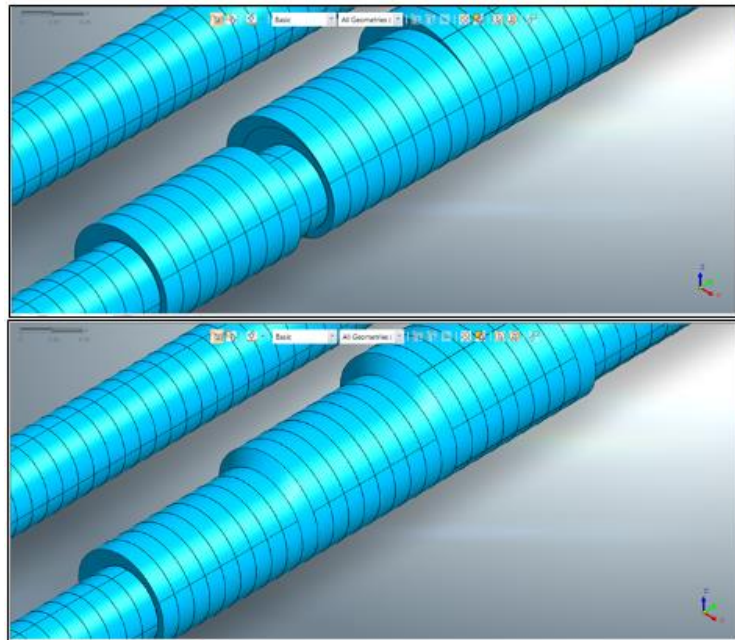


Figure 6.8-Transition Section problem and solution

6.3.2 Load and boundaries definition

The only load considered in the calculation is the ground's self-weight, represented in the model as a static load produced by gravity acting on the elements in vertical direction, defined by a unit vector.

Regarding boundary conditions, Midas works with a “Degree of Freedom” (DOF) constraint system that constrains the displacement of an arbitrary node or the DOF component when merging elements with different DOF’s for each node. Because of the domain’s dimensions, constraints are placed where there is nearly no change in stress or displacement due to the excavation.

The rules are created using the “Auto-constraint” function, restricting horizontal movement of the model’s walls and all displacements in the bottom (vertical and horizontal). It is important to restrict horizontal displacements at the bottom of the model because the excavation is not symmetrical in the vertical axis. The top of the model is free of constraints.

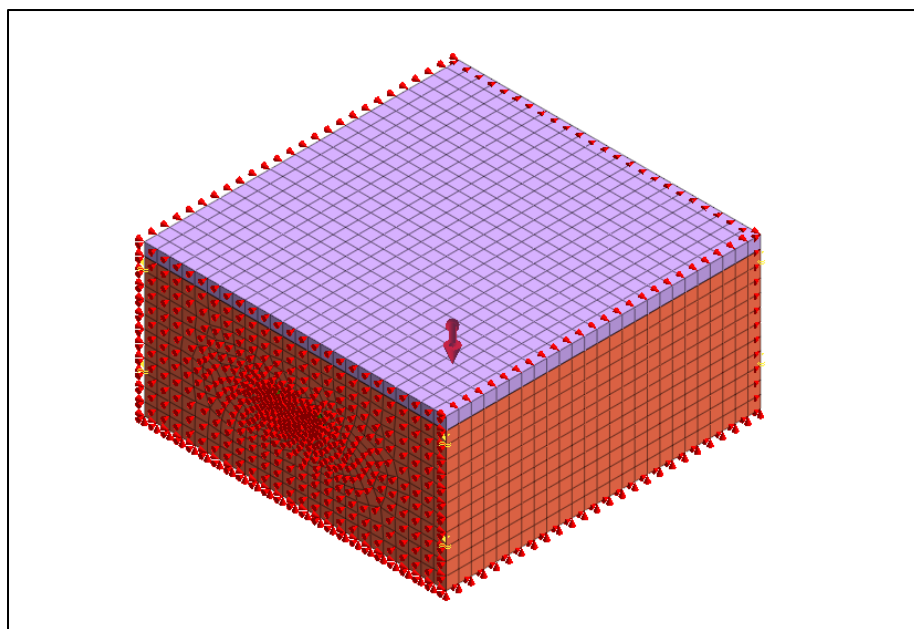


Figure 6.9-Model’s loads and constraints

6.4 Ground Characteristics

As presented in section 4.2., the geological profile of the zone of interest shows an upper layer of fill, followed by a clayey layer over a Breccia bedrock. Because the interest is centered in the rock’s behavior, in the model the two first layers will be merged in one called “Overburden” with a thickness of 5 meters.

To study how the scissor crossover responds to different ground characteristics, two models will be created with the rock mass represented as a homogeneous formation. To define their properties, information of class III and IV breccia rocks founded in the area will be used, with the aim of comparing results of a stable rock with the output of a more damaged material.

6.4.1 Failure Criteria

To represent the ground behavior, a Mohr-Coulomb model will be used because of its practicality and its wide applications in the field, so the model uses standard parameters. This yield criteria is represented by a linear function as shown in Figure 6.10, that states the failure for Mohr's circles in an effective stresses-shear stresses field.

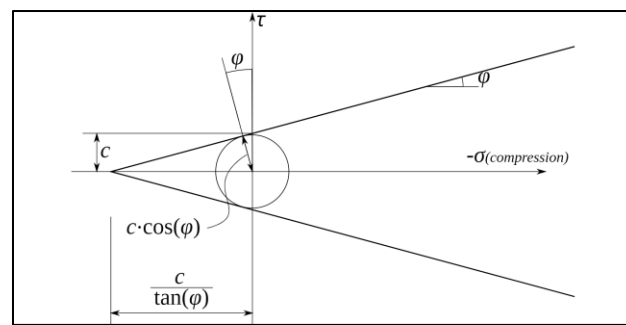


Figure 6.10- Mohr-Coulomb's Criterion.(Hudson & Harrison, 1997)

The key parameters of this model are the cohesion “c”, which is the intercept, and the slope or friction angle “φ”. So, the main relationship governing the response is the following:

$$\tau = \sigma * \tan(\varphi) + c \quad (6.4)$$

Soils have different cohesion and friction angle depending on their type and these values are applied to the shear strength equation. Ground, unlike other construction materials, has very little resistance to tension and in most cases shear failure occurs. When an external force or self-weight is applied, shear stress occurs in the ground. The strain increases with stress

increase and as this effect progresses, it works along a plane causing what is known as shear failure. The shear stress induces shear resistance and the shear resistance limit is called shear strength.

This criterion is most suitable at high confining pressures when the material does, in fact, fail through development of shear planes. At lower confining pressures, and in the uniaxial case, it has been proved that the phenomenon of failure occurs when micro-cracks increase their number in the direction of the principal stress.

Despite the difficulties associated with application of the criterion, it does remain in use as a rapidly calculable method for engineering practice, and is especially significant and valid for discontinuous rock masses.

6.4.2 Overburden

To represent the layer of fill and clay in the model, the characteristics of the latter one will be used because of the scarce and poor quality of the fill. Bulk density of the Clayey soil is assumed 19 kN/m^3 referring to previous studies done in the site.

By laboratory tests performed to soil samples Atterberg's Limits were determined obtaining 48% of Liquid Limit, 21% of Plastic Limit and a Plasticity Index of 27%. This sample is classified as Clay with low plasticity CL.

With this information it is possible to establish a relationship between friction angle and Plasticity index as follows:

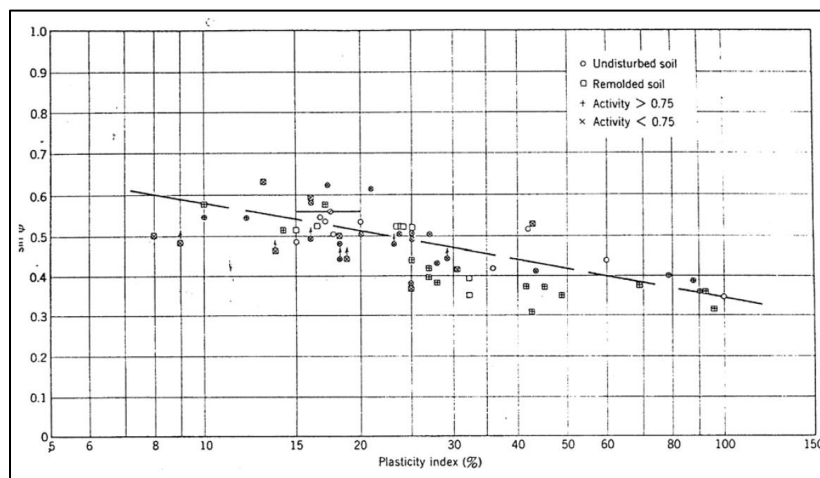


Figure 6.11-Relationship between $\sin \phi$ and plasticity index for normally consolidated soils. (Mitchel & Soga, 2005)

From here and considering the results obtained in the Triaxial Test performed to the sample, values of $\phi = 26^\circ$ and $c = 5\text{kPa}$ are considered.

To define the elasticity parameters, the correlations between N_{spt} and Young's Modulus should be used only in deposits well-characterized from a geotechnical point of view. In this kind of material, it is suggested to use the equations proposed by Stroud (1974) that correlate deformability parameter E_s to both blow count value (N_{spt}) and Plasticity Index (PI). The design value used is equal to 10Mpa.

6.4.3 Class III and IV Breccia

To characterize the ground with a Mohr-Coulomb model, Midas takes as input the values of the cohesion and the friction angle, so a link between these parameters and the ones that characterize the rock mass must be established.

One of the few and more diffused techniques available for estimating the rock mass strength from geological data is used, the Hoek-Brown criterion (Evert Hoek & Brown, 1980). This method is recommended when working with formations that present isotropic behavior and the size of the sample is not in the same order that the structure under study, as in this case.

For the situation analyzed, there is not a family of discontinuities particularly weaker than the rest, so no joint should be treated individually.

Hoek-Brown's criterion is based on the accumulation of empirical data, using the best-fit curve to represent the failure of the intact rock. This method is based in the relationship:

$$\sigma'_1 = \sigma'_3 + \sigma_{ci} \left(m_b \frac{\sigma'_3}{\sigma_{ci}} + s \right)^a \quad (6.5)$$

where “ σ'_1 ” and “ σ'_3 ” represent the principal stresses, “ σ_{ci} ” is the Uniaxial Compressive Strength of the intact rock, “ a ” is constant that takes the value of 0,5 for intact rock, and “ m_b ” and “ s ” result from the curve fit but they can be physically interpreted, relating m_b to the degree of particle interlocking and s to the degree of fracturing present on the rock sample.

The link between the Mohr-Coulomb's parameters and Hoek-Brown's criterion is done by fitting an average linear relationship to the curve generated by solving equation 6.5 for a range of minor principal stress values defined by $\sigma_t < \sigma_3 < \sigma_{3max}$, as illustrated in Figure 6.12. The fitting process involves balancing the areas above and below the Mohr-Coulomb plot.

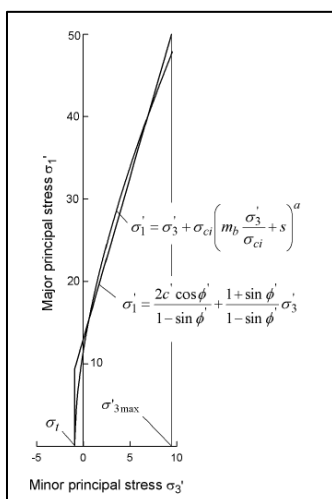


Figure 6.12 Mohr-Coulomb's fit with Hoek-Brown's criterion.

This balance results in the following relationships:

$$\varphi' = \sin^{-1} \left[\frac{6am_b(s + m_b\sigma'_{3n})^{a-1}}{2(1+a)(2+a) + 6am_b(s + m_b\sigma'_{3n})^{a-1}} \right] \quad (6.6)$$

$$c' = \frac{\sigma_{ci}[(1+2a)s + (1-a)m_b\sigma'_{3n}](s + m_b\sigma'_{3n})^{a-1}}{(1+a)(2+a)\sqrt{1 + (6am_b(s + m_b\sigma'_{3n})^{a-1})/((1+a)(2+a))}} \quad (6.7)$$

It is clear that an appropriate value of confinement $\sigma_{3\max}$ must be established in order to obtain a reliable fit. For the case of shallow tunnels, where the depth under the surface is less than 3 tunnel diameters, Hoek suggest the following relationship:

$$\frac{\sigma'_{3\max}}{\sigma'_{cm}} = 0,47 \left(\frac{\sigma'_{cm}}{\gamma H} \right)^{-0,94} \quad (6.8)$$

Where σ'_{cm} is the rock mass strength, γ is the unit weight of the rock mass and H is the depth of the tunnel below the surface. For this case, a depth of 20 meters has been considered.

Following this logic, the first to do is obtain Hoek-Brown's parameters presented in equation 6.5 with the following relationships:

$$m_b = m_i \exp\left(\frac{GSI - 100}{28 - 14D}\right) \quad (6.9)$$

$$s = \exp\left(\frac{GSI - 100}{9 - 3D}\right) \quad (6.10)$$

$$a = \frac{1}{2} + \frac{1}{6} \left(e^{-\frac{GSI}{15}} - e^{-\frac{20}{3}} \right) \quad (6.11)$$

Where,

- σ_{ci} : Uniaxial Compressive strength of the intact rock

- D :Disturbance factor. Although the excavation of the running tunnels will generate small disturbances because of its construction method, the effect produced by the excavation of the caverns must be considered, especially when working with the class IV rock. So, a value of $D=0,5$ is considered.
- m_i :Material constant. This value is assumed 19, as suggested by Hoek for breccia rock.
- GSI :Geological Strength Index

The GSI was introduced by Hoek in 1994 and is a number which, when combined with the intact rock properties, can be used for estimating the reduction in rock mass strength for different geological conditions. The determination of this value has evolved with the passing of the years and now the most recommended way to estimate it is with the use of tables that relate the lithology, strength and surface conditions of the discontinuities. Due to the impossibility of getting access to the actual samples, a method that relates GSI with the Rock Mass Rating is used as it was done before the publication of the above mentioned tables, although is not the most recommended approach.

The Rock Mass Rating (RMR) established by Bieniawski in 1989 is a classification system that has the advantage that with a few geometrical and mechanical parameters of the rock mass it is possible to give a characterization to the material. This criteria is based on five main parameters of the formation: the strength of the intact rock, the drill core quality (% RQD) (Deere, 1963) which is the percentage of intact drill core pieces longer than 10 cm recovered during a single core run, the space and condition of the discontinuities and the groundwater condition. Each of these criteria gets a score as presented in the following image:

A. CLASSIFICATION PARAMETERS AND THEIR RATINGS

Parameter		Ranges of values							
1	Strength of intact rock material	Point-load strength index (MPa)	>10	4 - 10	2 - 4	1 - 2	For this low range, uniaxial compressive test is preferred		
		Uniaxial compressive strength (MPa)	>250	100 - 250	50 - 100	25 - 50	5 - 25	1 - 5	<1
		Rating	15	12	7	4	2	1	0
2	Drill core quality RQD (%)		90 - 100	75 - 90	50 - 75	25 - 50	<25		
			Rating	20	17	13	8	3	
3	Spacing of discontinuities		>2m	0.6 - 2m	200 - 600mm	60 - 200mm	<60mm		
			Rating	20	15	10	8	5	
4	Condition of discontinuities		Very rough surfaces Not continuous No separation Unweathered wall rock	Slightly rough surfaces Separation <1mm Slightly weathered wall rock	Slightly rough surfaces Separation <1mm Highly weathered wall rock	Slickensided surfaces or Gouge <5mm thick or Separation 1 - 5mm Continuous	Soft gouge >5mm thick or Separation >5mm Continuous		
			Rating	30	25	20	10	0	
5	Groundwater	Inflow per 10m tunnel length (l/min)	None	<10	10 - 25	25 - 125	>125		
		ratio (joint water pressure)/(major principal stress)	0	<0.1	0.1 - 0.2	0.2 - 0.5	>0.5		
		General conditions	Completely dry	Damp	Wet	Dripping	Flowing		
			Rating	15	10	7	4	0	

Figure 6.13-Bieniawski Classification.(Bieniawski, 1989)

The parameters presented in tables 6.1 and 6.2 to apply the RMR classification are obtained from the documents of the Mumbai case for the worst samples of the geotechnical units Weathered Grade Three and Four defined in Chapter 5 Section 2:

Class III (TBH-80 from 12 to 14,5m)	Value	Rating
1. Uniaxial Compressive Strength	10 Mpa	2
2. Drill Core Quality RQD	57 %	11
3. Spacing of discontinuities	115mm	6
4. Condition of Discontinuities	Rough surfaces with separation less than 1 mm	25
5. Groundwater	Wet	7
RMR		51

Table 6.1-RMR Class III

Class IV (NTBH-13A from 10,5 to 12m)	Value	Rating
1. Uniaxial Compressive Strength	7,5 Mpa	1
2. Drill Core Quality RQD	10 %	2
3. Spacing of discontinuities	33mm	4
4. Condition of Discontinuities	Surfaces slightly rough and highly weathered.	20
5. Groundwater	Wet	7
RMR		34

Table 6.2-RMR Class IV

Because the rock mass GSI is an inherent parameter of the rock, to relate it to the value of RMR the conditions of the site must be obviated, so the corrected Rock Mass Rating (RMR_{corr}) is defined. The RMR_{corr} is obtained by not considering the presence of water in the mass, so the groundwater condition is defined as dry (rating=15). The value of GSI is the following:

$$\text{Class III: } GSI = RMR_{corr} - 5 = 59 - 5 = 54$$

$$\text{Class IV: } GSI = RMR_{corr} - 5 = 42 - 5 = 37$$

	Unit Weight	Hoek-Brown		Mohr-Coulomb	Global Strength of the Rock Mass	Tensile Strength of Rock Mass	
	(MN/m ³)	m _b	s	φ (°)	c(kPa)	σ _{cm} (Mpa)	σ _t (Mpa)
Class III	0,0224	2.125	0.0022	52	114	1,94	-0.010
Class IV	0,021	2.003	0.0009	43	65	0,91	-0.0043

Table 6.3-Rock Mass Parameters

Using as input the UCS of the rock mass, the GSI, the Material constant m_i , the disturbance factor and the excavation depth is possible to solve the previous equations through the RocData (Rocscience Inc., n.d.) software to estimate Hoek-Brown's parameters and the corresponding Mohr-Coulomb's fit. Also, this program provides information about the resistance of the rock mass that will be used in the analysis of the results. The outputs are shown below:

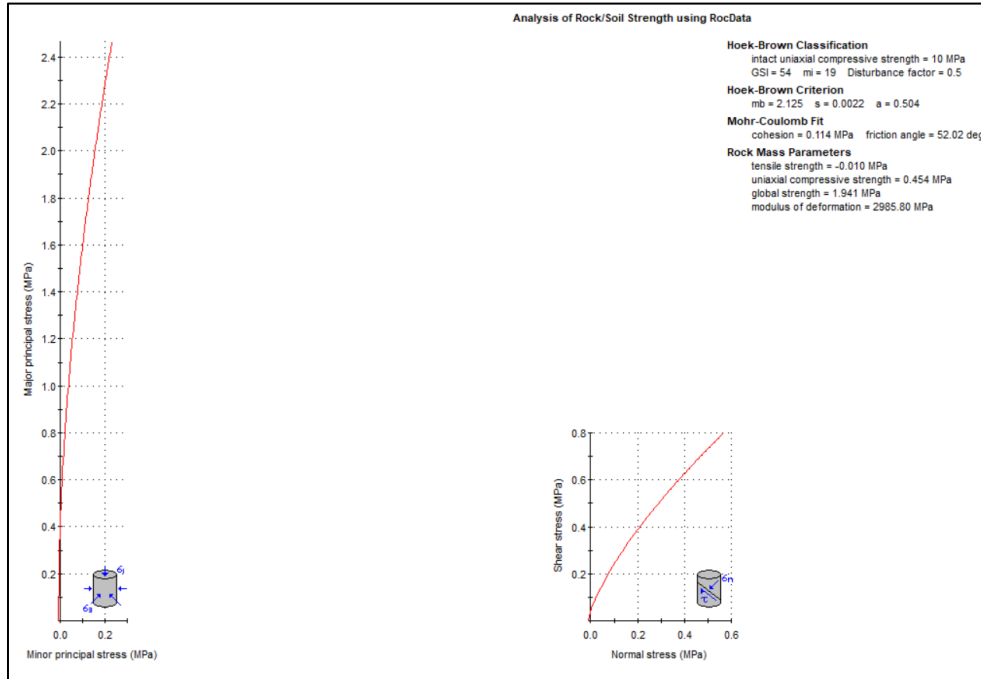


Figure 6.14-RocData Output. Breccia Class III

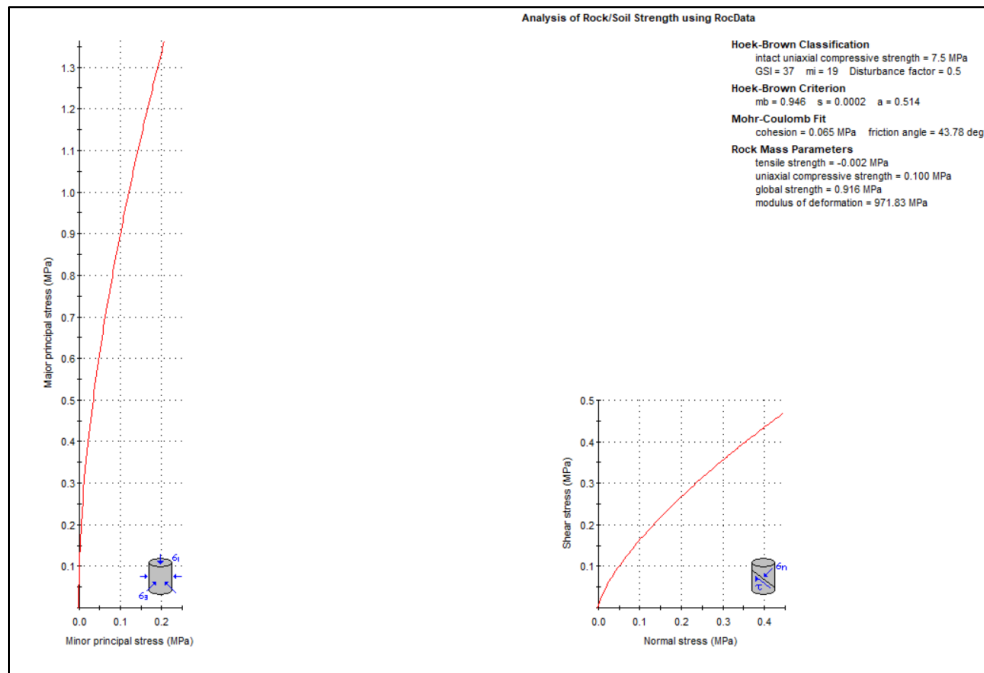


Figure 6.15-RocData Output. Breccia Class IV

For the estimation of rock mass elastic modulus, the following empirical estimation proposed (E. Hoek & Diederichs, 2006) has been used, according to the equation:

$$E_{rm} = E_i \left(0,02 + \frac{1 - \frac{D}{2}}{1 + e^{\left(\frac{60+15D-GSI}{11}\right)}} \right) \quad (6.12)$$

where E_i is the modulus of the intact rock obtained from laboratory tests. Again, the samples that present the lowest values are used, assigning $E_i = 1900\text{Mpa}$ for Class III and $E_i = 1150\text{Mpa}$ for Class IV, giving as result $E_{rm} = 700\text{Mpa}$ and $E_{rm}=420\text{Mpa}$ correspondingly.

For the definition of the coefficient of Lateral Earth Pressure K_0 that relates the value of horizontal and vertical stresses there are not particular studies performed on the site. It is widely used in literature a relationship that involves the use of Poisson coefficient to calculate K_0 but it gives more reliable results when it can be supposed that the material is not affected by its geological history, which is not the case. So, by experience of excavations of breccia rock in the region a value of $K_0=0.65$ is considered.

As it was stated in section 4.2, a permeability of $1,5 \times 10^{-6} \text{m/s}$ is used for the rock mass and the value of $1,59 \times 10^{-8} \text{m/s}$ is assigned to the soil.

In the following table the design values that work as input in the Midas GTS NX model are summarized:

	γ (kN/m ³)	E (Mpa)	ϕ (°)	c(kPa)	K ₀	Permeability(m/s)
Overburden	19	10	26	5	0,65	1,59x10 ⁻⁸
Class III Breccia	22,5	700	52	114	0,65	1,5x10 ⁻⁶
Class IV Breccia	21	420	43	65	0,65	1,5x10 ⁻⁶

Table 6.4-Parameters used in the model

6.5 Support Characteristics

6.5.1 First Phase Lining

The following empiric methodology is followed to define the characteristics of the initial support that will be placed while the caverns are constructed ensuring a safe advancement, (Trabada Guijarro, 2003):

- Characterize the rock mass with the RMR classification, as done in the previous section. The RMR obtained for both formations were 50 for breccia Class III and 34 for Class IV rock. Because the water influence will not be considered in the loading, the values of RMR_{corr} will be used (59 and 42 respectively).
- Determinate Barton's Q parameter to the corresponding RMR value through the following expression, with the values of Q_{III}=4,74 and Q_{IV} = 0,8 respectively.

$$Q = e^{\frac{RMR-44}{9}} \quad (6.13)$$

- Establish the Excavation Support Ratio following the criteria presented in the following table suggested by Burton (1947), considering the excavation as Category D for this case:

Excavation Category	Description	ESR
A	Temporary mine openings	3-5
B	Permanent mine openings, water tunnels for hydro power (excluding high pressure penstocks), pilot tunnels, drifts and headings for large excavations.	1,6
C	Storage rooms, water treatment plants, minor road and railway tunnels, surge chambers, access tunnels.	1,3
D	Power stations, major road and railway tunnels, civil defense chambers, portal intersections.	1,0
E	Underground nuclear power stations, railway stations, sports and public facilities	0,8

Table 6.5-Excavation Support Ratio. Burton (1947)

- Enter the abacus presented in Figure 6.16, proposed by Grimstad and Barton (1993) with the values of Q and ESR, also considering the span to support. To avoid unnecessary constructive complications, all bolts are considered with a length of 3 meters. Tables 6.6 and 6.7 express the information of the primary support for both ground conditions:

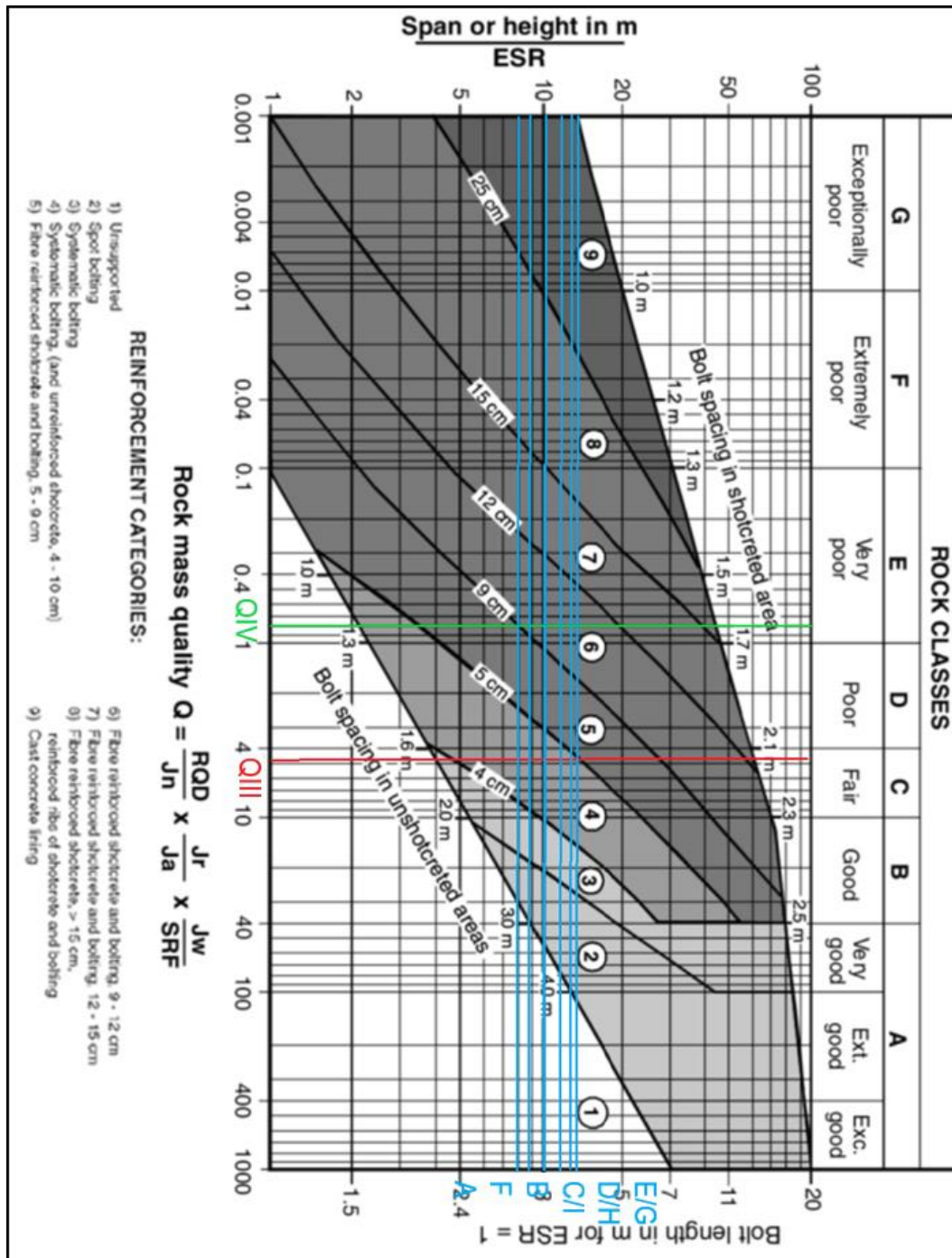


Figure 6.16-Aproximation of support, Grimstad and Barton (1993)

Cavern	Span	Shotcrete		Bolts		
		Reinforced	Thickness(cm)	Number	Length(m)	Spacing(m)
A	8,7	Yes	4	8	3	2
B	10	Yes	5	9	3	2
C	12	Yes	5	10	3	2
D	13,5	Yes	5	11	3	2
E	14,6	Yes	7	12	3	2
F	8,08	Yes	4	-	-	-
G	14,9	Yes	7	12	3	2
H	13,8	Yes	5	11	3	2
I	12,1	Yes	5	10	3	2

Table 6.6- Initial support for caverns. Class III breccia

Cavern	Span	Shotcrete		Bolts		
		Reinforced	Thickness(cm)	Number	Length(m)	Spacing(m)
A	8,7	Yes	9	8	3	1.6
B	10	Yes	10	9	3	1.6
C	12	Yes	10	10	3	1.6
D	13,5	Yes	10	11	3	1.6
E	14,6	Yes	12	12	3	1.6
F	8,08	Yes	9	-	-	-
G	14,9	Yes	12	12	3	1.6
H	13,8	Yes	10	11	3	1.6
I	12,1	Yes	10	10	3	1.6

Table 6.7-Initial support. Class IV breccia

Shotcrete's characteristics are presented below following the indications presented in the Indian standard (PLAIN AND REINFORCED CONCRETE CODE OF PRACTICE-4th Revision, 2007):

Parameter	Value	Code Section
Characteristic cube compressive strength	30 Mpa	IS456 Section 6.2.1 – Table 2
Unit weight	25 kN/m ³	IS456 Section 19.2.1
Design compressive strength	13,4 Mpa	IS456 Section 38.1.c
Characteristic tensile strength	3,83 Mpa	IS456 Section 6.2.2
Design tensile strength	2,56 Mpa	IS456 Section 36.3.1
Modulus of elasticity	27.386 Mpa	IS456 Section 6.2.3.1
Poisson ratio	0,2	

Table 6.8-Shotcrete Characteristics

Also is planned the installation of lattice girders for every step of advancement with the following properties:

Parameter	Value	Code Section
Characteristic strength	500 Mpa (Fe500)	IS456 Section 38.1.f
Design strength	435 Mpa	IS456 Section 36.3.1
Modulus of elasticity	200.000 Mpa	IS456 Section 5.6.3
Poisson ratio	0,3	
Area	11,19 cm ²	
Inertia	148 cm ⁴	
Bars	2φ20+1Φ25, steel rebars Φ10 connection bars	

Table 6.9-Lattice girders characteristics

To represent these materials in the computational model, a shell-type surface will be created considering equivalent elastic modulus that represent the behavior of both materials acting together. By considering the steel area per meter present in the support (separation between girders equal to length of advancement) and subtracting it the thickness of the sprayed shotcrete, is possible to calculate an equivalent stiffness:

$$Eeq * Aeq = Ec * \left(Ac + \frac{Es * As}{Ec} \right) [MPa * m^2/m] \quad (6.14)$$

where As is the steel area per meter and Ac is the thickness of shotcrete minus As . The value of the elastic modulus varies with the thickness of the shotcrete, so the corresponding values used in the model are presented below:

Thickness (cm)	Eeq (Mpa)
4	30.404
5	29.800
7	29.110
9	28.725
10	28.590
12	28.390

Table 6.10-Elasticity Modulus of support.

The properties of the rock bolts are the following:

Parameter	Value
Characteristic strength	500 Mpa (Fe500)
Modulus of elasticity	200.000 Mpa
Poisson ratio	0,3
Unit weight	78,6 kN/m ³
Section	Circular Φ 25
Area	4,91 cm ²

Table 6.11-Rock bolts characteristics

This element will be represented in the model as a 1D embed element, ensuring that their nodes will interact correctly with the surrounding rock.

6.5.2 Final Lining and Segmental Lining

Once the safety of the advancement is ensured by the primary support, the construction of a cast-in-place concrete lining is planned for the caverns. This structure will act as permanent tunnel lining and fulfill the environmental constraints, provide support for fixed permanent

services and mobile equipment and will have a waterproofing purpose. It is recommended the installation of a waterproof geotextile, but because it will not be represented in the numerical model, no further details will be given regarding this material.

Because of the dimensions of the caverns it is proposed to build formworks capable of materializing each structure in only one stage of pouring. This will create monolithic lining avoiding unnecessary joints.

To represent the concrete layer in the model, the same shells used for the initial lining are used with a change of their properties applied when necessary with the following characteristics:

Parameter	Value	Code Section
Characteristic cube compressive strength	35 Mpa	IS456 Section 6.2.1 – Table 2
Unit weight	25 kN/m ³	IS456 Section 19.2.1
Design compressive strength	15,63 Mpa	IS456 Section 38.1.c
Characteristic tensile strength	4,14 Mpa	IS456 Section 6.2.2
Design tensile strength	2,76 Mpa	IS456 Section 36.3.1
Modulus of elasticity	29,580 Mpa	IS456 Section 6.2.3.1
Poisson ratio	0,2	
Thickness	0,5 m	

Table 6.12-Final Lining characteristics

For the segmental rings used as support during the excavation with the TBM, the Universal Ring System is chosen, composed of a set of trapezoidal segments that together conform the ring, closed by a key segment that enables an entire 360° rotatability of every segmental ring.

This rings with no parallel faces have the advantage that with only one set of formworks is possible to cast all the segments of the alignment. With the appropriate rotation of the rings is possible to create the curves of the track and correct the inevitable, though small, TBM driving errors.

The smallest radius that can be constructed is related to the taper, this is, the difference between l' and l'' (Figure 6.17). The ring is composed by three kinds of segments: normal or rectangular, counter-key segments and a key segment. This last ones closes the ring and it is useful to control the curvature of the alignment. By turning each ring 180° in reference to the previous one the excavation follows a straight line and by changing this rotation vertical and horizontal radius are created.

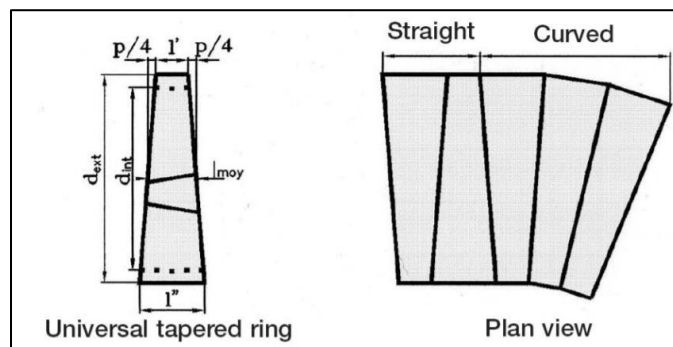


Figure 6.17-Universal Ring.

Property	Value
Extrados Diameter	6,35 m
Intrados Diameter	6,05m
Ring Width	1,6 m
Taper total	48 mm
Minimum Horizontal Curve Radius	200 m
Minimum Vertical Curve Radius	1500 m
Number of Segments	5+1 key
Type of concrete	M50
Elastic Modulus of Concrete	35,35 Mpa
Unit Weight	25 Mpa

Table 6.13- Segmental rings information.

6.6 Groundwater

In the original project, because of the good characteristics of the rock mass, the low permeability of the formation, the complications that implies the preparation of a drainage system and the urban condition of the surface, it was decided not to disturb the water level of the ground. It was assumed that groundwater inflows could happen during the excavation of the cavern and were predicted through analytical formulas.

For the case of the model, the influence of the groundwater is neglected to achieve a better understanding of the results produced by the excavation process.

6.7 Construction stages

Both models have a total of 396 computational construction stages starting from the undisturbed ground and finishing with the installation of the final lining, including the excavation of the TBM tunnels and the collocation of the segmental lining, the creation of

the caverns and the placing of its corresponding support. In this section it is detailed how the constructive process explained in section 3.2 is represented using the geotechnical analysis software. In order to achieve a clear explanation of the procedure, the almost 400 steps are grouped in 3 general stages:

Stage 1 (from 1 to 156): Excavation of the running tunnels and the installation of the segmental lining. Starting from an initial situation with no displacements, the removal of the clusters that represent the twin tubes begins, with the immediate collocation of the shell surfaces that represent the concrete rings in a cyclic operation, with a length of step of 1,6 meters performed in the 125 meters of the domain.

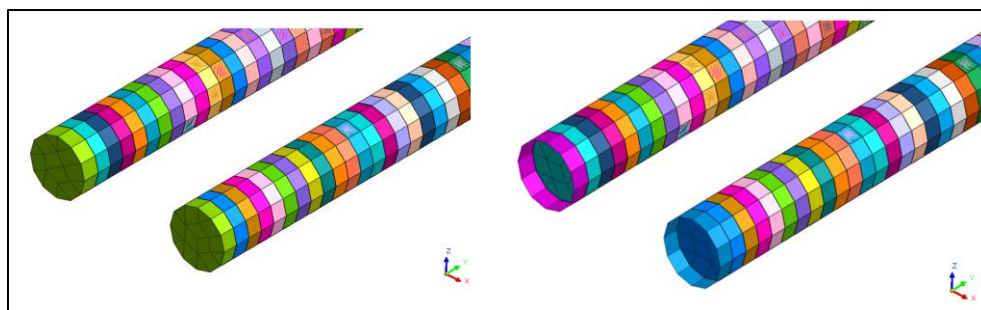


Figure 6.18-Excavation of TBM tunnels and installation of segment lining

Stage 2 (from 157 to 390): Construction of the caverns. As exposed in section 3.2, two directions of construction are followed. One starting from cavern A to E, and the other from I to G meeting before the execution of cavern F. Depending on the size of the cross section, the excavation of each cavern can take more steps in order to complete the sequence in which the face is divided. To illustrate the procedure, one round of cavern I is shown below:

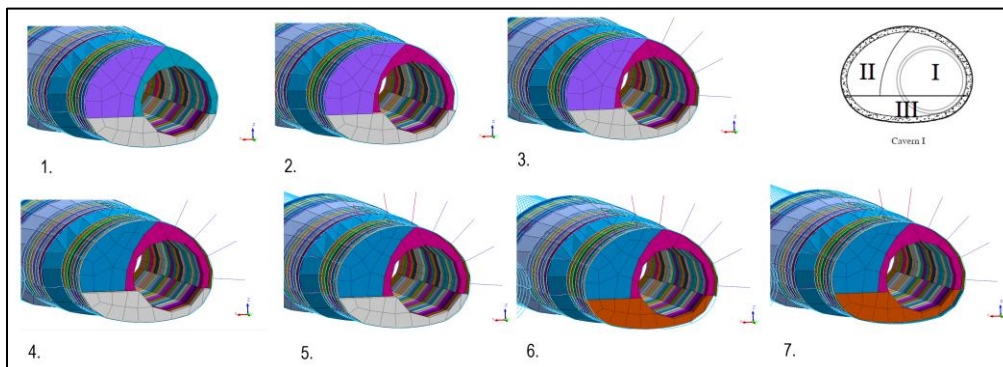


Figure 6.19-Cavern I construction sequence.

The sequence in Figure 6.19 is the following:

- 1. Removal of one concrete ring.
- 2. Excavation of section I of the cavern in a length of 1,6 meters.
- 3. Collocation of rock bolts and shotcrete for section I.
- 4. Excavation of section II of the cavern in a length of 1,6 meters.
- 5. Collocation of rock bolts and shotcrete for section II.
- 6. Excavation of section III of the cavern in a length of 1,6 meters.
- 7. Collocation of shotcrete for section III.

This procedure is followed in both directions for all the caverns (Figure 3.5).

Stage 3 (from 390 to 396): Once the caverns are excavated and the primary support is placed, the characteristics of the shell elements that represent the layer of shotcrete are changed to materialize the final lining. As explained in section 3.2, the concrete layer of each cavern is placed in one stage in the following sequence:

- 1. Cavern A (Direction 1) and I (Direction 2).
- 2. Cavern B (Direction 1) and H (Direction 2).
- 3. Cavern C (Direction 1) and G (Direction 2).
- 4. Cavern D (Direction 1).
- 5. Cavern E (Direction 1).

- 6. Cavern F (Direction 1).

6.8 FEM models results

In this section short comments about the results obtained from Midas GTS NX after the simulation are done with the comparison of the two models, each one with different rock characteristics. The analysis will focus on how the ground moved after the excavation, the stresses that were generated in the rock mass and how severe are the deformations of the material. Most of the inquiry will be centered in a cross section placed at 87 meters from the edge of the model in the direction of the TBM tunnels, where cavern F is located and most critical values are expected, as explained in section 3.3. The outputs of the software are shown in Appendix 3.

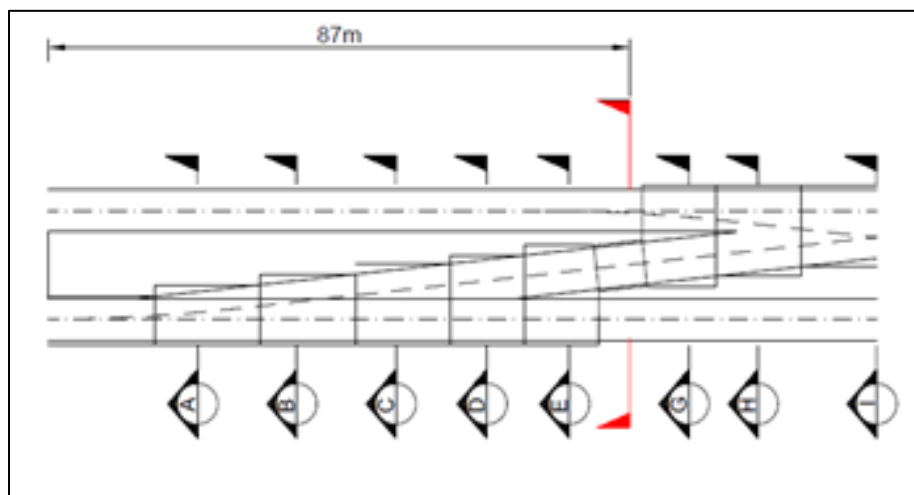


Figure 6.20- Analyzed section

6.8.1 Displacements

As it was previously mentioned in this document, because of the urban location of the work settlements on the surface must be controlled to predict how the structures in surrounding will be affected.

The results presented in the Appendix 3 show how the displacements at the end of the construction range from 3 to 5 millimeters at the surface in the model with the rock mass class III, being these values low as it is considered that from settlements bigger than 1 centimeter the damage produced in the surface starts to be considerable (Figure 10.13). When changing the parameters of the rock mass, the value of settlements in the surface increases, ranging from 5 to 8 millimeters over the excavation and almost reaching the centimeter in the surroundings of the cavern (Figure 10.20). Nevertheless, still these values are considered low.

Most of this ground movement is attributed to the construction of the caverns, due to the fact that the deformation produced by the advancement of the TBMs does not even reach the millimeter in the surface in both models (Figures 10.14 and 10.21) when settlements are analyzed in the stage in which twin tunnels construction ends:

An output of the construction of cavern G is presented to study the extrusion of the face during the construction of this cavern which is the one with the most important dimensions. It can be appreciated that the movements of the face through the excavation are almost unnoticeable, being 2,4 millimeters the higher value for breccia class III and 6 millimeters for breccia class IV (Figures 10.15 and 10.22).

6.8.2 Principal Stresses

Additionally, in Appendix 3 are presented the results of the model that represent the value of the maximum and minimum stress on each point of both models, σ_1 and σ_3 . In the columns between the excavations are present the limit values of the section (Figures 10.16 and 10.17) but considering that the resistance calculated for this mass was of 1940 Kpa for compression and 10 Kpa for tension for the class III rock mass, the stresses generated should not cause important deformation in the mass.

For the weak formation the results slightly overpass the rock's mass resistance to compression in the surroundings of the cavern F (Figures 10.23 and 10.24), that has a value of 910 kPa. This could compromise the stability of the excavation when reaching this section.

As a reminder, Midas shows with positive values tensile stresses and with negative values compression stresses.

6.8.3 Plastic Status

To understand the severity of the deformations produced in the ground after the construction, in the Appendix are presented the parts of the excavation that reached plastic behavior. Beyond some particular nodes, most of the model with the class III rock mass presents no plastic points (red points) and only unload/reload points with elastic behavior. Although there is a concentration of points that are subjected to movements in the perimeters of cavern F, most of them show an elastic deformation so there is no risk of failing.

In contrast to the previous case, this time a plastic behavior is present around the excavation of cavern F, in accordance with the stresses presented in this region. Also, the cloud of mobilized points is denser in relation to the poor characteristics of the material.

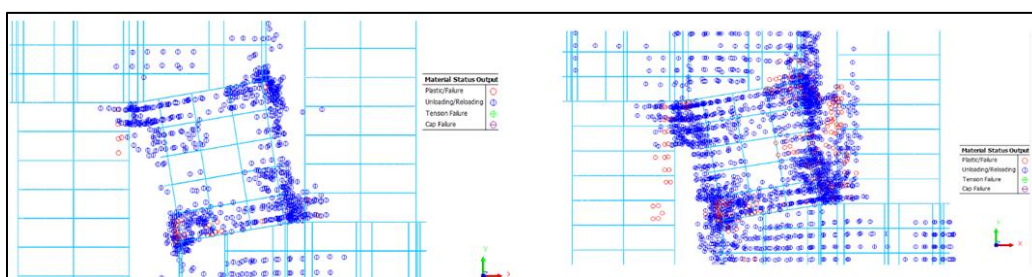


Figure 6.21-Plastic status. Plan view around cavern F. Breccia class III(left) and IV (right).

6.8.4 Original Cavern Model:

Two other computational simulations were done in the exact same ground conditions than the scissor crossover model, seeking to compare how the rock reacts to both crossover methodologies.

For the representation of the big cavern, the guidelines exposed in section 1.2 of this document were followed. Starting from the excavation of a vertical shaft with a connection tunnel that allows the access to the cavern zone, boring first the TBM tunnels and then the cavern, dividing its face to do it sequentially. As in the previous case, because of the symmetry of the model only half of the model was constructed, making a small change in the length of the cavern in order to fit precisely with the length of the segments that control the advancements step.

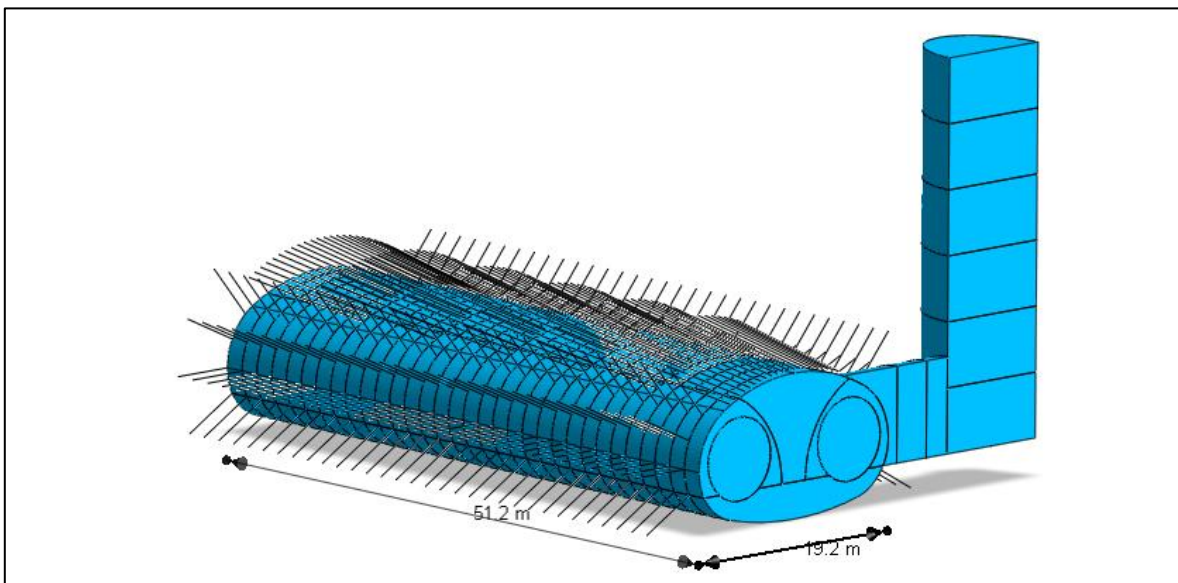


Figure 6.22-Original cavern model

In this project, a pipe umbrella support was thought to be installed before starting the excavation of the cavern in order to provide additional resistance to the ground that is about to suffer the extraction of an important quantity of volume. The proposed length of the pipes

is equal to 12 meters with an overlap of 4 meters between each set of bars ensuring permanent support. The characteristics of this material are the followings:

Parameter	Value
Number	25 over the crown of the cavern
Outer Diameter/Wall Thickness	114,3/6,3mm
Steel	IS2062 (S235JR)
Young's Modulus	200.000Mpa
Unit weight	78,6 kN/m ³

Table 6.14- Steel Pipes characteristics

For the support materials, Burton's methodology was again used with the same Q values calculated previously for each rock formation. For a free span of 19,2 meters, the abacus of Grimstad and Barton suggests a layer of reinforced shotcrete of 7 and 12 centimeters, with the placement of five meters long rock bolts in the side benches of the cavern. The characteristics of the material remain the same as those used in the scissor crossover.

Regarding the reinforcement of the shaft and the access tunnel, only a layer of shotcrete is applied with the characteristics of the smallest span caverns of each model. In the case of the class III breccia rock, the thickness is 4 centimeters and for the model with the weaker rock, the layer of shotcrete in these excavations is 9 centimeters thick.

After this, the pouring of final lining is completed dividing the 50 meters of the cavern in five final stages, according to the length of actual formworks with similar section dimensions.

The computational stages that recreate the construction follow the same guidelines that in the scissor crossover.

- Stage 1: Construction of the side vertical shaft at the center of the crossover as shown in Figure 3.2.
- Stage 2: Installation of the support of the shaft.
- Stage 3: Excavation of the twin TBM tunnels with a length of advancement of 1,6 meters.
- Stage 4: Collocation of the corresponding segmental lining.
- Stage 5: Excavation of access tunnel allowing to reach the face of the cavern.
- Stage 6: Installation of the support of the access tunnel.
- Stage 7: Installation of umbrella pipe system over the T section of the crown providing overhead protection.
- Stage 8: Removal of the ring of the down line to start excavation of section I of the face.
- Stage 9: Excavation of section I, growing from the space made by the boring machine.
- Stage 10: Collocation of the support of the excavated drift.
- Stage 11: Repeat Stage 8 for the left side of the cavern.
- Stage 12: Repeat Stage 9 for section II of the face.
- Stage 13: Repeat stage 10 for the excavated section.
- Stage 14: Excavation of the middle drift of the face.
- Stage 15: Collocation of the middle support.
- Stage 16: Excavation of the bench of the cavern.
- Stage 17: Final lining concrete pouring, using formworks of approximately 10 meters long.

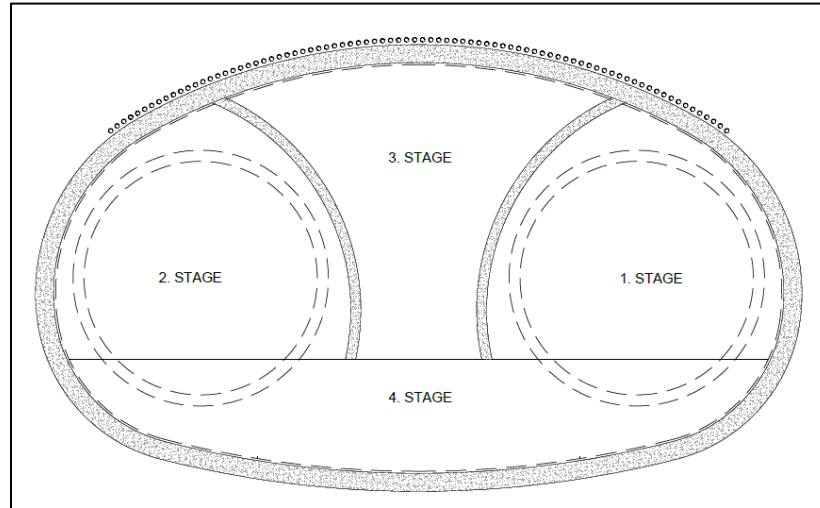


Figure 6.23-Original Cavern Sequence.

The main objective of these secondary models is to confront the scissor crossover in terms of displacements. An increase in the values of the displacements is noticed with respect to the previous models and this difference will be analyzed with further details in Chapter 7.

6.8.4.1 Breccia Class III

The results of the vertical settlements produced in this model are the followings:

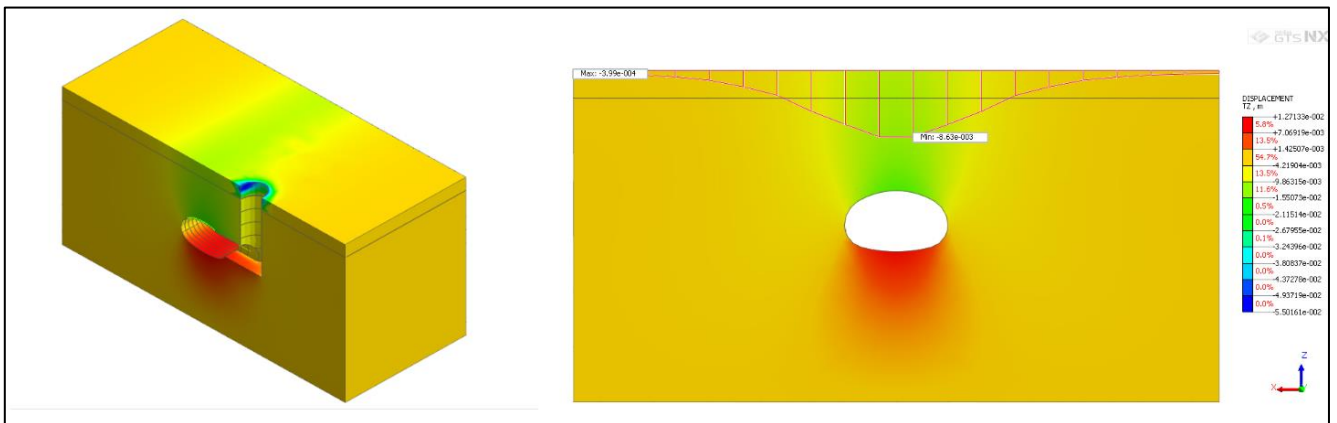


Figure 6.24-Original Cavern superficial Settlements. Breccia Class III

6.8.4.2 Breccia Class IV

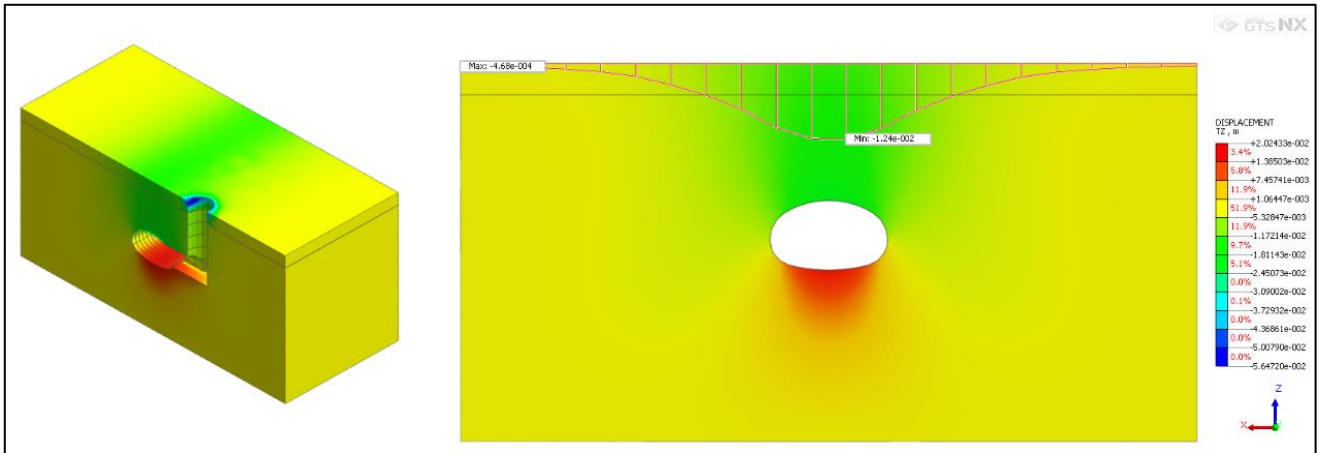


Figure 6.25-Original Cavern superficial Settlements. Breccia Class IV

Chapter 7: Discussion

7.1 Viability of the crossover in the two rock masses

In terms of stresses, it can be said that both formations can stand the construction of the caverns. For the case with good ground characteristics, its materialization should not present any particular difficulty, due to the fact that the stresses found in the mass are low compared to the resistance values. Also, almost no plastic points are present in the surroundings of the excavation with the exception of isolated points.

In the case of the rock mass with weak parameters, the ground responded pretty well in the most part of the model but presented plastic deformation around the perimeter of cavern F, as expected at the beginning of the study. In an extreme case this could lead to the failure of the material and detachment of blocks in this area. To address this issue, two different solutions are proposed:

One is to anchor the columns formed between cavern F and the running tunnels to provide additional resistance to the rock mass in this potentially risky region. The other alternative is to construct a unique cavern with similar dimensions to the one constructed in Mumbai covering from the limits of cavern E and G, where is seen in the results that almost no plastic points are generated.

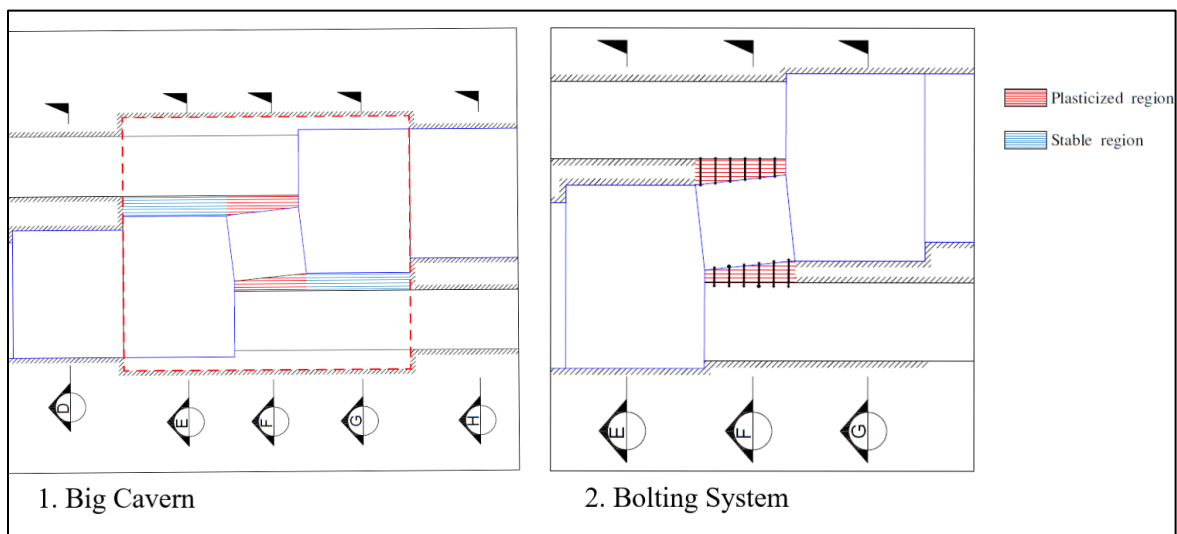


Figure 7.1-Alternative solutions for Breccia Class IV

To study how severe are the settlements produced on the surface, a damage analysis on the surrounding structures is made. It is based on the theories established by Boscardin & Cording and Bjerrum, that relate the value of the horizontal strain (ϵ_h) and angular distortion (β) with the damage produced in the structure:

Damage Field	Damage description	Crack width (mm)
Negligible	Micro-cracks	<0,1
Very Slight	Architectural	<1
Slight	Architectural	<5
Moderate	Functional	5-15
Severe	Structural	15-25

Table 7.1- Boscardin & Cordin classification (1989)

β	Description
<1/500	Negligible Damage
1/500 – 1/300	Cracking
1/300 – 1/150	Tilting becomes visible
>1/150	Structural Damage

Table 7.2 - Bjerrum Classification (1963)

As a supposition in the model, a line of 40 meters long has been drawn perpendicular to the excavation advancement axis in the center of all four models representing the edge of a building in the surface. To make the comparison reasonable, the line is in the same coordinates in all the models. With the values of vertical and horizontal displacements provided by Midas and the position in the space of the points is possible to calculate the values of ϵ_h and β to plot them with the mentioned criteria (software outputs Appendix 4):

Scissor Class III		Scissor Class IV		Original Class III		Original Class IV	
ϵ_h (10-3)	β (10-3)	ϵ_h (10-3)	β (10-3)	ϵ_h (10-3)	β (10-3)	ϵ_h (10-3)	β (10-3)
0.041	0.149	0.046	0.274	0.026	0.387	0.004	0.402
0.003	0.173	0.205	0.491	0.250	0.295	0.276	0.487
0.068	0.156	0.158	0.613	0.298	0.413	0.397	0.553
0.137	0.473	0.304	0.944	0.410	0.509	0.603	0.893
0.139	0.641	0.328	1.206	0.352	0.612	0.528	0.909
0.172	0.003	0.182	1.186	0.393	0.527	0.582	0.832
0.131	0.545	0.091	0.196	0.208	0.343	0.301	0.556
0.134	0.291	0.018	0.205	0.113	0.242	0.157	0.498
0.019	0.203	0.063	0.214	0.030	0.310	0.052	0.461

Table 7.3- Horizontal strains and angular distortions of the models.

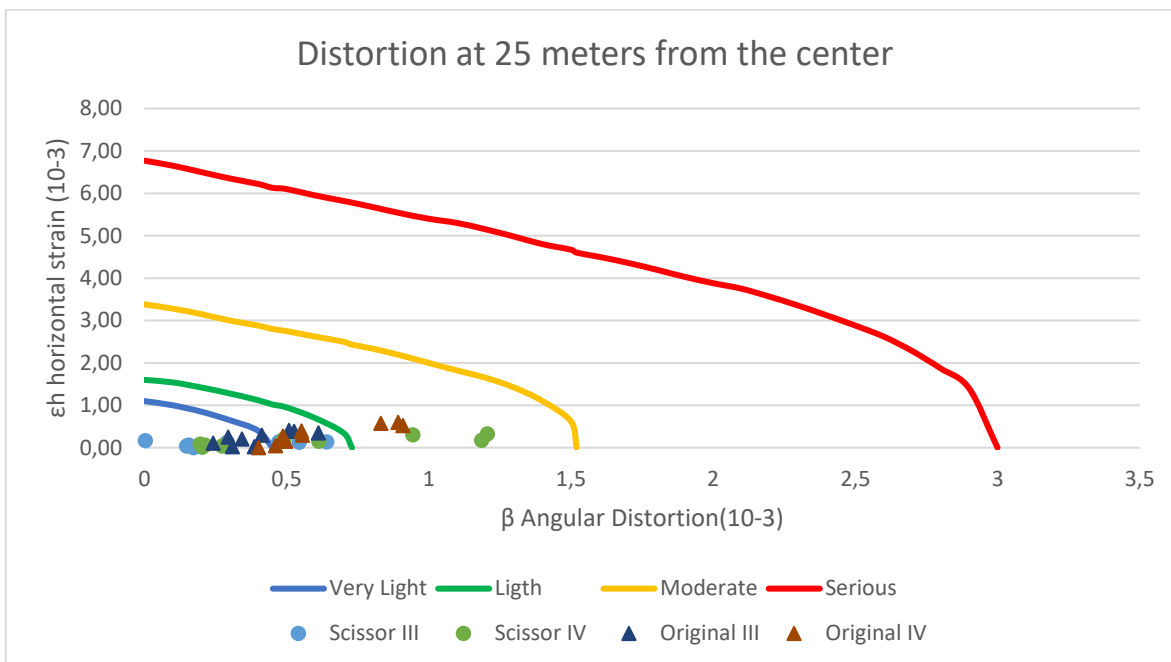


Figure 7.2-Superficial Structures damage. Boscardin & Cordin (1989).

Scissor Class III		Scissor Class IV		Original Class III		Original Class IV	
ϵ_h (10 ⁻³)	β (10 ⁻³)	ϵ_h (10 ⁻³)	β (10 ⁻³)	ϵ_h (10 ⁻³)	β (10 ⁻³)	ϵ_h (10 ⁻³)	β (10 ⁻³)
0.024	0.168	0.055	0.205	0.024	0.321	0.051	0.467
0.228	0.502	0.025	0.191	0.752	0.822	1.056	1.164
0.009	0.709	0.091	0.183	0.381	0.435	0.544	0.908
0.188	0.033	0.299	0.620	0.365	0.154	0.525	0.235
0.101	0.644	0.190	0.682	0.392	0.002	0.568	0.008
0.224	0.470	0.283	0.052	0.365	0.150	0.529	0.219
0.060	0.120	0.026	0.707	0.420	0.945	0.594	0.809
0.017	0.126	0.353	0.753	0.795	0.640	1.128	1.193
0.036	0.135	0.033	0.256	0.025	0.323	0.043	0.472

Table 7.4-- Horizontal strains and angular distortions of the models.(50 meters from the center)

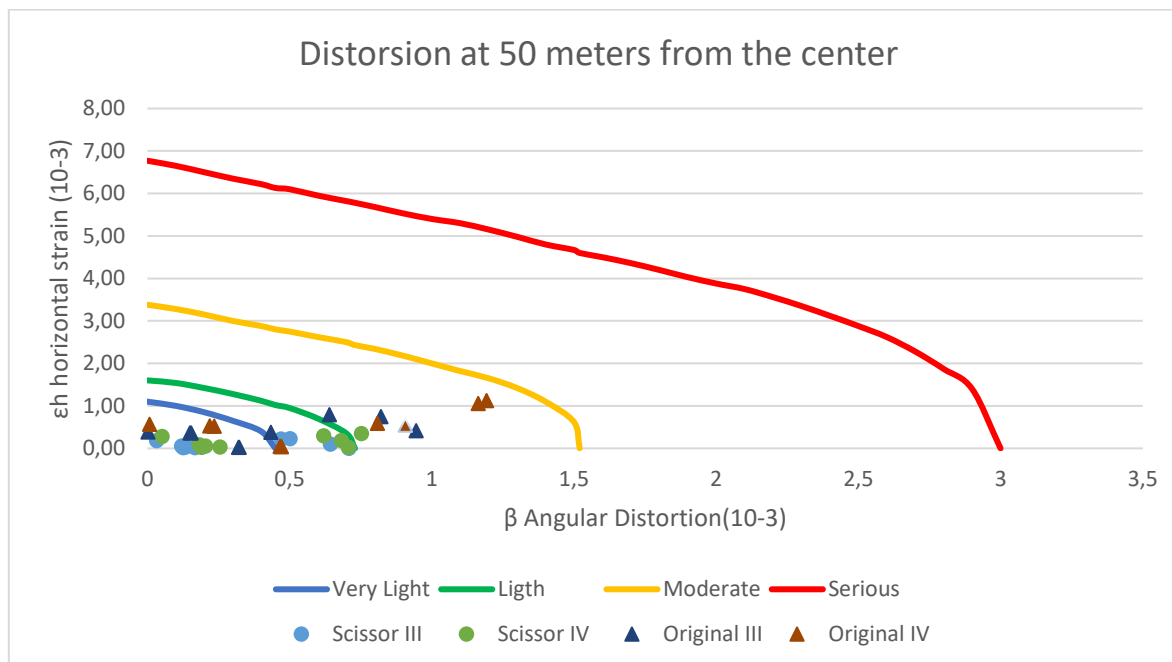


Figure 7.3-Superficial Structures damage. Boscardin & Cordin (1989).

As appreciated on the graphs, most of the results range from very light to light damage for all four models, with some points almost reaching a moderate damage for the case of the original cavern at 50 meters from the center of the crossover. This means that the settlements produced would not affect the structures on the surroundings of the excavation in general terms.

It also can be seen that in the building closer to the center of the crossover, the scissor method presents more problems than its alternative, especially for the model with the rock mass class IV. This coincides with the results obtained from Midas, where it was showed that around cavern F the rock mass presented plastic behavior so worst distortions are expected.

Instead, when the building is supposed at 50 meters from the crossover center, the scissor alternative presents a less harmful behavior. Following this reasoning, the intervention proposed of constructing a cavern of big dimensions between caverns E and G potentially could reduce the surface affectations in the most critical area, obtaining better results in the

whole length of the interchange. As it was said before, this is a proposal only for the case of a class IV rock mass.

7.2 Comparison with original project

As it was explained previously on this document, the construction of one big cavern allows the possibility of industrialize the construction process, because although it requires the construction of access tunnels and the placements of an umbrella piping system, once these operations are ended the procedure becomes repetitive. Also, once the excavation is finished, a great underground volume is generated that provides freedom for the installation of needed infrastructure.

Instead, although is true that the scissor crossover consists on a system of smaller caverns (in the transversal direction), its execution needs a high level of precision due to the geometric particularities of each cavern, and also gives tight space for the placement of the railway system.

It was demonstrated in section 6.8.1 that the models of the scissor crossover result in smaller superficial displacements, that as it was said, they are the key parameter to be controlled in an urban area. But the difference between one model and the other for the same rock mass parameters are approximately 5 millimeters, which is a small value. Also, in the previous section it was proved that none of the four models produce relevant damage on the superficial structures, but with correct interventions the scissor alternative certainly provokes milder effects.

A comparison between the volume of ground excavated and the shotcrete used for each methodology is done to confront them in economic terms. The values of shotcrete thickness correspond to the models with Breccia Class III:

Surface (m²)	Length (m)	S/C thickness (m)	S/C Area (m²)	Rock Vol. (m³)	S/C Volume (m³)
178.65	102.88	0.07	3.46	18379.51	355.96

Table 7.5-Original Model Volumes

Cavern	Surface (m²)	Length* (m)	S/C thickness (m)	S/C Area (m²)	Rock Vol. (m³)	S/C Volume (m³)
A	54.96	32.00	0.04	1.05	1758.72	33.60
B	71.92	28.80	0.05	1.50	2071.30	43.20
C	87.87	28.80	0.05	1.68	2530.66	48.38
D	102.50	22.40	0.05	1.83	2296.00	40.99
E	116.26	22.40	0.07	2.75	2604.22	61.60
F	35.26	16.00	0.04	0.84	564.16	13.44
G	118.16	22.40	0.07	2.78	2646.78	62.27
H	106.94	25.60	0.05	1.88	2737.66	48.13
I	87.79	22.40	0.05	1.68	1966.50	37.63
TOTAL					19176.00	389.25

Table 7.6 - Scissor Crossover volumes. *The length of each cavern is multiplied by 2.

It is noticed that the proposed alternative results in higher excavation and shotcrete volumes, so it would not be economically advantageous either.

7.3 Distance between tubes

During the design of the geometry of the crossover, the necessity of starting in a previous chainage appeared in order to progressively increment the section, leave enough space between the caverns and the next tunnel and to correctly fit the transition excavation (cavern F).

Like the case of Istanbul, a wider space between the running tunnels gives more freedom in the design and allows the use of a smaller railway radius, that at the end controls the geometry of the project.

It is clear that the more space between the twin tunnels, the more convenient the scissor crossover becomes and the less useful it turns the idea of excavating a unique cavern that covers the whole area. More space between the tunnels would lead to a decrease of the excavated volumes when using the scissor alternative and to a reduction of the plastic regions, taking more advantage of the small surface distortions.

Chapter 8: Conclusions

During the construction of Line 3 of the metro system of the city of Mumbai, the necessity of constructing a crossover between two stations has been established, allowing the trains to change track and facilitate the operation of the railway line.

The job done in the present thesis was based on the study of using the scissor crossover alternative to solve the above mentioned problem. Starting from the geometric design of each individual cavern, including the determination of their support and the organization of the execution in construction stages, to the calculation of the ground parameters needed to recreate the problem in a numerical model. This was followed by the analysis of the outputs of the simulation and confrontation with the results of the real-case model and the available information of this case.

As a primary conclusion it can be said that the construction of the scissor crossover in the ground and geometric presented conditions it is viable. In terms of the rock mass structure and displacement development, the methodology presented a correct behavior for a stable rock mass and a formation with poor characteristics, beyond the eventual interventions to make it feasible in this last case. Nevertheless, it has been demonstrated that the alternative chosen by the company in charge of the project requires less constructive materials and a smaller excavation volume.

The benefits in terms of superficial settlements of the scissor alternative do not have enough relevance to justify a change of methodology in this case, due to the fact that the displacements generated by its competitor do not affect the superficial structures to an alarming degree. So, it can be said that for the crossover studied in the Line 3 of Mumbai, the execution of a big cavern is the most advantageous choice.

Still, if a smaller affectation is required, the scissor alternative could fulfill this need in both ground conditions, but executing the big cavern where the ground presents important

deformations for the case of the class IV rock mass. Probably, in a case where the running tunnels present more separation between each other this method could become the best option, obtaining more design liberty to avoid the weak points generated in this case.

Finally, for future investigations it would be interesting to better understand until what point the separation of the running tunnels controls the method election, establishing a minimum distance between the twin tunnels for which the scissor crossover results more convenient than the excavation of a unique cavern. Additionally, including the water table to the analysis will allow to consider this alternative in a wider range of ground conditions.

Chapter 9: References

- Bieniawski, Z. T. (1989). *Engineering Rock Mass Classifications*. John Wiley & Sons, Inc.
- PLAIN AND REINFORCED CONCRETE CODE OF PRACTICE-4th Revision, Indian Standard 1 (2007). <http://www.iitk.ac.in/ce/test/IS-codes/is.456.2000.pdf>
- Chamorro Ramos, O. (2005). *Análisis de los movimientos del terreno producidos por la excavación mecánica del túnel de la L9 en la zona de Santa Coloma de Gramenet* [UNIVERSITAT POLITÈCNICA DE CATALUNYA]. <https://upcommons.upc.edu/handle/2099.1/3270>
- El País. (2007). *El hundimiento del metro del Carmel: la peor crisis*. https://elpais.com/diario/2007/06/29/catalunya/1183079238_850215.html
- Hansford, M. (2012). *No.11 Nicoll Highway collapse*. <https://www.newcivilengineer.com/latest/no-11-nicoll-highway-collapse-02-05-2012/>
- Harper, K. (2000). *Managers “overlooked risk” in airport tunnel collapse*. <https://www.theguardian.com/uk/2000/jul/06/keithharper>
- Hoek, E., & Diederichs, M. S. (2006). Empirical estimation of rock mass modulus. *International Journal of Rock Mechanics and Mining Sciences*, 43(2), 203–215.
- Hoek, Evert, & Brown, E. T. (1980). *Underground Excavations in Rock* (H. . P. . Rossmanith (ed.)). E & FN Spon.
- Hudson, J. A., & Harrison, J. P. (1997). *Engineering Rock Mechanics* (1st ed.). Elsevier Science Ltd.

ITA Working Group. (2009). *General Report on Conventional Tunnelling Method* (Issue April).

Maidl, U. (2011). Slurry Shields. In B. Maidl, M. Herrenknecht, U. Miadl, & G. Wehrmeyer (Eds.), *Mechanised Shield Tunnel* (2nd ed., pp. 223–228). Ernst & Sohn.

Medaña Saavedra, F. (2003). El proyecto de Túneles. In C. López Jimeno (Ed.), *Manual de Túneles y Obras Subterráneas* (Segunda Ed, pp. 82–88; 90–94).

MIDAS Information Technology. (2019). *Midas GTS NX*.

STANDARDIZATION AND INDIGENISATION OF METRO RAILWAYS, SYSTEMS AND SUB-SYSTEMS, (2013). <http://mohua.gov.in/upload/uploadfiles/files/Report1Base Paper on STANDARDIZATION AND INDIGENISATION Copy.pdf>

Mitchel, J. K., & Soga, K. (2005). Fundamentals of Soil Behavior. In *Soil Science* (Third, Vol. 158, Issue 1). John Wiley & Sons, Inc. <https://doi.org/10.1097/00010694-199407000-00009>

MORETTO, O., PECK, R. B., ALBERRO, J., ENDO, M., JENNINGS, J. E., KUESEL, T., & WARD, W. H. (1969). *DEEP EXCAVATIONS AND TUNNELLING IN SOFT GROUND EXCAVATIONS*. 536–537. https://doi.org/10.1007/978-3-319-73568-9_174

Potts, D. M., & Zdravkovic, L. (2001). *FEM analysis in geotechnical engineering 2 Application*.

Quiñones-Rozo, C. (2010). *LUGEON TEST INTERPRETATION, REVISITED*.

Rafie, K. (2019). Sequential excavation method tunnelling. *Tunnels and Tunnelling, Tunnelling*, 40.

Rocscience Inc. (n.d.). *RocData* (v3.0). <https://www.rocscience.com/software/rocddata>

Trabada Guijarro, J. (2003). Excavación en terrenos blandos. In C. López Jimeno (Ed.), *Manual de Túneles y Obras Subterráneas* (Segunda Ed, pp. 220–224). U.D.Proyectos.

Chapter 10: Appendices

10.1 Appendix 1: Scissor Crossover cross sections

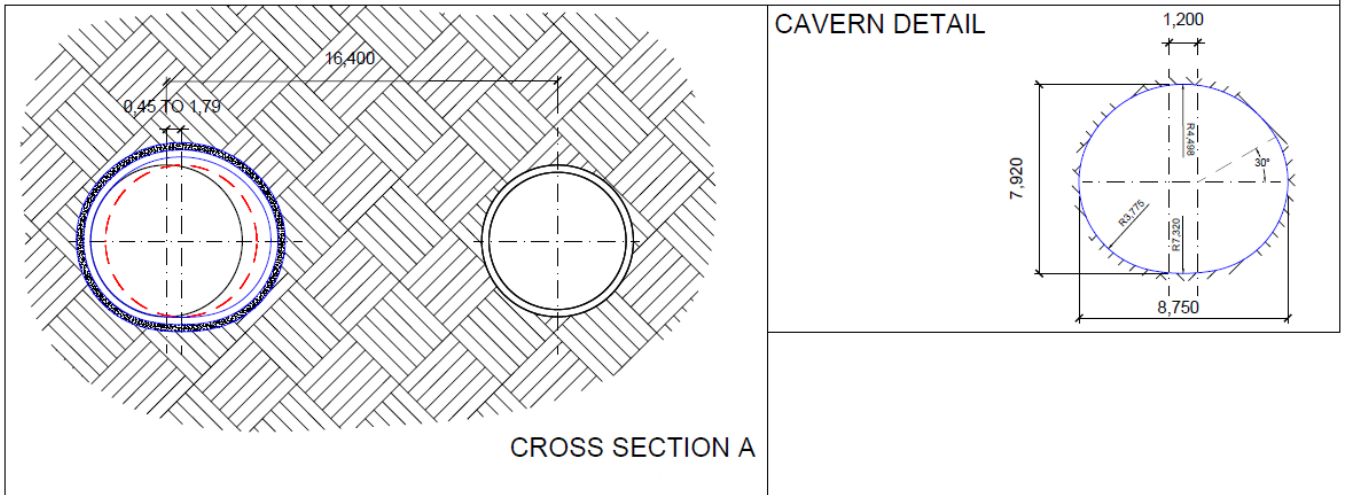


Figure 10.1-Cavern A

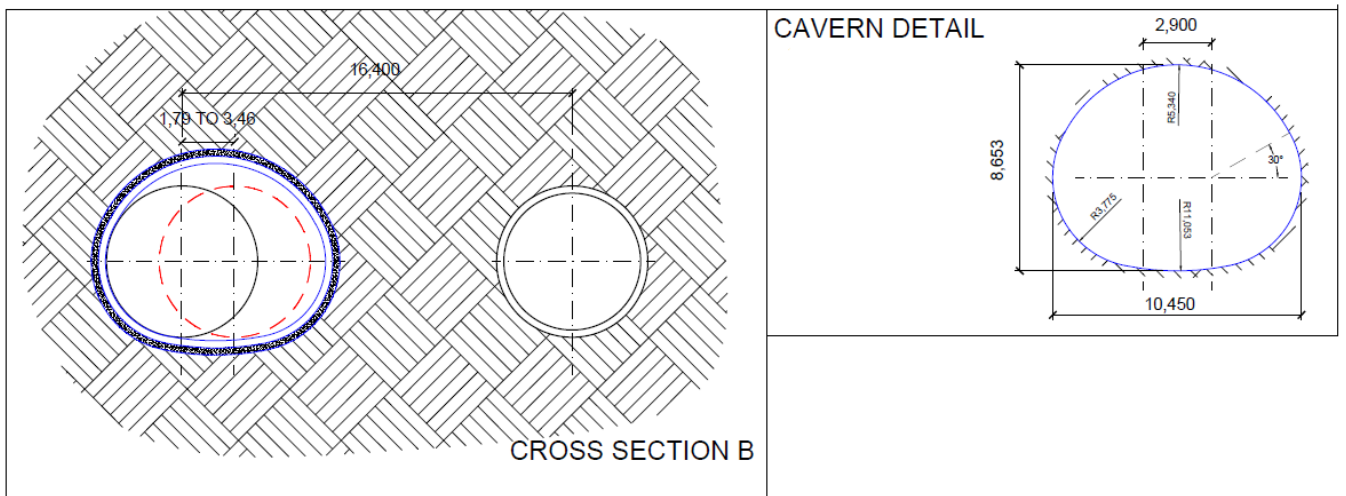


Figure 10.2-Cavern B

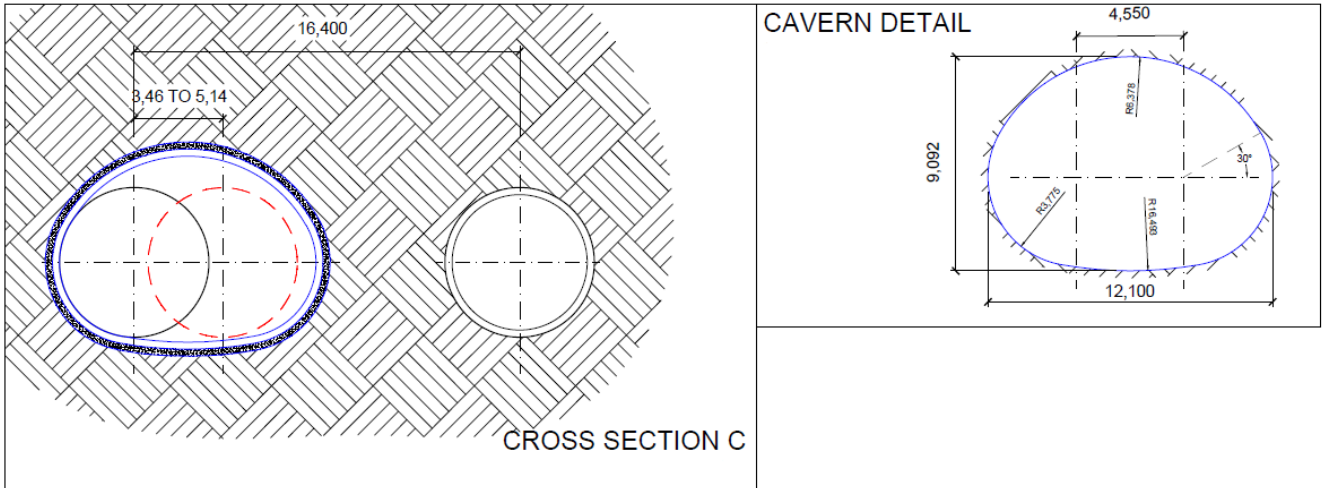


Figure 10.3- Cavern C

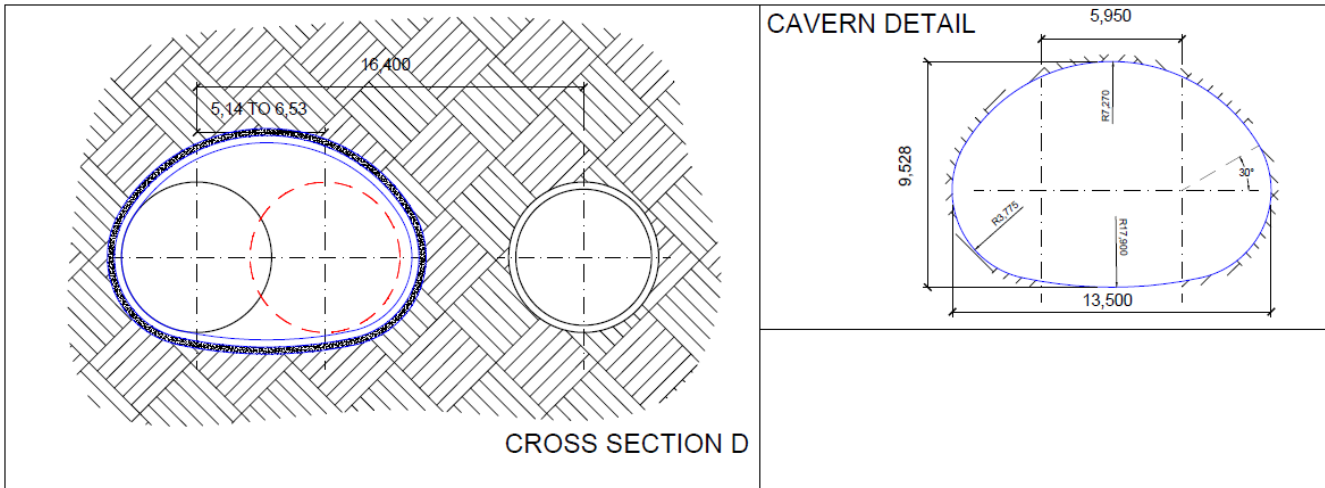


Figure 10.4- Cavern D

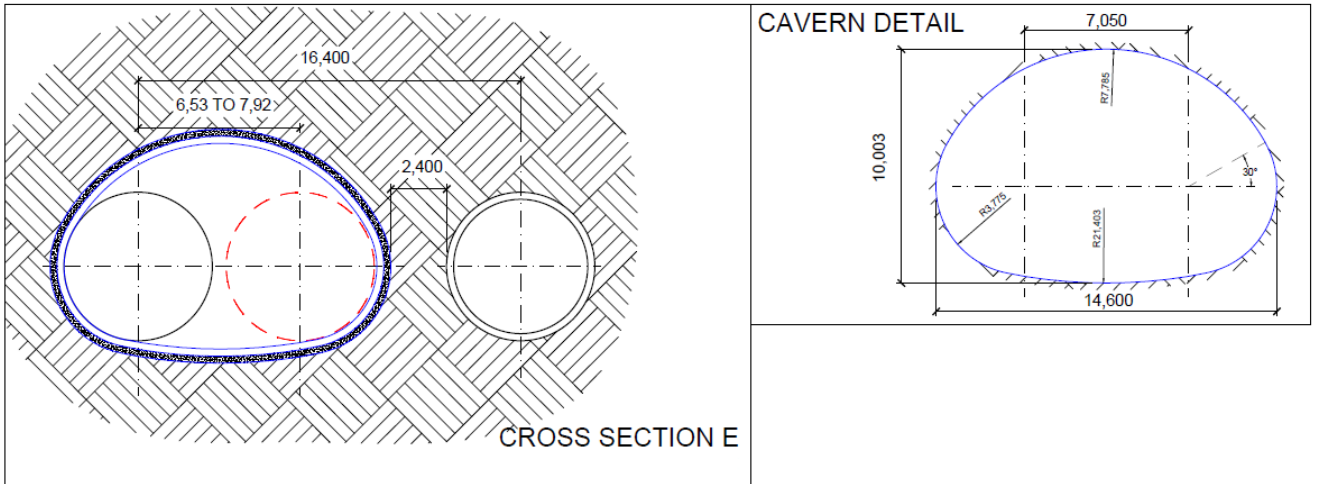


Figure 10.5- Cavern E

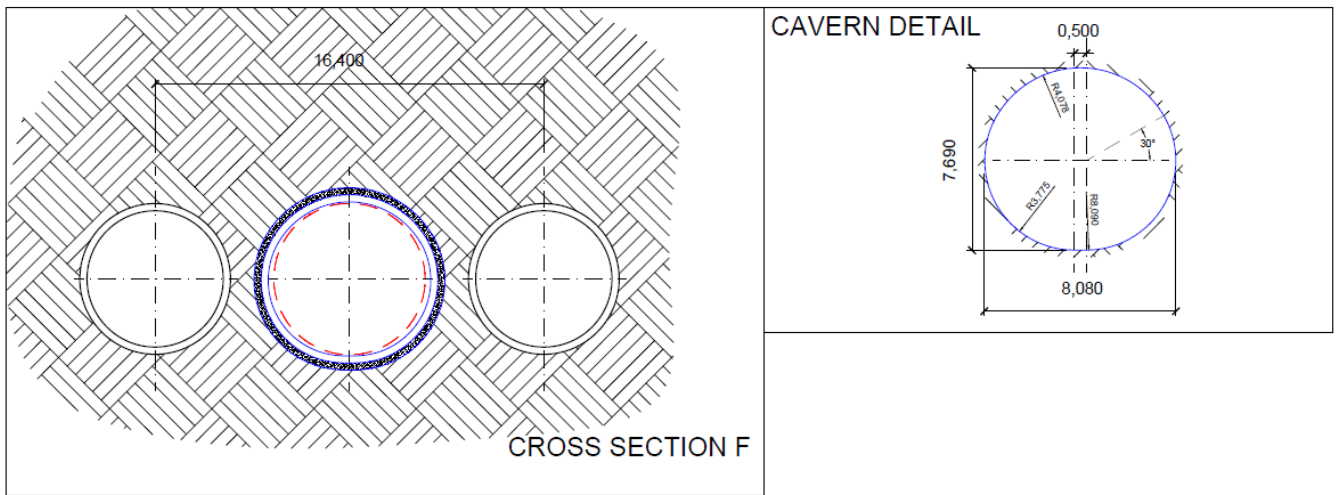


Figure 10.6 - Cavern F

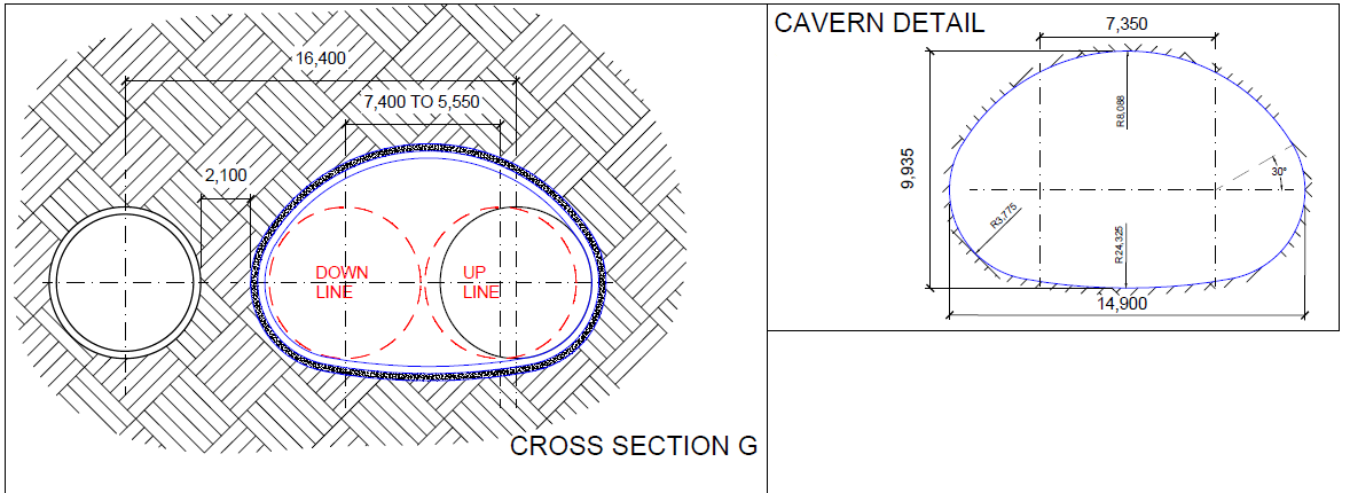


Figure 10.7 - Cavern G

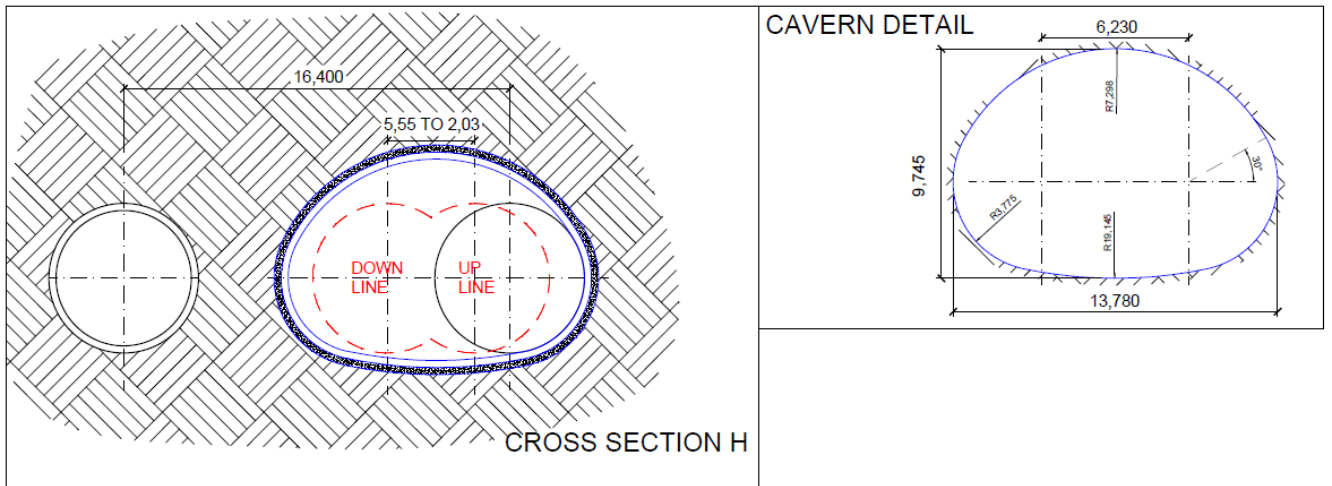


Figure 10.8 - Cavern H

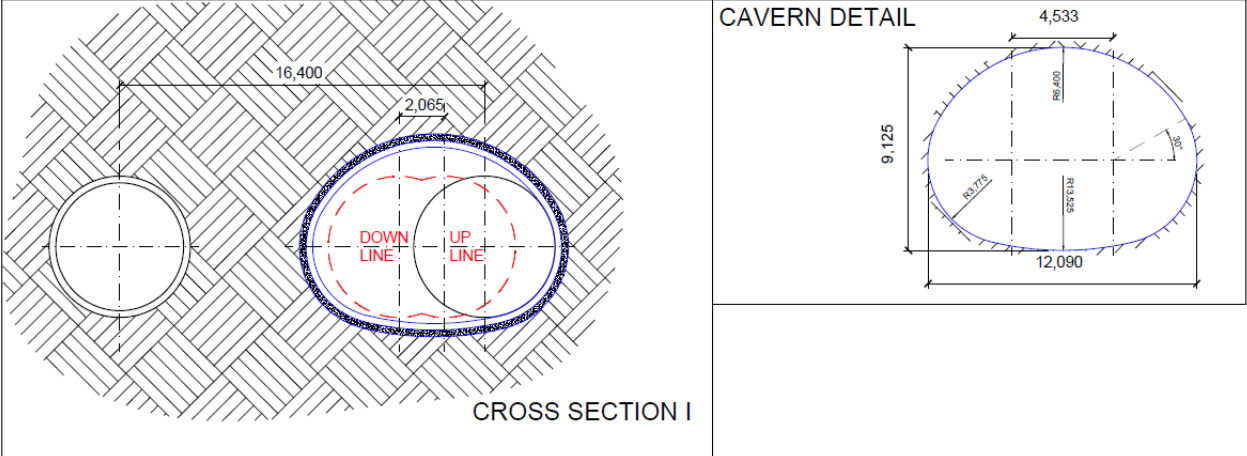


Figure 10.9 - Cavern I

10.2 Appendix 2: Crossover geological information

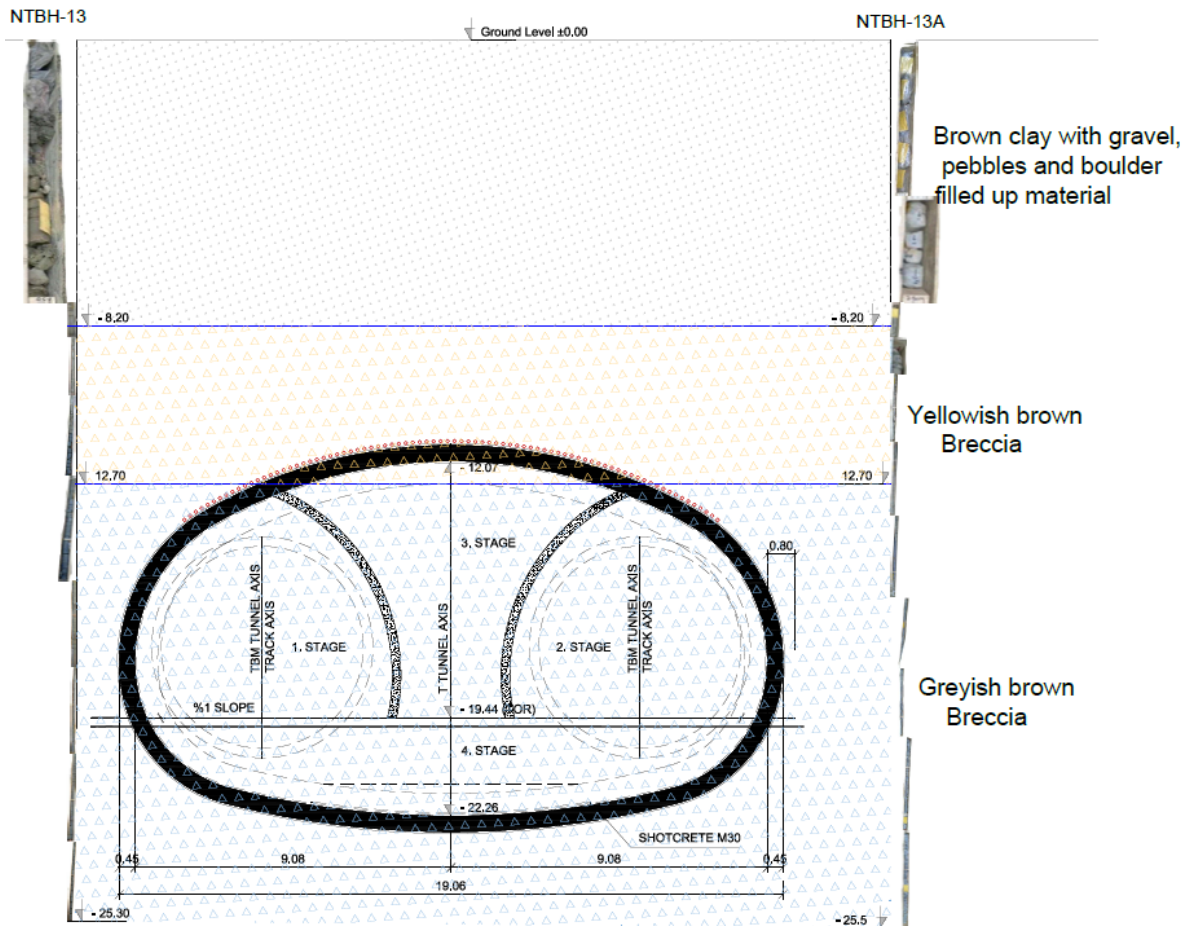


Figure 10.10-Borehole information in the section

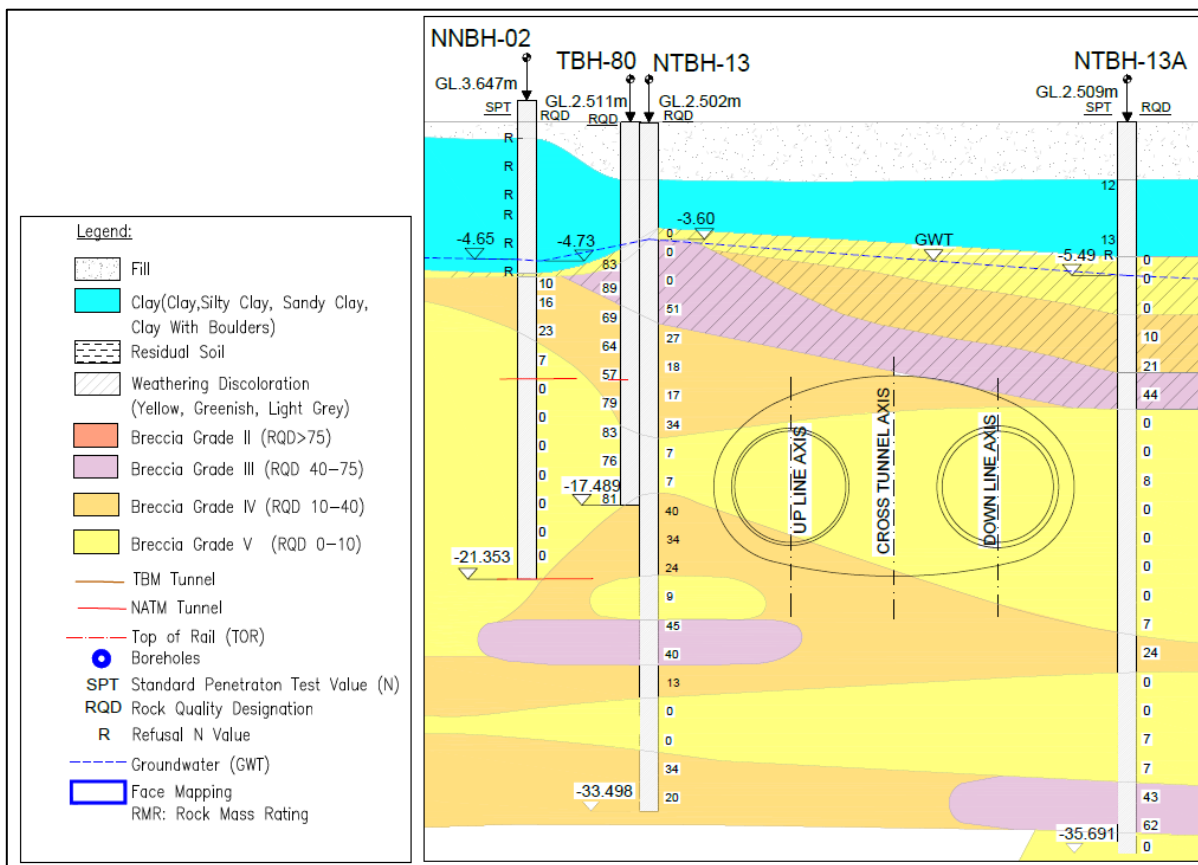


Figure 10.11- Geological profile. Cross section.

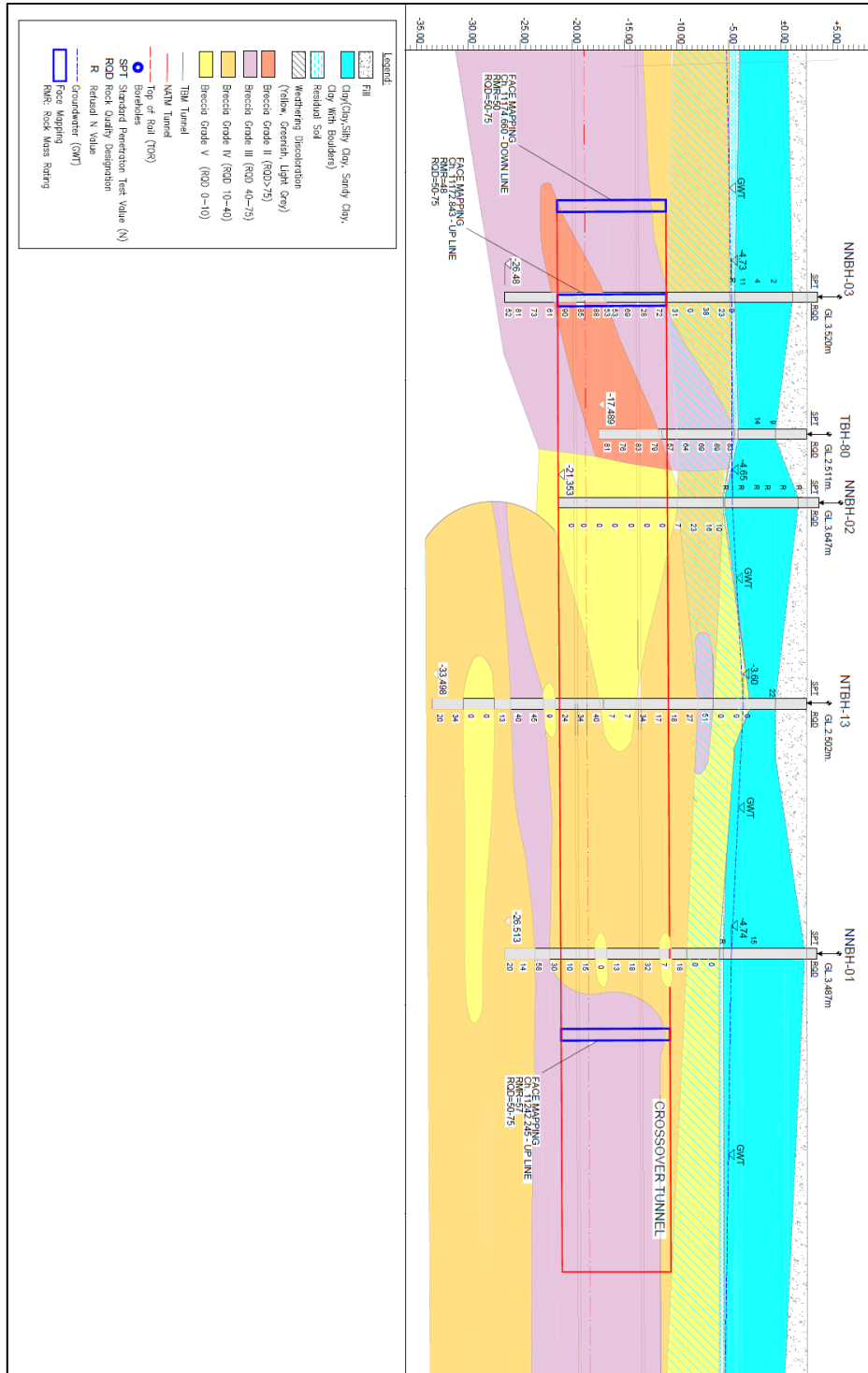


Figure 10.12- Geological Profile. Longitudinal Section.

10.3 Appendix 3: Scissor crossover results

10.3.1 Breccia Class III

10.3.1.1 Displacements

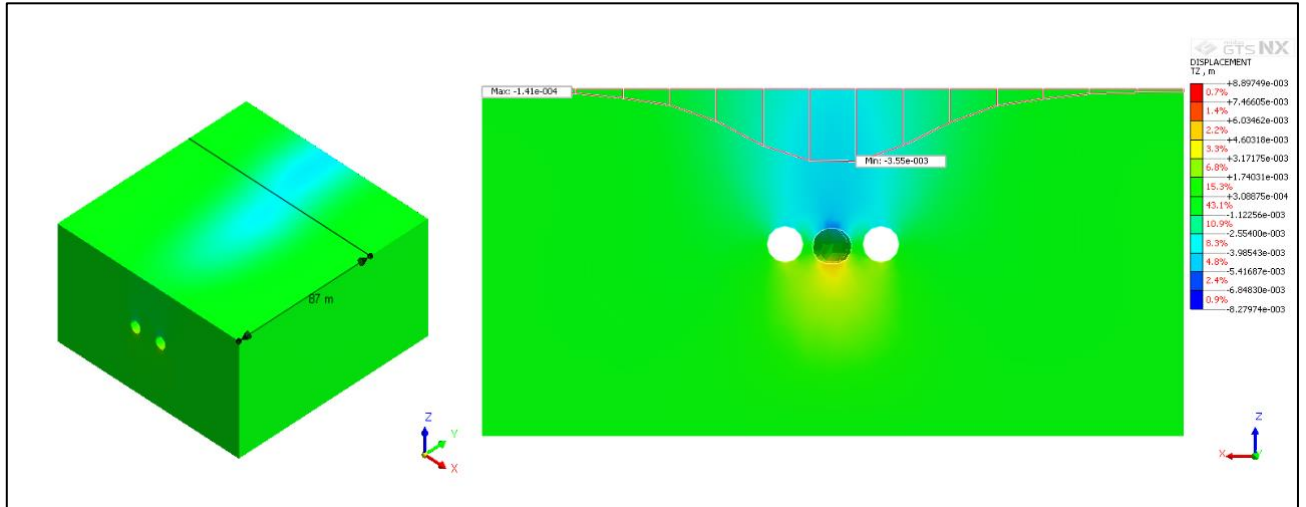


Figure 10.13- Superficial Settlements. Breccia Class III.

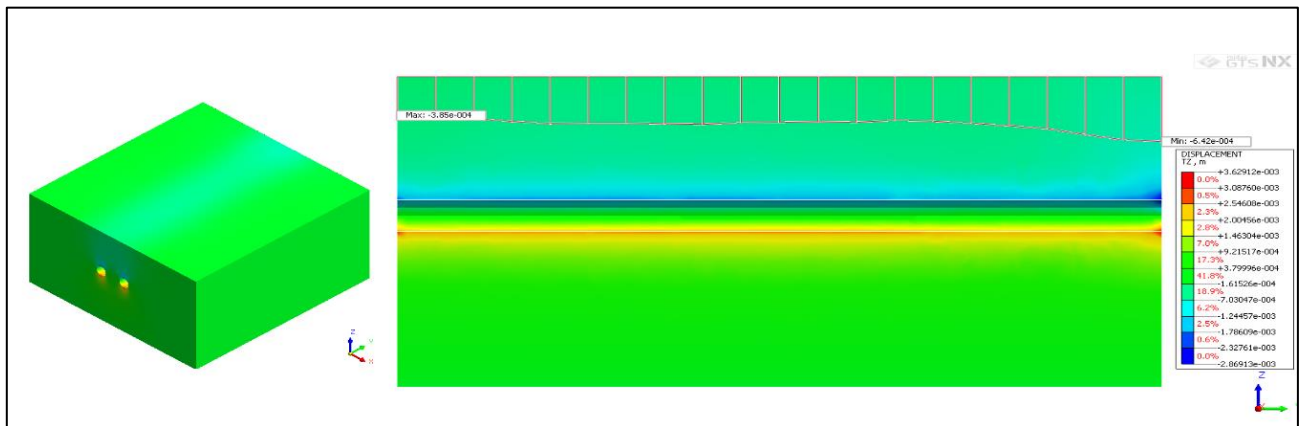


Figure 10.14- Superficial Settlements before the construction of the caverns. Breccia Class III.

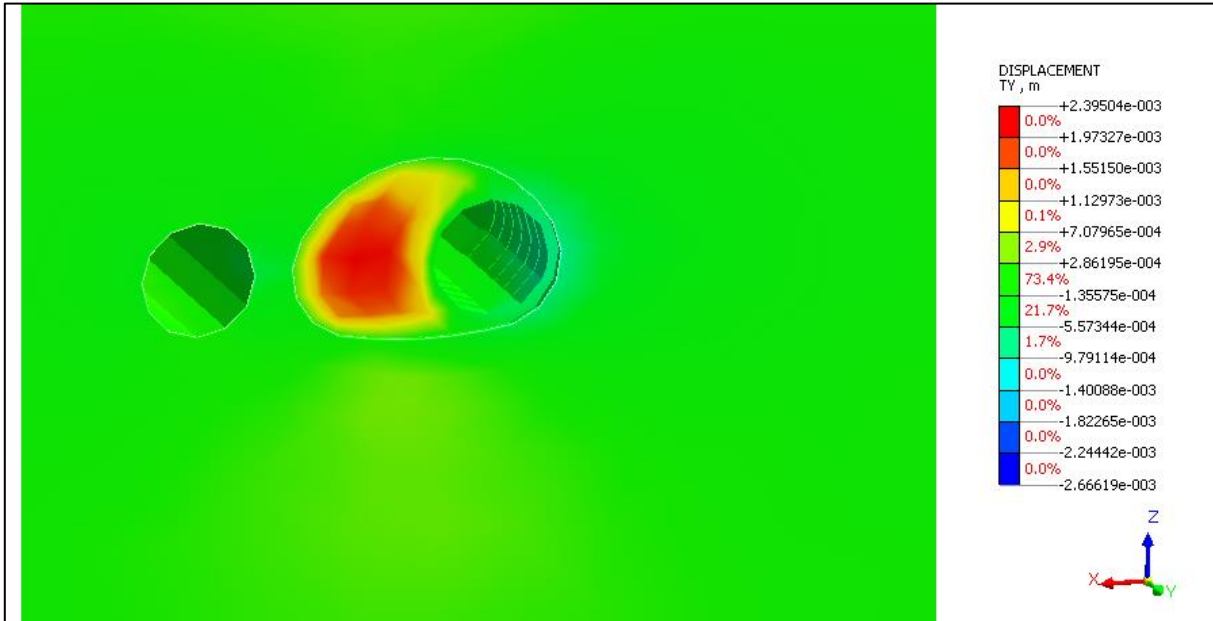


Figure 10.15-Cavern G face displacements in Y direction. Breccia Class III.

10.3.1.2 Principal Stresses

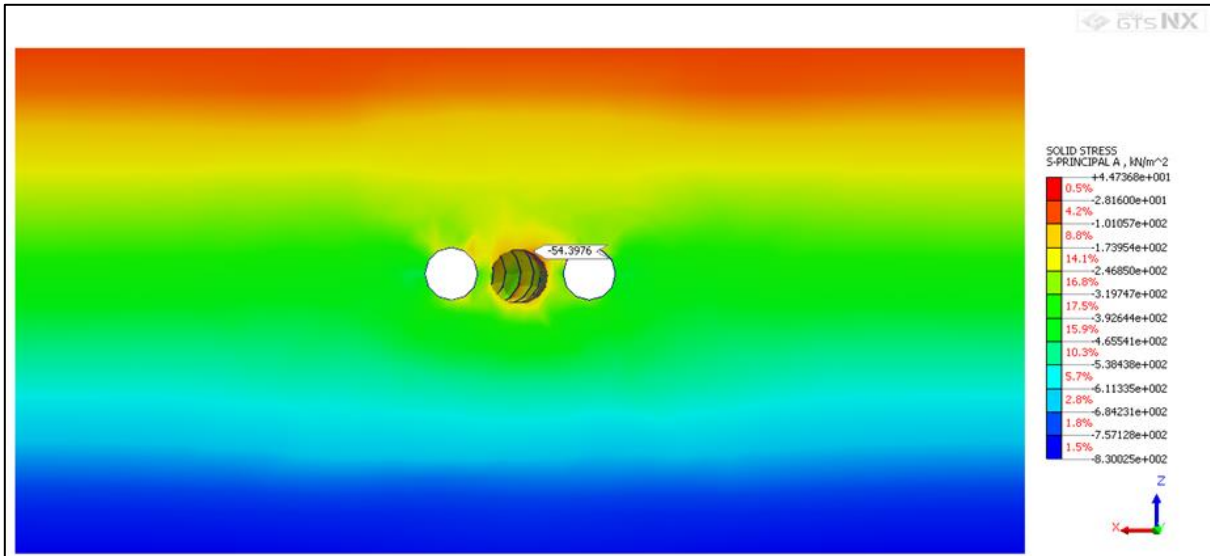


Figure 10.16- σ_1 in the analyzed section

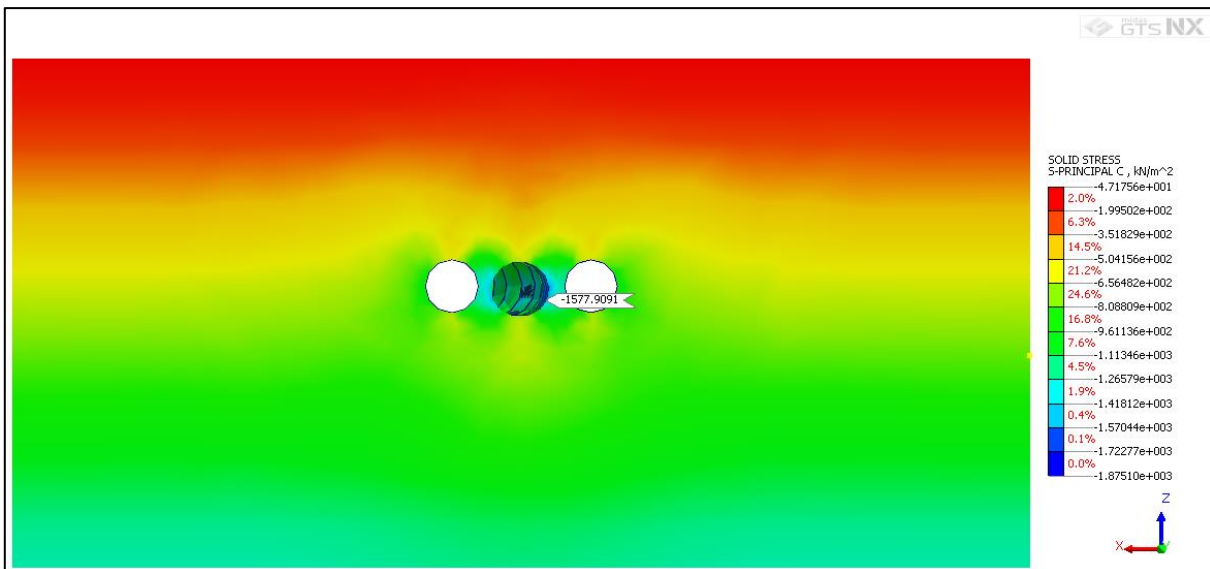


Figure 10.17- σ_3 in the analyzed section

10.3.1.3 Plastic Status

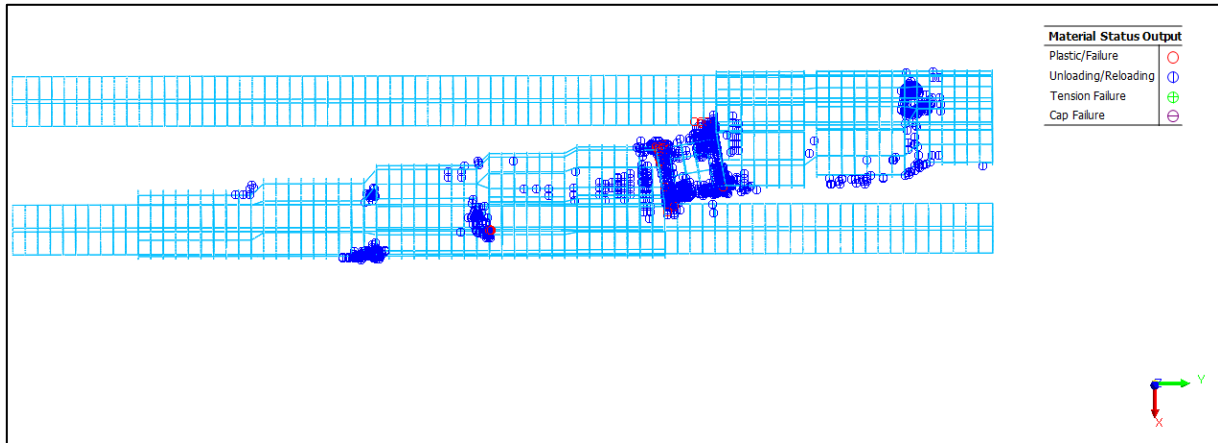


Figure 10.18- Plasticity analysis. Plan view

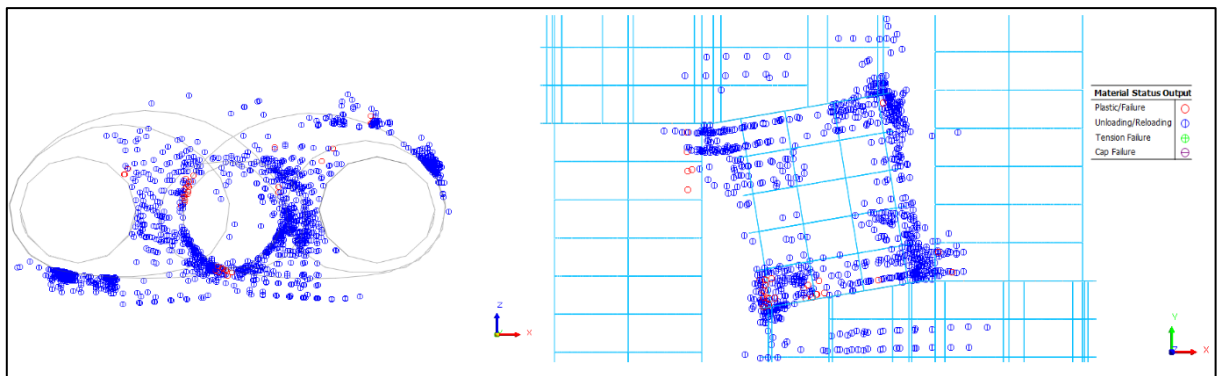


Figure 10.19-Plasticity analysis. Cavern F cross section and plan view detail

10.3.2 Breccia Class IV

10.3.2.1 Displacements

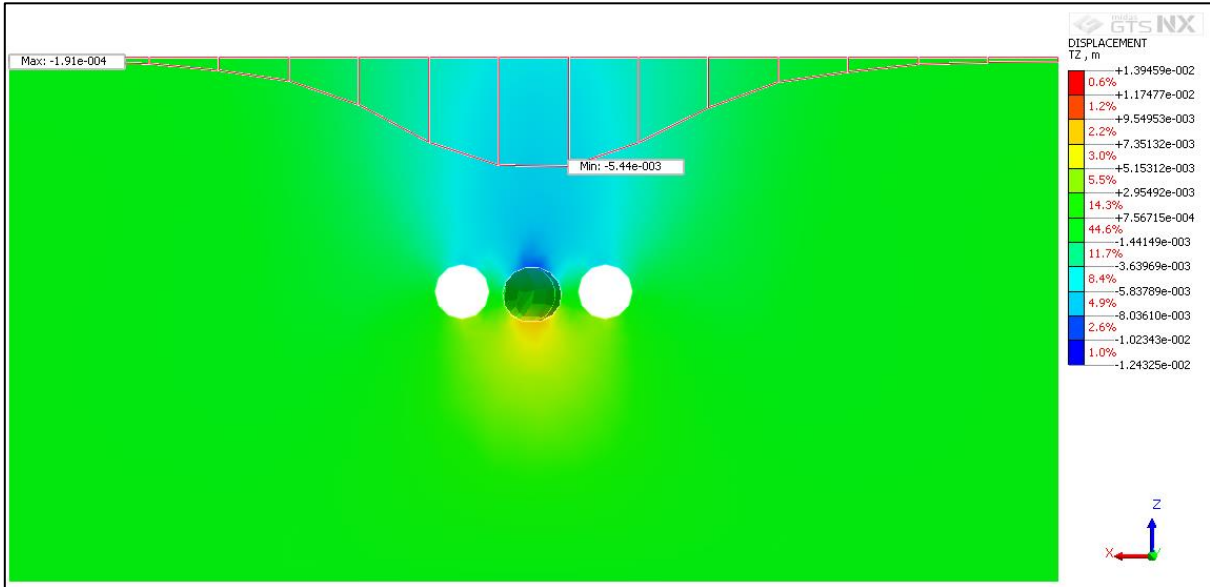


Figure 10.20-Superficial settlements

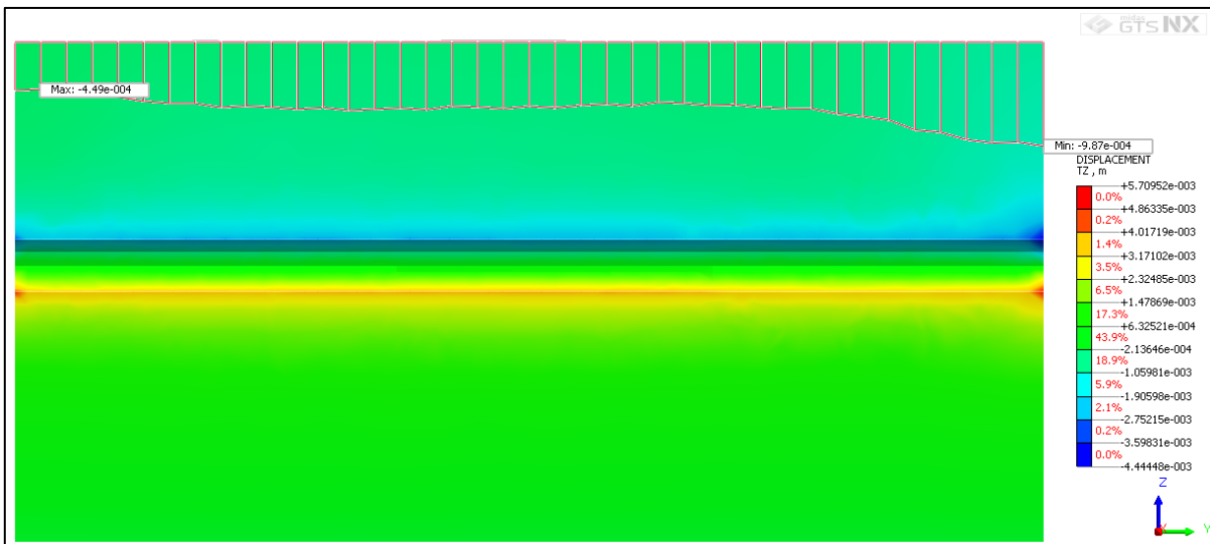


Figure 10.21-Superficial Settlements before the construction of the caverns

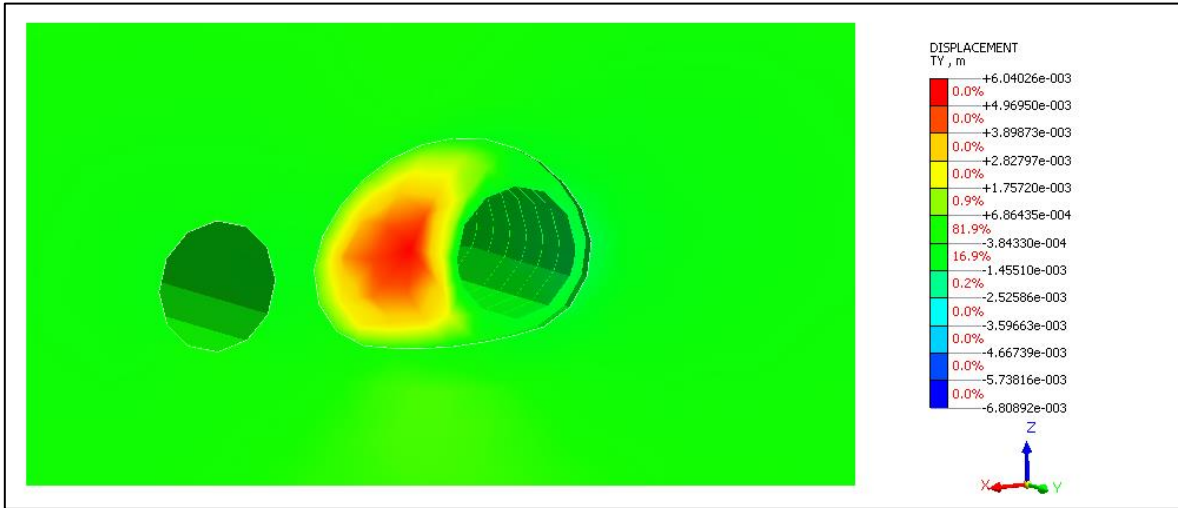


Figure 10.22-Cavern G face displacements in Y direction

10.3.2.2 Principal Stresses

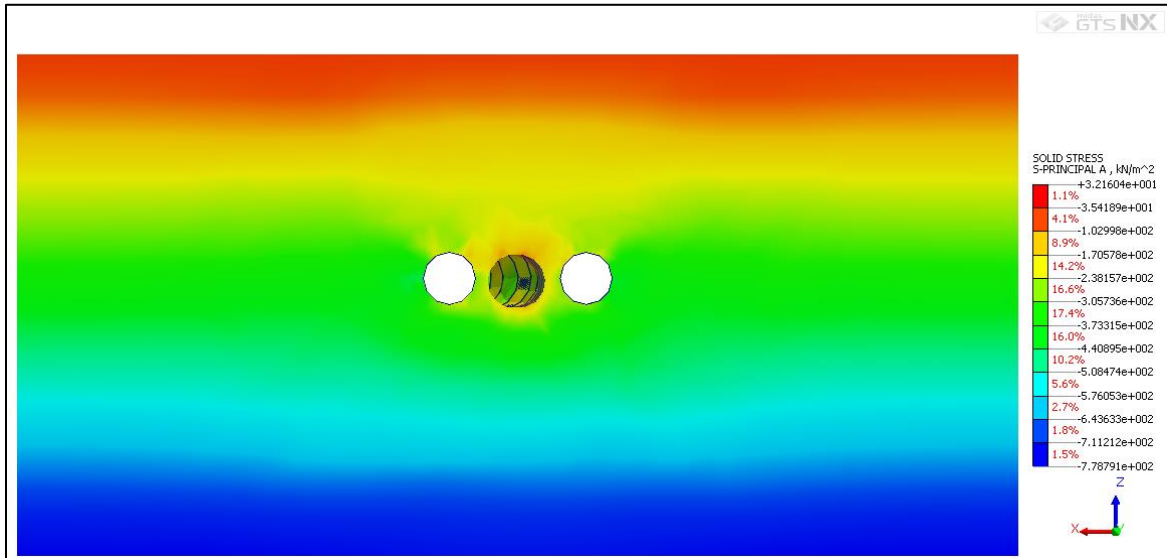


Figure 10.23- σ_1 in the analyzed section

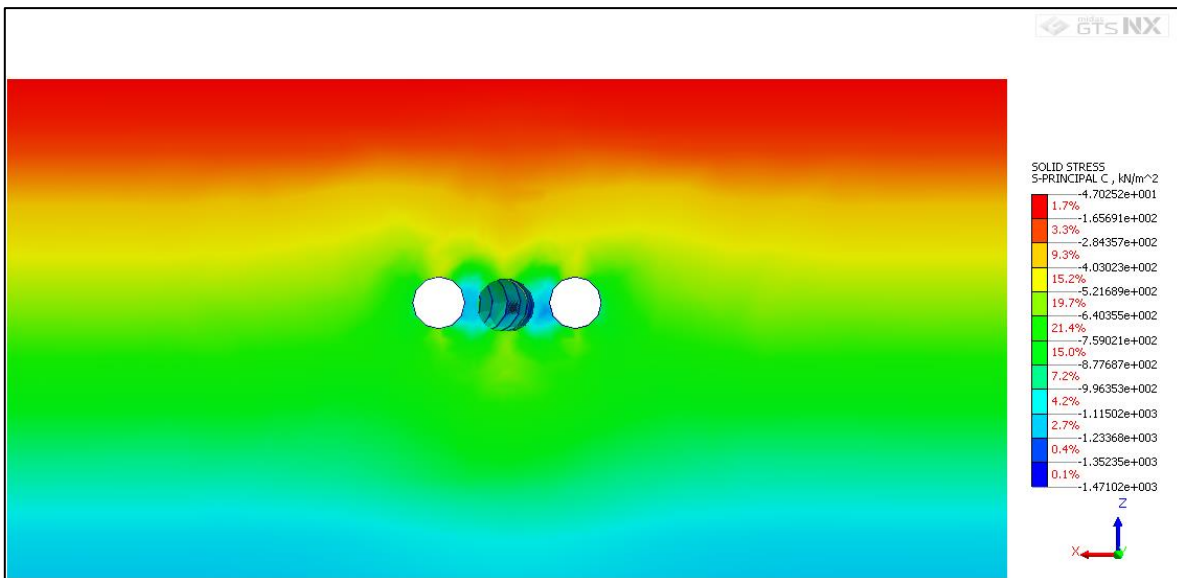


Figure 10.24- σ_3 in the analyzed section

10.3.2.3 Plastic Status

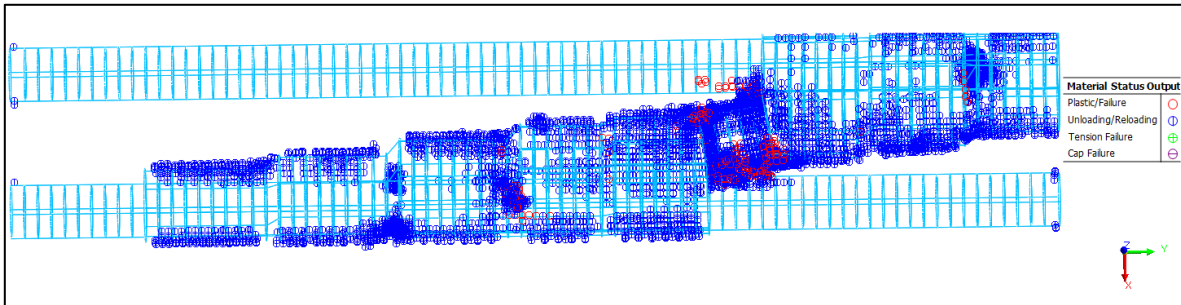


Figure 10.25-Plasticity analysis. Plan view

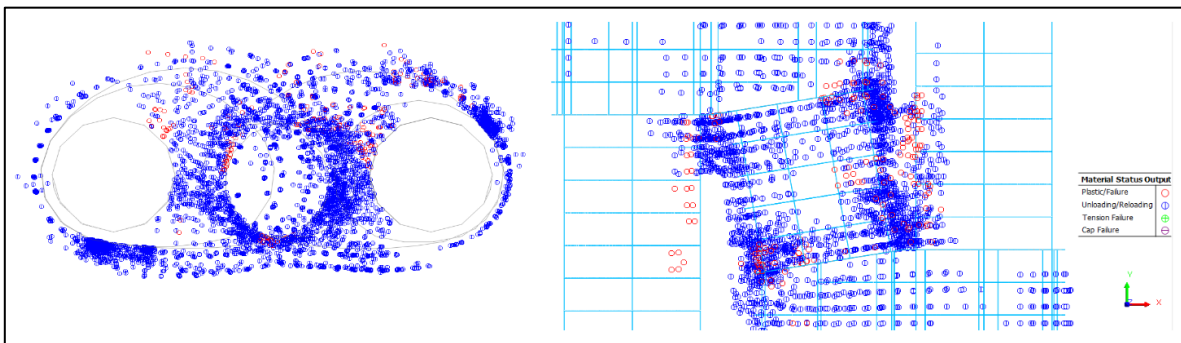


Figure 10.26-Plasticity analysis. Cavern F cross section and plan view detail

10.4 Appendix 4: Values of Superficial Displacements

ID	X (m)	Y (m)	Z (m)	Uv(m)	Uh(m)	Norm X	ϵ_h	β
1	20.00	100.00	30.000	-0.001	-0.002	0.00		
2	15.56	100.00	30.000	-0.002	-0.002	4.44	0.041	0.149
3	11.11	100.00	30.000	-0.003	-0.002	8.89	0.003	0.173
4	6.67	100.00	30.000	-0.003	-0.001	13.33	0.068	0.156
5	2.22	100.00	30.000	-0.001	-0.001	17.78	0.137	0.473
6	-2.22	100.00	30.000	-0.004	0.000	22.22	0.139	0.641
7	-6.67	100.00	30.000	-0.004	0.001	26.67	0.172	0.003
8	-11.11	100.00	30.000	-0.002	0.001	31.11	0.131	0.545
9	-15.56	100.00	30.000	-0.003	0.002	35.56	0.134	0.291
10	-20.00	100.00	30.000	-0.002	0.002	40.00	0.019	0.203

Table 10.1- Superficial Displacements Scissor Crossover. Breccia Class III. 25m from crossover center

ID	X (m)	Y (m)	Z (m)	Uv(m)	Uh(m)	Norm X	ϵ_h	β
1	20.00	100.00	30.000	-0.003	0.003	40.000		
2	15.56	100.00	30.000	-0.004	0.003	35.556	0.006	0.236
3	11.11	100.00	30.000	-0.005	0.002	31.111	0.101	0.219
4	6.67	100.00	30.000	-0.005	0.001	26.667	0.186	0.160
5	2.22	100.00	30.000	-0.006	0.000	22.222	0.226	0.075
6	-2.22	100.00	30.000	-0.006	-0.001	17.778	0.230	0.001
7	-6.67	100.00	30.000	-0.005	-0.002	13.333	0.224	0.078
8	-11.11	100.00	30.000	-0.004	-0.002	8.889	0.190	0.169
9	-15.56	100.00	30.000	-0.003	-0.003	4.444	0.092	0.241
10	-20.00	100.00	30.000	-0.002	-0.003	0.000	.018	0.236

Table 10.2-Superficial Displacements Scissor Crossover. Breccia Class IV. 25m from crossover center

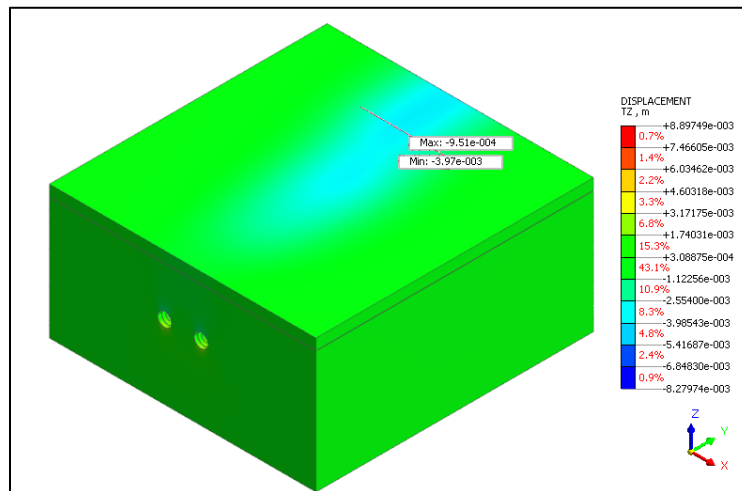


Figure 10.27- Building Edge, at 25 meters from Crossover center. Scissor Crossover.

ID	X (m)	Y (m)	Z (m)	Uv(m)	Uh(m)	Norm X	ϵ_h	β
1	20.00	25.00	30.00	-0.004	-0.004	0.00		
2	15.56	25.00	30.00	-0.005	-0.004	4.44	0.028	0.287
3	11.11	25.00	30.00	-0.006	-0.004	8.89	0.111	0.295
4	6.67	25.00	30.00	-0.008	-0.003	13.33	0.217	0.413
5	2.22	25.00	30.00	-0.009	-0.001	17.78	0.375	0.209
6	-2.22	25.00	30.00	-0.009	0.001	22.22	0.468	0.012
7	-6.67	25.00	30.00	-0.008	0.003	26.67	0.376	0.227
8	-11.11	25.00	30.00	-0.007	0.004	31.11	0.219	0.243
9	-15.56	25.00	30.00	-0.005	0.004	35.56	0.113	0.342
10	-20.00	25.00	30.00	-0.004	0.004	40.00	0.027	0.310

Table 10.3- Superficial Displacements Original Crossover. Breccia Class III. 25m from crossover center

ID	X (m)	Y (m)	Z (m)	Uv(m)	Uh(m)	Norm X	ϵ_h	β
1	20.00	25.00	30.00	-0.005	-0.006	0.00		
2	15.56	25.00	30.00	-0.007	-0.006	4.44	0.058	0.507
3	11.11	25.00	30.00	-0.009	-0.005	8.89	0.147	0.440
4	6.67	25.00	30.00	-0.011	-0.004	13.33	0.306	0.372
5	2.22	25.00	30.00	-0.012	-0.001	17.78	0.538	0.286
6	-2.22	25.00	30.00	-0.012	0.002	22.22	0.679	0.010
7	-6.67	25.00	30.00	-0.011	0.004	26.67	0.544	0.270
8	-11.11	25.00	30.00	-0.010	0.005	31.11	0.315	0.363
9	-15.56	25.00	30.00	-0.008	0.006	35.56	0.158	0.436
10	-20.00	25.00	30.00	-0.005	0.006	40.00	0.048	0.506

Table 10.4-Superficial Displacements Original Crossover. Breccia Class IV. 25m from crossover center

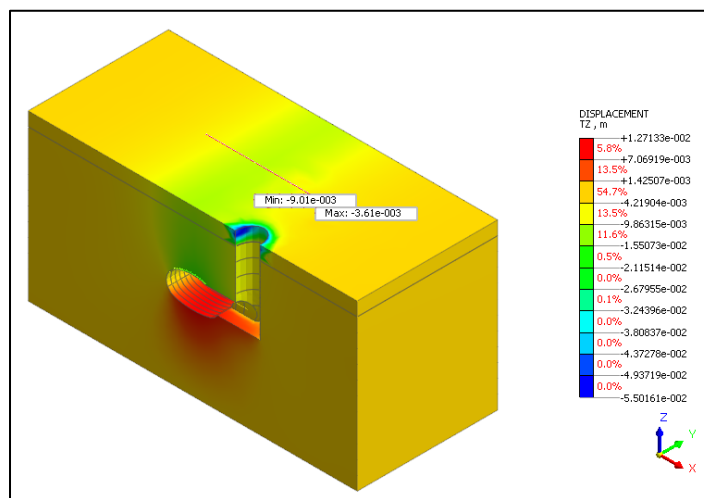


Figure 10.28- Building Edge, at 25 meters from Crossover center. Original Crossover.

ID	X (m)	Y (m)	Z (m)	Uv(m)	Uh(m)	Norm X	ϵ_h	β
1	20.00	75.000	30.000	-0.002	-0.002	0.00		
2	15.56	75.000	30.000	-0.003	-0.002	4.44	0.024	0.168
3	11.11	75.000	30.000	0.000	-0.001	8.89	0.228	0.502
4	6.67	75.000	30.000	-0.004	-0.001	13.33	0.009	0.709
5	2.22	75.000	30.000	-0.004	0.000	17.78	0.188	0.033
6	-2.22	75.000	30.000	-0.001	0.000	22.22	0.101	0.644
7	-6.67	75.000	30.000	-0.003	0.001	26.67	0.224	0.470
8	-11.11	75.000	30.000	-0.002	0.002	31.11	0.060	0.120
9	-15.56	75.000	30.000	-0.002	0.002	35.56	0.017	0.126
10	-20.00	75.000	30.000	-0.001	0.002	40.00	0.036	0.135

Table 10.5- Superficial Displacements Scissor Crossover. Breccia Class III. 50m from crossover center

ID	X (m)	Y (m)	Z (m)	Uv(m)	Uh(m)	Norm X	ϵ_h	β
1	-20.00	75.000	30.000	-0.002	0.002	40.000		
2	-15.56	75.000	30.000	-0.003	0.003	35.556	0.055	0.205
3	-11.11	75.000	30.000	-0.004	0.003	31.111	0.025	0.191
4	-6.67	75.000	30.000	-0.004	0.002	26.667	0.091	0.183
5	-2.22	75.000	30.000	-0.002	0.001	22.222	0.299	0.620
6	2.22	75.000	30.000	-0.006	0.000	17.778	0.190	0.882
7	6.67	75.000	30.000	-0.005	-0.001	13.333	0.283	0.052
8	11.11	75.000	30.000	-0.001	-0.001	8.889	0.026	1.070
9	15.56	75.000	30.000	-0.004	-0.003	4.444	0.353	0.753
10	20.00	75.000	30.000	-0.003	-0.003	0.000	0.033	0.256

Table 10.6-Superficial Displacements Scissor Crossover. Breccia Class IV. 50m from crossover center

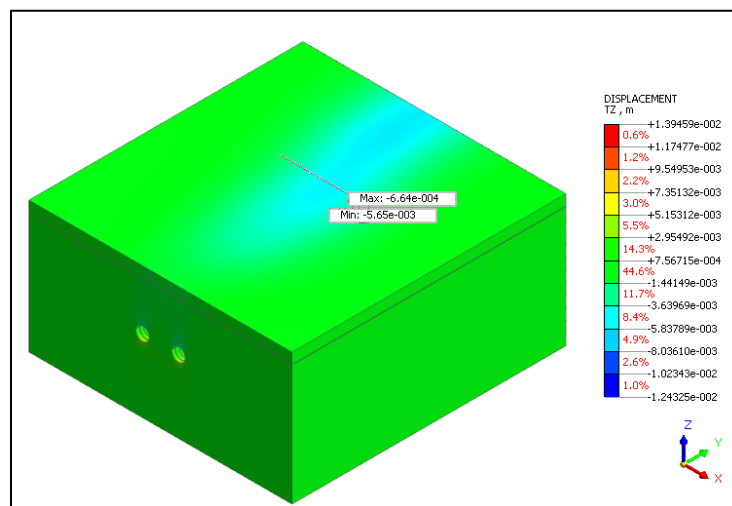


Figure 10.29- Building Edge, at 50 meters from Crossover center. Scissor Crossover.

ID	X (m)	Y (m)	Z (m)	Uv(m)	Uh(m)	Norm X	ϵ_h	β
1	20.00	50.00	30.00	-0.004	-0.004	0.00		
2	15.56	50.00	30.00	-0.005	-0.004	4.44	0.024	0.321
3	11.11	50.00	30.00	-0.002	-0.001	8.89	0.752	0.822
4	6.67	50.00	30.00	-0.008	-0.002	13.33	0.381	1.435
5	2.22	50.00	30.00	-0.009	-0.001	17.78	0.365	0.154
6	-2.22	50.00	30.00	-0.009	0.001	22.22	0.392	0.002
7	-6.67	50.00	30.00	-0.008	0.003	26.67	0.365	0.150
8	-11.11	50.00	30.00	-0.002	0.001	31.11	0.420	1.449
9	-15.56	50.00	30.00	-0.005	0.004	35.56	0.795	0.840
10	-20.00	50.00	30.00	-0.004	0.004	40.00	0.025	0.323

Table 10.7- Superficial Displacements Original Crossover. Breccia Class III. 50m from crossover center

ID	X (m)	Y (m)	Z (m)	Uv(m)	Uh(m)	Norm X	ϵ_h	β
1	20.00	50.00	30.00	-0.005	-0.006	0.00		
2	15.56	50.00	30.00	-0.007	-0.006	4.44	0.051	0.467
3	11.11	50.00	30.00	-0.002	-0.001	8.89	1.056	1.164
4	6.67	50.00	30.00	-0.011	-0.004	13.33	0.544	2.077
5	2.22	50.00	30.00	-0.012	-0.001	17.78	0.525	0.235
6	-2.22	50.00	30.00	-0.012	0.001	22.22	0.568	0.008
7	-6.67	50.00	30.00	-0.012	0.004	26.67	0.529	0.219
8	-11.11	50.00	30.00	-0.002	0.001	31.11	0.594	2.089
9	-15.56	50.00	30.00	-0.008	0.006	35.56	1.128	1.193
10	-20.00	50.00	30.00	-0.005	0.006	40.00	0.043	0.472

Table 10.8-Superficial Displacements Original Crossover. Breccia Class IV. 50m from crossover center

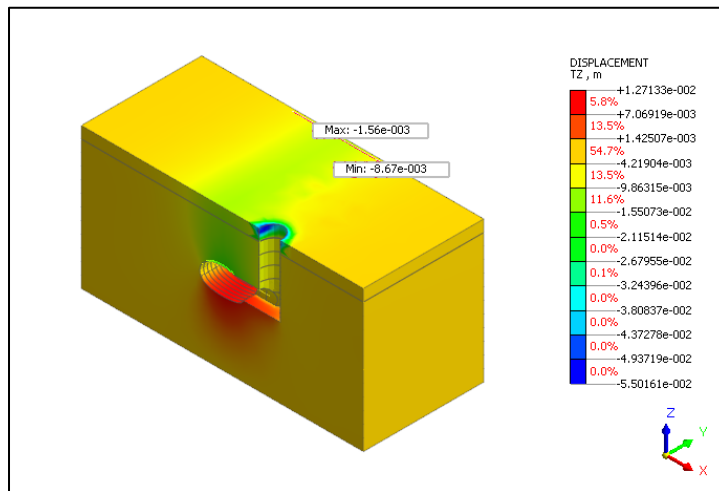


Figure 10.30- Building Edge, at 50 meters from Crossover center. Original Crossover.